IDENTIFICATION OF HOST AND VIRAL FACTORS OF ARTHRITIC ALPHAVIRUS PATHOGENESIS: THE ROLE OF MANNOSE BINDING LECTIN AND THE VIRAL N-LINKED GLYCANS

Bronwyn Mei Gunn

A dissertation submitted to the faculty of the University of North Carolina at Chapel Hill in partial fulfillment of the requirements for the degree of Doctor of Philosophy in Department of Microbiology and Immunology.

Chapel Hill
2013

Approved by:

Mark T. Heise, Ph.D.

Aravinda deSilva, Ph.D.

Ralph S. Baric, Ph.D.

Dirk P. Dittmer, Ph.D.

Barbara Sherry, Ph.D.

ABSTRACT

BRONWYN MEI GUNN: Identification of host and viral factors of arthritic alphavirus pathogenesis: the role of mannose binding lectin and the viral N-linked glycans
(Under the direction of Mark T. Heise)

Arthritogenic alphaviruses such as Ross River virus (RRV) and chikungunya virus are mosquito-borne viruses that cause epidemics of debilitating myositis and polyarthritis in humans in various areas around the world. Studies conducted in a mouse model of RRV-induced disease have demonstrated a critical role for the inflammatory response in the development of disease. In particular, the host complement system contributes significantly to damage within target tissues through activation of CR3-bearing inflammatory cells. However, the precise mechanism and ligands leading to complement activation and disease following RRV infection are not known. In these studies, we have identified critical roles for the host innate immune protein mannose binding lectin (MBL) and the viral N-linked glycans in mediating complement activation and disease following RRV infection. Using mice deficient in MBL, we demonstrated that the MBL activation pathway of the host complement system is the primary pathway required for complement activation and disease following infection. MBL recognizes and binds to terminal carbohydrates, such as mannose found on glycosylated viral proteins or on infected cells. The RRV E2 envelope glycoprotein contains two N-linked glycosylation sites that are glycosylated with a combination of high mannose and complex glycans when replicating in mammalian cells. We hypothesized that MBL recognizes the E2 N-linked glycans to activate the complement system, leading to disease. Using a panel of RRV mutants lacking one or more envelope

glycans, we have found that the RRV E2 N-linked glycans contribute to MBL binding to RRV infected cells and development of disease. Viruses lacking either E2 N-linked glycosylation sites cause reduced disease in mice, while a virus lacking both sites causes very mild disease. In addition, the role of the E2 glycans is independent of replication within host tissues and recruitment of inflammatory cells. Rather, the E2 glycans were required for MBL deposition and complement activation within target tissues in vivo. These results suggest that interactions between the viral N-linked glycans and the MBL pathway play a central role in development of severe alphavirus-induced arthritis and may be an effective target for therapeutic treatment in patients infected with RRV.

To my parents, Michael and Bee Fong,

who have always supported me

with unconditional love and constant encouragement,

even from the other side of the world.

You have given me every opportunity possible,

and I am so proud to be your daughter.

And to my brother Jonathan,

who has been my best friend and advocate my entire life.

ACKNOWLEDGEMENTS

There are so many people to thank for shaping me into the scientist that I am today. First, I would like to thank my thesis advisor Mark Heise, who has been a truly wonderful mentor. He has taught me so much about virology, pathogenesis, and immunology, but most importantly, he has taught me how to be a rigorous, methodical, independent, and creative scientist. He has always supported and encouraged me, and I cannot thank him enough for his patience, kindness, advice, and guidance throughout my graduate career. I am very proud to be a Heise Lab trainee, and I look forward to many more years of continued mentorship.

I have been incredibly fortunate to have had worked with all the members of the Heise lab, past and present, and I have learned so much from everyone both scientifically and personally. I would particularly like to thank Tem Morrison, who has been a great mentor, collaborator, and role model throughout the years. I would especially like to thank Kristin Long who made all of the projects in the BSL-3 possible by maintaining the facility in impeccable working order, and I thank her for all the advice and support during my time in the lab. Alan Whitmore has always inspired me to stay positive and enthusiastic about science and to never stop having fun. I would also like to thank Marty Ferris, Charlie McGee, and Adam Cockrell for friendship, mentorship, and good times in the lab. I feel extremely lucky to have worked beside Jason Simmons, Cathy Cruz, Alina Lotstein, and Amy Wollish, who I value not only as scientific colleagues but also as wonderful and true friends. I would also like to thank Lauren Neighbours, Bianca Trollinger, Charissa Kam,

TABLE OF CONTENTS

LIST OF TABLES

LIST OF FIGURES

LIST OF ABBREVIATIONS

BBB	blood brain barrier
BHK	baby hamster kidney
BMDC	bone marrow derived dendritic cell
BSL-3	biosafety level three
CC	Collaborative Cross
CHIKV	Chikungunya virus
CL-11	collectin-11
CLR	C-type lectin receptor
CNS	central nervous system
CPE	cytopathic effect
CRD	carbohydrate recognition domain
CR3	complement receptor 3
CR4	complement receptor 4
DCs	dendritic cells
DENV	dengue virus
DF	dengue fever
DHF	dengue hemorrhagic fever
DKO	double knockout
DM	double mutant
dpi	days post infection
EBD	Evans Blue dye
EEEV	Eastern equine encephalitis virus

ELISA	enzyme linked immunosorbent assay
EM	electron microscopy
EMCV	encephalomyocarditis virus
ER	endoplasmic reticulum
fB	factor B
FITC	fluorescein isothiocyanate
GFP	green fluorescent protein
GlcNAc	N-acetylglucosamine
HIV	human immunodeficiency virus
HS	heparan sulfate
HSV-2	herpes simplex virus-2
H&E	hemotoxylin and eosin
IFN	interferon
IHC	immunohistochemistry
IRI	ischemic reperfusion injury
kDa	kilo-dalton
LCA	leukocyte common antigen
MAC	membrane attack complex
Mam-RRV	mammalian cell-derived RRV
MASPs	MBL-associated serine proteases
MBL	mannose binding lectin
MCP-1	monocyte chemotactic protein
mDC	myeloid dendritic cells

MEFs	mouse embryonic fibroblasts
MIF	macrophage migration inhibitory factor
MOI	multiplicity of infection
Mos-RRV	mosquito cell-derived RRV
NK	natural killer
NLR	NOD-like receptor
NRAMP	natural resistance associated macrophage protein
NSAID	nonsteroidal anti-inflammatory
NTPase	nucleoside triphosphatase
ONNV	O'nyong nyong virus
PFA	paraformaldehyde
PFU	plaque forming units
PRR	pattern recognition receptor
RA	rheumatoid arthritis
RLR	RIG-I like receptor
RRV	Ross River virus
RT-PCR	real time polymerase chain reaction
SARS-CoV	severe acute respiratory syndrome coronavirus
SINV	Sindbis virus
SFV	Semliki Forest virus
TLR	toll-like receptor
TNF	tumor necrosis factor
UTR	untranslated region

VEEV	Venezuelan equine encephalitis virus
WEEV	Western equine encephalitis virus
WNV	West Nile virus
WT	wild-type

CHAPTER ONE:
INTRODUCTION

1.1. Alphaviruses.

Alphavirus classification.

The alphavirus genus is part of the *Togaviridae* family of enveloped viruses that have a single stranded positive sense RNA genome. The *Togavirus* family is divided into two groups, the alphaviruses and the rubiviruses, and the family was initially named for their members' cloak-like appearance under the electron microscope; the word "*Toga*" is Latin for "cloak". To date, over forty alphaviruses have been identified, many of which have been associated with human disease, and can be found on all continents of the globe and in a wide range of hosts (78). Rubella virus is the only rubivirus to date, and is an important childhood human pathogen. The two genus of *Togaviridae* are further defined by their similar genomic organization with the four nonstructural genes at the 5' end of the genome followed by the structural genes whose expression is driven from a subgenomic promoter in the latter third at the 3' end of the genome. While alphaviruses and rubiviruses share similar genome organization and virion structure, they differ significantly in replication strategies, types of disease they cause, as well as how they are transmitted. Rubella virus is transmitted human to human through aerosol droplets and causes a flu-like disease that is characterized by an extensive rash (101), whereas alphaviruses are transmitted by arthropod vectors from small mammals to humans and are associated with arthritis/myositis or encephalitis (78).

Of the forty alphaviruses that have been described, twenty-nine cause human disease and are classified into seven distinct antigenic and genetic groups (reviewed in (78, 242)). These groups have been classified based on sequence similarity within the E1 glycoprotein as well as cross-reactivity of sera and members of each complex generally share similar disease characteristics (175). The Semliki Forest (SF) complex includes many of the arthritic alphaviruses such as the namesake Semliki Forest virus (SFV), Ross River virus (RRV), chikungunya virus (CHIKV), and O'nyong nyong virus (ONNV). The VEE and EEE complexes encompasses encephalitic viruses such as Venezuelan equine encephalitis virus (VEEV), eastern equine encephalitis virus (EEEV), and the WEE antigenic complex includes viruses that are associated with both arthritic and encephalitic viruses such as Sindbis virus (SINV), and western equine encephalitis virus (WEEV). Many aspects of alphavirus biology have been elucidated using two prototype alphaviruses: SINV of the WEE antigenic complex and SFV of the SF antigenic complex. While there are some differences between these viruses and the other alphaviruses such as RRV and CHIKV, the basic biology of replication and structure learned in SINV and SFV studies applies to the replication all alphaviruses.

Of note, alphaviruses were originally categorized with the *Flaviviridae* family of viruses as Group A and B arboviruses, respectively, based upon similarities in transmission and disease (125). However, once viruses from both groups were sequenced, it became clear that the genome organization was too different to classify them together. However, since the disease and transmission of alphaviruses and flaviviruses are similar, it has been useful to compare and contrast aspects of disease pathogenesis and interaction with both mosquito and mammalian host proteins between the two groups of viruses.

Geographic distribution and epidemics.

Alphaviruses have a global distribution and can be found on all continents. While not all alphaviruses are associated with disease pathology, the ones that do cause disease are roughly separated into two general groups: the Old World and the New World alphaviruses. This grouping is based both on the type of disease associated with each virus and geographic location. The Old World alphaviruses are found mostly in Africa, Asia, and Oceania and tend to cause polyarthritis and arthralgia in humans. New World alphaviruses are found in the Americas and are more closely associated with encephalitis.

The New World viruses include EEEV, WEEV, and VEEV, and cause encephalitis in humans and horses in various regions around the Americas. EEEV has been found in parts of eastern North America, as well as parts of Central America and is particularly virulent in humans, causing up to 70% mortality in symptomatic cases, and the horse fatality rate is 80-90% (42, 206). WEEV is found in western parts of the North America and South America, and is reportedly aerosol transmitted as well as mosquito-borne and has a 10% human fatality rate (78, 180). VEEV has been identified in the tropical regions of South America and epizootic outbreaks have involved over 75, 000 people (185).

Old world alphaviruses, including CHIKV, RRV, SINV, and ONNV, are present throughout parts of Africa and Oceania and are associated with large-scale outbreaks of arthritis, arthralgia, myalgia, and rash. CHIKV was first isolated in modern day Tanzania, and is currently found throughout India, Southeast Asia, and sub-Saharan Africa, and most recently has been associated with epidemic in areas surrounding the Indian Ocean that affected upwards of 6 million people (27). ONNV has been found in regions in East

Africa and caused an epidemic of rash and fever involving 2 million people in 1959 (247). RRV is found in Oceania, and is endemic within many areas of Australia and throughout Papua New Guinea and the surrounding islands (86). Outbreaks of RRV-induced disease have occurred on coastal areas of Western Australia, in the southern states of New South Wales and Victoria, as well as within Papua New Guinea, Fiji, and the Cook and Solomon Islands affecting over 50, 000 people. SINV exhibits a broad geographic distribution and can be found in Northern Europe, Africa, Southeast Asia, and Oceania (78).

The worldwide distribution of alphaviruses that are associated with human disease and the ability to cause periodic and explosive outbreaks involving millions of people highlight the importance of understanding how these viruses cause disease in order to design a vaccine, develop therapeutics, as well as develop appropriate measures to prevent infection and future epidemics.

Transmission of alphaviruses.

Alphaviruses are generally maintained in an enzootic cycle where the viruses transmit between their arthropod vectors and a reservoir host organism, usually birds, small mammals, or primates. The reservoir hosts vary for the different alphaviruses, but generally support high levels of viral replication and viremia that allow for infection of the competent arthropod species. The arthropods, typically mosquitoes, become persistently infected with the virus, and are capable of transmitting virus through their saliva 2-7 days after initial infection (206). *Aedes* and *Culex* species are the primary enzootic vectors for most alphaviruses, and certain species of *Aedes* such as *Ae. aegypti*

4

and *Ae. albopictus,* as well as the *Anopheles* mosquitoes can act as additional vectors during epidemics (reviewed in (242)).

Human disease typically occurs through a spillover effect when humans come into contact with the infected mosquito or arthropod. Seasonal outbreaks of alphavirus-induced disease have been noted and are well documented with RRV in Australia, and alphaviruses can also enter into an urban epidemic cycle where viruses can transmit between humans and the mosquitoes without a reservoir host. This is thought to have occurred in nearly every large-scale epidemic of alphavirus-induced disease.

The factors that affect the emergence of disease to bring on an epidemic can be both environmental and genetic. Climatic events, such as unusually heavy rainfall, can alter the mosquito vector host range and bring epidemic mosquito vectors into endemic regions (240). Genetic changes within the virus genome also play a role in the epidemic potential of the virus. The evolution rate of alphaviruses is approximately 1×10^4 bases/year, which is slower than some other RNA viruses due to the fact that alphaviruses are maintained in two disparate hosts (241). Alphaviruses can acquire changes in the genome that confer an ability to replicate within an additional mosquito vector or allow for more efficient replication within a host organism. Such a change was observed during the most recent CHIKV epidemic where a mutation in the E1 glycoprotein allowed for spread of the virus from an additional mosquito vector, *Ae. albopictus* (227).

Clinical disease and pathology of arthritic alphaviruses: Ross River virus.

Reports of seasonal epidemics of joint swelling and rashes began as early as 1928 in Australia, but the etiological agent was not identified as RRV until about 1959 (46).

There had been additional epidemics noted prior to 1959 throughout the Northern Territory, Queensland, and Papua New Guinea during the Second World War, but it was not until an epidemic in Murray Valley in Southeast Australia in 1956 that researchers began to suspect that the disease was caused by an arbovirus. CHIKV had recently been associated with an outbreak of acute virus polyarthritis in Tanganyika (Tanzania) in Africa that shared some similarities with the Australian epidemic. The Australian patient sera were assayed for cross-reactivity to other group A arbovirus including SFV and CHIKV. While some cross-reactivity was observed, Shope and Anderson concluding that the outbreak in Australia was due to a yet undescribed group A arbovirus (214). Doherty *et al* then isolated a virus from a pool of trapped *Aedes vigilax* mosquitoes by the Ross River in Northern Queensland, which reacted strongly with patient sera (46). The virus isolated was formally named Ross River virus, and the strain isolated was dubbed T48 (Townsville and mosquito pool 48). T48 is the type strain of RRV and is the strain used in the laboratory to study RRV.

The largest outbreak of RRV occurred in 1979-1980 when RRV spread to islands in the South Pacific, including Fiji, Samoa, and the Cook Islands. An estimated 50, 000 people throughout the region were infected and presented with arthritis and/or arthralgia. RRV was isolated from several patients by several different research groups (1, 191, 225) confirming that the epidemic was associated with RRV. The sudden outbreak of infection in the region is thought to be due to high levels of viremia in many of the affected individuals evaluated (191), and RRV transmission throughout the region was likely sustained through a human-mosquito-human transmission cycle.

Annual seasonal outbreaks of RRV-induced disease occur in Australia, most notably in Queensland, resulting in about 5000 reported cases of RRV-associated polyarthritis each year (86). Incidence of infection correlates with the presence of the mosquito vector and most of the infections reported occur in the late summer-early fall. The reservoir hosts for RRV are thought to be marsupials such as wallabies and kangaroos as well as fruit bats (86). RRV has been isolated from about 42 different types of mosquito but is transmitted to humans primarily *Ae. vigilax* and *Ae. camptorhynchus* on the coast, and *Culex annulirostris* in the inland areas (194).

The incubation period for RRV in humans is thought to be about 7 to 9 days following infection by mosquito bite (56). Joint pain and arthritis affecting the ankles, wrist, fingers, and knees are the most common symptom in RRV-induced disease in humans, and patients have also reported pain in the back, neck, and elbows (86). Myalgia is another common symptom reported in patients, and about half of infected patients develop a macropapular rash that can cover the torso and limbs. Many patients develop a fever, and experience fatigue and malaise that can last for several weeks to months. Less common symptoms of RRV-disease include headache, splenomegaly, hematuria, photophobia, and sore throat. The disease symptoms can generally last up to three weeks, with the joint pain and swelling most severe in the first week, and many patients are incapacitated by the debilitating pain and are unable to work during that time. Furthermore, many patients continue to have chronic joint pain and arthritic symptoms for several months after initial infection (86).

Analysis of synovial aspirates from RRV-infected patients revealed the presence of inflammatory cells within affected joints. In particular, monocytes, macrophages and

natural killer (NK) cells were found in the synovial fluid, and the NK cells had equivalent cytotoxic activity as those derived from the periphery (91). Activated macrophages within the synovium were observed (32, 57), and subsequent studies in mouse models of RRV-induced disease demonstrate that the activated macrophages play a critical role in development of clinical disease signs (135). In contrast to other arthritic diseases where disease is driven in part by immune complexes with antigen, the presence of immune complexes was not observed within the synovium of affected joints from RRV-infected patients (57, 58).

Clinical disease and pathology of arthritic alphaviruses: Chikungunya virus.

Chikungunya virus (CHIKV) was first isolated from a patient in Tanganyika, which is present day Tanzania, in the early 1950s (188), however it is very likely that the epidemics of disease had occurred prior to its identification, and were mistakenly attributed to dengue virus (29). The word "chikungunya" means "that which bends up" in the Makonde language, and is thought to describe the debilitating symptoms associated with virus infection (188).

There had been periodic outbreaks of disease between the 1950s and the early 2000s (221), but it wasn't until a large-scale epidemic of disease that lasted from 2004 to 2011 that public health officials and researchers recognized the virus as a significant public health threat. The epidemic began in 2004 in Africa and spread to neighboring countries and islands in the Indian Ocean. Notably, the virus infected two-thirds of the population of the French island La Reunion, and ultimately is estimated to have infected over 6 million people during the epidemic (221). While the majority of transmission

8

events occurred in the areas surrounding the Indian Ocean such as India, Sri Lanka, and many countries in Southeast Asia, the virus was detected in patients in over 40 countries around the world, including the United States and Australia (27). Importantly, sustained local transmission of CHIKV between residents who had not visited affected areas occurred in regions of Italy and France that were previously free of the virus (181), raising fears that the virus may be able to spread to other countries such as United States.

A major factor in the ability of CHIKV to re-emerge in such an explosive manner is thought to be due to the presence of a single mutation in the E1 glycoprotein at position 226 (227). This mutation, a change from an alanine to a valine, allowed for more efficient entry and replication within an additional mosquito species, *Aedes albopictus* (227). Interestingly, a change at this same amino acid in SFV that confers cholesterol independence has been associated with enhanced viral fusion with mosquito cells leading to more efficient replication within the mosquito (4, 230). The *Ae. albopictus* mosquito is an aggressive species that lives in urban areas in close proximity to humans and has a worldwide distribution. Thus, a natural mutation at E1 226 that allows for efficient replication within *Ae. albopictus* has allowed CHIKV to spread rapidly throughout the regions where the mosquito vector was present.

The onset of CHIKV-induced disease can occur immediately following the incubation period that lasts on average 2-4 days. The disease is characterized by polyarthritis along with severe arthralgia and myalgia affecting multiple joints, and is often accompanied by a high fever (19, 27, 188). Other common symptoms include photophobia, headaches, and a rash. The polyarthritis is a prominent feature of the disease and up to 95% of patients develop painful symmetrical swelling in multiple joints

(19). While many of the main symptoms subside about 1-2 weeks following onset, a subset of patients may experience chronic arthralgia for months to years (18). The basis for the chronic arthralgia is has been proposed to be due to viral persistence. Indeed, CHIKV antigen has been detected in muscle biopsies from patients up to 18 months post infection (100), and viral RNA is detectable within joints of mice in a mouse model of CHIKV infection up to 3 weeks post infection (159). Similar to RRV, the pathology of CHIKV is associated with inflammation into the joints and muscle. Monocytes, macrophages, $CD4^+$ T cells, and high levels of NK cells are found within synovial aspirates from CHIKV patients (100), and elevated levels of pro-inflammatory cytokines such as IL-1β and IL-6 have been associated with severity of clinical disease (166).

In general, the current therapies for CHIKV and RRV-induced disease as well as other arthritic alphavirus diseases are merely palliative. Most patients are simply administered nonsteroidal anti-inflammatory drugs (NSAIDs), analgesics, and aspirin and are advised to rest and engage in physical therapy (86, 221). Given the potential long-term treatment due to the prolonged nature of the disease, long-term use of NSAIDs is not ideal, and development of alternative therapeutics is needed.

1.2. Molecular biology of alphaviruses.

Genome organization and structure of alphaviruses.

The genome of alphaviruses is encoded on a capped, positive sense RNA that is about 11.5kb in length with a poly adenylated tail and can be translated similar to host mRNA (219). The four nonstructural proteins (nsP1, nsP2, nsP3, and nsP4) are encoded

at the 5' end of the genome, and once translated, make up the replicase complex that allows for both positive and minus strand genome synthesis. The structural proteins (capsid, E3, E2, 6K, and E1) that compose the virion particle are encoded on a subgenomic mRNA that is transcribed and translated from the minus strand genomic template. The alphavirus genome also has a 5' UTR and a 3' UTR that contain virulence determinants and are required for efficient genome replication and translation (59, 84, 245).

The structure of the alphavirus virion has been determined through cryo-electron microscopy (EM) and X-ray reconstructions of SFV, SINV, and CHIKV (87, 88, 133, 162, 174, 234-236). The virion is approximately 70nm in diameter, and is composed of a nucleocapsid core that contains a single copy of genomic RNA, and an outer layer that is comprised of a lipid bi-layer derived from the host membrane and an exterior glycoprotein shell. The glycoprotein shell on each virion has 240 copies of E1 and E2 that are organized into of 80 trimeric E1-E2 heterodimers, with E1 lying parallel to the lipid bi-layer and E2 protruding to the surface to form spikes. The E2 glycoprotein is thought to mediate receptor interaction on the surface of host cells and the E1 glycoprotein mediates fusion of the virus to the host cell (113).

Overview of the lifecycle of alphaviruses.

The lifecycle of alphaviruses are outlined in Figure 1.1 and is described in detail in subsequent sections. Briefly, alphaviruses enter host cells through receptor-mediated endocytosis, and release the viral RNA genome into the cytoplasm following fusion of the virus membranes with host membranes in the endosome. Since the alphavirus genome

is a positive sense, capped RNA, it can be immediately translated by host translational machinery. The nonstructural polyprotein forms the viral replicase complex, which mediates minus-strand RNA synthesis. From the minus-strand template, additional copies of positive strand RNA are generated and either translated or packaged into virions. Synthesis of the viral structural proteins from the subgenomic RNA leads to synthesis of the capsid protein, which will go on to form the nucleocapsid, and the viral glycoproteins are translocated into the ER and then the Golgi, where they undergo post-translational modification including glycosylation. The glycoproteins are cleaved in the Golgi, and are transported to the plasma membrane. Interactions between the viral glycoproteins and the nucleocapsid drive viral budding and egress from the host cell plasma membrane to the extracellular milieu.

Entry of alphaviruses into host cells.

Entry of alphaviruses into host cells is thought to primarily occur through receptor-mediated endocytosis through engagement of the alphavirus protein E2 on the virion with receptors and attachment factors, although direct fusion of virus with host membranes has been proposed (49). While several putative receptors have been identified for some alphaviruses, there does not appear to be any one single receptor that mediates entry for all alphaviruses. Rather, since alphaviruses can infect a broad range of hosts and cell types, the prevailing trend is that alphaviruses can use a diverse set of receptors that vary according to cell type and host.

A ubiquitously expressed membrane laminin receptor was first identified as a putative SINV mammalian receptor into BHK-21 cells, and for VEEV into mosquito

cells (140, 238). However, the laminin receptor does not appear to mediate entry into all types of host cells, such as the chick embryo fibroblasts (238), suggesting either that alphaviruses can use multiple receptors or that laminin acts more as an attachment receptor rather than a true receptor. Additional host factors have been identified as attachment factors that aid entry into particular cell types. Klimstra *et al.* showed that certain members of innate immune receptors called C-type lectins (CLRs) such as DC-SIGN and L-SIGN, mediate entry of mosquito-derived SINV into dendritic cells (120). The type IV α1β1 collagen receptor has been proposed to be a putative receptor for RRV (128), as RRV bound specifically to α1β1-coated ELISA plates. However, RRV entry into α1-knockout MEFs was not completely abolished, and further supports the overall hypothesis that alphavirus can use multiple receptors and attachment factors to gain entry into cells. More recently, the ubiquitously expressed divalent metal ion transporter NRAMP was identified as a receptor for SINV into both insect (dNRAMP) and mammalian cells (NRAMP2) through an RNAi screen in *Drosophila* cells (190). Interestingly, the usage of NRAMP2 was specific to SINV as RRV entry into mammalian cells was not dependent on NRAMP2. Thus, the alphavirus receptor is still elusive.

Of note, heparan sulfate (HS) is also thought to be an attachment receptor for alphaviruses, and mutations that confer binding to HS modulate virulence in some alphaviruses (67, 195). Passage of alphaviruses in cell culture have led to rapid acquisition of mutations in E2 that can introduce basic amino acid residues and alter the charge of the glycoprotein, leading to an increase in positive charge within E2 and higher efficiency and tighter binding to HS molecules on the cell surface (121).

Receptor engagement induces a conformational change in E1 and E2 that allow for internalization into the host cell through clathrin-mediated endocytosis (43). Subsequent acidification of the endosome destabilizes the E2 and E1 heterodimer and exposes the fusion peptide on the distal end of E1 (3, 130). The fusion peptide inserts into the host cell membrane and leads to E1 trimerization and subsequent formation of the fusion pore by bringing the viral membrane and host membranes together (reviewed in (125)). The nucleocapsid is released into the cytoplasm, where it disassociates and releases the viral RNA. Since alphavirus genomic RNA is a capped positive strand RNA, it can be translated directly by the host translation machinery. The nonstructural proteins are synthesized as a single polyprotein either as nsP123 or nsP1234. The production of nsP1234 is a result of read-through of the opal stop codon at the end of nsP3 that occurs about 10-20% of the time (219). Many alphaviruses including SINV, RRV, VEEV, EEEV, and WEEV contain the opal codon (219). The polyprotein P123 and the viral RNA dependent RNA polymerase, nsP4, acts as a replication complex to initiate minus strand synthesis of the viral RNA. The polyprotein is then cleaved into mature nsP1, nsP2, and nsP3, and these proteins, along with nsP4 can act to generate many copies of the positive strand viral RNA for packaging and further replication (125).

Roles of the alphavirus nonstructural proteins.

While the formal roles of most of the alphavirus nonstructural proteins (nsPs) are involved in some aspect of genome replication, nearly all of nsPs are likely to be involved modification of the host response in one way or another to modulate infection and viral pathogenesis.

The alphavirus nsP1 has multiple functions in viral replication. First, it mediates association of the viral replicase complex with cell membranes through palmitoylation groups on the protein (171). Furthermore, nsP1 acts as a methyltransferase and guanylyltransferase to cap the viral genomic and subgenomic RNAs (152, 153). Eukaryotic mRNAs contain a 5' cap structure, which is a guanine nucleotide that has been methylated at the 7-position (m^7G). The 5' cap has multiple functions in mRNA stability and export from the nucleus, as well as promoting translation of the mRNA transcript. In order to be efficiently translated from host cells, most viruses also have a mechanism to cap their mRNA. Furthermore, cytoplasmic RNA innate immune sensors, such as RIG-I, recognize RNA motifs like 5' triphosphates that are hidden from detection by the 5' cap structure (139). Thus, the capping capacity of nsP1 acts to ensure efficient translation of the viral RNAs and serves to evade detection by cytoplasmic RNA sensors. Indeed, mutations that affect the capping ability of nsP1 in SINV and RRV induce more type I IFN compared to a wild-type virus in a RIG-I/MDA5 dependent manner (38).

The nsP2 protein is the largest of the alphavirus nonstructural proteins and also has multiple functions. The N-terminus of the protein is an RNA helicase that unwinds RNA, an NTPase, and a 5' triphophatase, and the C-terminus of the protein is papain-like protease that cleaves the viral nonstructural polyprotein (45, 73, 85, 184, 218, 231). In old world alphaviruses, nsP2 is thought to mediate host translational shutoff as a mechanism to prevent activation of the type I IFN system (69, 70).

The function of the alphavirus nsP3 protein has been elusive for a number of years. It has an essential role in viral RNA synthesis, and the N-terminus is pretty well conserved throughout the different alphaviruses, however, the C-terminus is

hypervariable and heavily phosphorylated (125). A recent study identified a putative role for the conserved SH3 domain within the C-terminus of nsP3 and appears to interact with amphiphysins and may act to regulate endocytosis and membrane trafficking (165). However, the overall role of the protein remains unknown.

Finally, the nsP4 protein is the RNA dependent RNA polymerase, and is the critical for replication. The nsP4 protein may interact with other nsPs through the N-terminus domain, but the functional consequences of these interactions are currently unknown (125, 213).

Synthesis of the alphavirus glycoproteins and viral budding.

The structural proteins are encoded on the subgenomic 26S mRNA, which is produced at roughly three times the amount of genomic 49S RNA (178). The capsid protein is translated first and immediately is cleaved from the polyprotein as it leaves the ribosome by the autoprotease activity that resides in the C-terminus (5, 81). Translation of the pE2 polyprotein follows capsid protein and contains E3 and E2. The cleavage of capsid protein from pE2 allows for the N-terminus of pE2 to translocate across the ER membrane, and signal sequences within E2 and 6K allow for 6K and E1, respectively, translocation across the membrane (125). Once in the ER lumen, pE2 and E1 undergo post-translational modifications. N-linked glycans are added to possible N-linked glycosylation sites on pE2 and E1 (discussed in more detail in following sections)(207), and palmitoylation occurs on pE2, E1, 6K (17). Maturation of the glycoproteins occurs in the Golgi where furin cleaves pE2 to generate E3 and E2 (40). Release of E2 from pE2 allows for E2 and E1 to form heterodimers and further N-linked oligosaccharide

processing occurs. E2 and E1 and then transported through the Golgi together as heterodimers, and finally to the plasma membrane by cytoplasmic vesicles (182, 258). Once at the plasma membrane, the mature E2-E1 heterodimers trimerize to form the glycoprotein spikes and subsequent interaction with the nucleocapsid to inititiate viral budding and egress from the host cell (125, 234, 235) The alphavirus glycoprotein spike is composed of three E1-E2 heterodimers and is easily visualized on the virion surface by cryo-EM.

Immediately following cleavage from pE2, the capsid protein begins to form the nucleocapsid. Capsid dimers form around the viral RNA and the protein interacts with the RNA through packaging signals in the viral RNA located within nsP1(244). To initiate budding, the nucleocapsid cores assemble and cluster at the plasma membrane. The mature glycoprotein E2-E1 trimer spikes are present on the surface of the plasma membrane and the interaction between the cytoplasmic tail of E2 and a hydrophobic pocket on capsid promotes formation of the virion and drives viral egress.

1.3. Alphavirus-induced disease.

Alphavirus pathogenesis models.

The diseases associated with alphavirus infections generally fall into two categories: encephalitic and arthritic. New World alphaviruses are more commonly associated with encephalitis and Old World alphaviruses with arthritis. Details of alphavirus pathogenesis have been elucidated primarily through the use of mouse models. Natural virus isolates associated with clinical disease have been identified through isolation either from infected patients or from mosquitoes located around sites of disease

outbreaks (78). Many of these isolates have been passaged through suckling mice to produce virus capable of efficient replication within the mouse. While both inbred and outbred strains of mice have been used to model alphavirus pathogenesis, the C57BL/6 line of inbred mouse is susceptible to alphavirus infection, and has been used extensively in many labs. Virus injected subcutaneously into the rear footpad is thought to first come into contact with Langerhans cells and dermal fibroblasts that are resident in the skin (141). Since infection of humans occurs by a mosquito bite, it is likely that some of the first cells that are infected are dendritic cells, and several host factors such as DC-SIGN and L-SIGN, as well as other unknown factors are thought to facilitate this interaction (120, 209). The virus replicates locally within the synovial fibroblasts in the ankle and is likely spread to the popliteal draining lymph node by infected dendritic cells (141). Once in the draining lymph node, the virus seeds a serum viremia and is able to spread throughout the host, infecting the various target tissues that are specific for the different groups of viruses. Virus is cleared through several mechanisms involving both innate and adaptive arms of the immune system. Activation of the type I interferon (IFN) system is critical in early control of virus replication for most alphaviruses (197, 202, 245, 248), and there is evidence for T cells as well and B cells and antibody in clearance of virus within tissues (22, 131).

Encephalitic alphaviruses.

The pathogenesis of encephalitic alphaviruses such as VEEV, WEEV, EEEV have been studied using a combination of young and adult mouse models, and recapitulate many neurologic disease symptoms that are observed in human disease (39).

18

While SINV infection in humans leads to arthralgia, SINV infection in mice causes an encephalitic disease that has been used to model acute encephalomyelitis, and studies from both SINV and VEEV have gained some insight into the mechanisms of disease following infection with neurovirulent viruses. Infection of adult mice with wild-type strains of VEEV and some strains of SINV causes a lethal neurologic disease (39, 93). Virus is thought to enter into the brain from the periphery through transient opening of the blood-brain barrier (BBB) (201). The opening of the BBB allows for viral infection of neurons and other cell types within the brain, leading to activation of pro-inflammatory cytokine response, and subsequent infiltration of inflammatory cells into the brain and CNS, leading to development of neurologic disease and eventually, death (203, 204).

Arthritic alphavirus pathogenesis: Ross River virus.

There have been several mouse models used to study arthritic alphavirus pathogenesis. Early studies of RRV pathogenesis used a young mouse model ranging from newborn mice to mice 10 days old where mice succumbed to viral infection (155). Non-lethal models of disease using older mice have been developed, and the most recent mouse model established to study RRV-induced disease was described by Morrison *et al*. (161), and is the mouse model used throughout this dissertation. Twenty-four day old C57BL/6 mice are subcutaneously infected with 1000 plaque forming units (PFU) of RRV T48 (RR64) in the left rear footpad, and go on to develop disease that is characterized primarily by hind-limb dysfunction.

The initial events following RRV infection are similar other alphaviruses outlined above. While virus can be detected in the liver, spleen, brain, heart, and spinal cord, RRV

replicates to the highest titers in the skeletal muscle and ankle joints (161). Peak viral titer within these tissues occurs at 24-48 hours post infection, and steadily declines throughout the course of disease, and is virtually undetectable by plaque assay by 10 days post infection (dpi) (161). While peak viral titer occurs within the first 2 days of infection, infected mice do not start to exhibit clinical disease signs until about 5 dpi (161). Mice begin to show signs of hind limb weakness and altered gait at 5 dpi as determined by a grip test (161). By 7 dpi, infected mice begin to lose the ability to grip with their hind limbs and a subset of mice display the inability to right. Peak disease severity occurs from 10-12 dpi where most infected mice are dragging their hind limbs and are unable to right themselves. However, by about 14 dpi mice are beginning to recover and regain use of their hind limbs, and then by 21 dpi the infected mice have recovered and are indistinguishable from uninfected mice (161).

Histopathological analyses of the target tissues within infected mice have shown that the disease signs observed in the mice correlate with the induction of the host inflammatory response rather than viral titer (135, 161). Inflammatory immune cells such as macrophages, monocytes, neutrophils, and eosinophils along with $CD8^+$ and $CD4^+$ T cells, B cells and NK cells begin to infiltrate into the tissues starting at about 5 dpi and reach peak inflammation by 10 dpi. The infiltration of these cells into tissues is thought to mediate tissue damage, and in particular the inflammatory macrophages have a critical role in damage within the skeletal muscle. Injection of macrophage-cytotoxic agents such as silica, carrageenan, and liposome-covered clodronate dramatically reduced disease symptoms in RRV-infected mice (134, 135). Furthermore, macrophage-derived inflammatory cytokines and products have been implicated in RRV-pathogenesis.

Monocyte chemotactic protein (MCP-1; CCL2) is involved in macrophage recruitment and chemotaxis of other immune cells, and inhibition of MCP-1 by administration of bindarit into mice abrogated RRV-induced disease by significantly reducing the numbers of CD11b$^+$ cells recruited into the skeletal muscle (193). Another cytokine, macrophage migration inhibitory factor (MIF), which acts as a powerful pro-inflammatory cytokine that regulates multiple aspects of the host inflammatory response (28), has an important role in regulating the infiltration of immune cells into target tissues following RRV infection (94). MIF$^{-/-}$ mice show reduced disease and tissue damage following RRV infection compared to WT mice, and correlated with a reduction in inflammation in the skeletal muscle rather than altering viral titer (94). Finally, arginase I, which is produced by alternatively activated macrophages and neutrophils, thwarts clearance of RRV from skeletal muscle and ankle joints, and allows for sustained replication and disease at later time points (216).

All of these studies indicate a critical role for the host inflammatory response in mediating RRV-induced disease. However, there are gaps in our understanding regarding the underlying mechanisms of how the inflammatory response is initiated and/or regulated following RRV infection. Furthermore, the specific RRV ligands that activate the inflammatory response have not been identified, thus many aspects of RRV pathogenesis remain unknown and understudied.

Arthritic alphavirus pathogenesis: chikungunya virus.

Development of appropriate CHIKV mouse models have been hampered somewhat by the lack of a mouse adapted CHIKV that spreads systemically from the site

of infection to replicate in distal tissues. However, several models using two different human isolates from the most recent CHIKV epidemic have been described. A young mouse model where 14 day old C57BL/6 mice and infected with a CHIKV isolate from Sri Lanka exhibits swelling, arthritis, tenosynovitis, and myositis in the injected foot, and shares many pathologic characteristics with the human CHIKV disease (159). Similar to RRV, CHIKV infection results in inflammation within the joints and skeletal muscle, although swelling of the joints occurs following CHIKV infection but is absent during the mouse model of RRV-induced disease. Pronounced swelling of the ankles occurs at 2-3 dpi and 6-7 dpi in the CHIKV mouse model. Analysis of the inflammatory cells infiltrating into the leg reveals that NK cells and neutrophils are the predominant infiltrating cell types at 5 dpi, although a heterogenous mix of NK cells, neutrophils, monocytes/macrophages and $CD8^+/CD4^+$ T cells were observed at 7 dpi (159). An older mouse model, where both feet of mice are injected with a CHIKV isolate from La Reunion Island, demonstrate similar disease characteristics as the young mouse model, albeit less pronounced, but may be more amenable to vaccination and therapeutic studies (68). Studies using a neonatal mouse model demonstrated the importance of type I IFN in protection from lethal CHIKV infection (202), further highlighting the critical role of the innate immune system in protection from alphavirus infection.

1.4. The host complement system.

The innate immune system is generally considered to be the first line of defense against invading pathogens and is critical in host protection. The host complement system is a branch of innate immunity that has many diverse functions including pathogen

22

recognition, signaling, initiation of inflammation, and direct pathogen lysis. The complement system is truly a "system" as there are well over thirty extracellular and cell-associated proteins that help orchestrate the immune response to a given pathogen. A general schematic of the complement system is shown in Figure 1.2.

Activation of complement is thought to occur through three main pathways: classical, lectin, and alternative pathways. Regardless of which pathway activates complement, the critical step in complement activation is cleavage of the C3 protein, which is central to the complement system (reviewed in (183)). Cleavage of C3 requires formation of the C3 convertases that are generated on target pathogens or cells following activation through either the classical or the lectin pathway. Cleavage of C3 results first in the generation of C3a and C3b, and C3b becomes covalently attached to the target surface through recognition of the reactive thioester group that is exposed upon cleavage on C3b and carbohydrate groups on the target surface. Interestingly, the specificity of the C3 thioester group for carbohydrates, and in particular terminal sugars on polysaccharides may have biological relevance since glycosylation on pathogens and stressed/infected cells can be different than healthy uninfected cells, and could be an additional safety guard to protect host cells from excessive complement activation (199). C3a is released and acts as a chemoattractant and anaphylatoxin to aid in activation of other arms of the immune response.

The C3b deposition on the target cell leads to formation of additional C3 convertases allowing for rapid accumulation of C3b on the surface of the cell. Eventually, the C5 convertase is formed (C4b2b3b) to cleave C5 into C5a and C5b. C5b can then interact with C6 and C7 to begin the membrane attack complex. The C5bC6C7 complex

inserts into the target membrane, allowing for C8 and then C9 to become part of the complex and generates a lytic pore called the membrane attack complex (MAC) that lyses the target cell. C5a is an additional anaphylatoxin that is released upon cleavage and acts on neutrophils and monocytes to induce rapid phagocytosis of opsonized targets.

In addition to the first C3 cleavage event that generates C3a and C3b, C3b is further cleaved by factor I in complex with CR1 that inactivates C3b, but generates iC3b and C3c, C3dg and eventually C3f and C3d, which all have biological functions in complement to aid in pathogen clearance (183). Perhaps the most effective cleavage product is iC3b. The iC3b cleavage product acts to opsonize the target cell and interacts with several complement receptors on phagocytic cells to promote phagocytosis and leukocyte signaling (183, 233, 251). Interactions with complement receptors such as CR3 and CR4 lead to enhanced phagocytosis of iC3b-opsonized cells and can trigger signaling downstream from both of the receptors (50, 183). CR3-mediated signaling within phagocytic cells, such as monocytes/macrophages and neutrophils, can act to initiate and enhance cytotoxic effector functions of the cells (173, 232).

The role of complement in alphavirus pathogenesis.

The role of the complement system in alphavirus infection is either protective or pathologic role depending on the virus. Complement has a protective role in mouse models of SINV and VEEV infections, but is pathologic in RRV infection (23, 97, 99, 158).

The role of complement following SINV infection is generally thought to be protective. Mice depleted for complement by cobra venom factor administration, which

24

consumes and depletes C3, had elevated levels of SINV in serum and in the brains compared to untreated infected controls (97, 98). Interestingly, inflammation in the brains of the complement depleted mice was increased compared to controls, and correlated with prolonged disease signs, suggesting that complement may also regulate inflammation (97). Analysis of the mechanisms of viral control by complement revealed that both the classical and alternative pathways were activated upon SINV infection even in the absence of virus-specific antibodies (99). Furthermore, mice genetically deficient in C5 displayed enhanced susceptibility to SINV infection, suggesting that formation of the MAC by complement is very important for control of serum viremia and infection within the tissues (96). Interestingly, despite the increase in viral titer with the CNS and serum, the C3 depleted mice did not show any enhanced mortality and actually had prolonged survival compared to undepleted mice (97), suggesting that there may be some pathology associated with presence of C3. The role of the lectin pathway has not been evaluated in the context of SINV infection.

In the context of VEEV infection, the complement system plays a role in host protection (23). Using a non-lethal model of VEEV infection where mice are infected with an attenuated strain of VEEV, V3533, Brooke *et al*. demonstrated that C3$^{-/-}$ mice are more susceptible to V3533 compared to WT mice (23). C3$^{-/-}$ mice displayed enhanced weight loss, and morbidity compared to WT mice in response to VEEV infection, and increased disease correlated with elevated levels of virus in the CNS and the periphery and increased inflammation with the brain. Furthermore, the role of complement in limiting viral replication and disease appeared to be most important in preventing spread of virus into the CNS from the periphery as C3$^{-/-}$ and WT mice inoculated with VEEV

25

directly into the brain showed no difference in mortality. Furthermore, $C5^{-/-}$ mice displayed wild-type kinetics and severity of disease, indicating that formation of the MAC was not required for limiting viral spread by complement. Instead, it is likely that other effector mechanisms involving C3 cleavage products have a key role in protection from VEEV infection.

The pathology and disease associated with RRV infection in humans and mice is primarily mediated by the host inflammatory response. Studies by Morrison *et al.* demonstrated that the complement system is activated following RRV infection (158). RRV-infected mice exhibited elevated levels of circulating C3 in the serum compared to mock-infected mice, and also had increased amounts of C3 cleavage products in the quadriceps muscle and ankle joints (158). In addition, human patients with RRV-induced polyarthritis had elevated levels of C3a, indicative of complement activation, within the synovial fluid compared to patients with the non-inflammatory arthritis disease osteoarthritis. Furthermore, the authors demonstrated that complement activation has a critical role in mediating damage and disease within target tissues. Mice deficient in C3, which is the central component of the complement system, developed a mild disease compared to wild-type mice. Interestingly, viral burden and localization of viral replication within the tissues was not affected by the presence or absence of C3, suggesting that complement regulated some aspect of inflammation. However, histopathologic analysis of both quadriceps muscle and ankle joints indicated the presence of inflammatory cells within the tissues, and flow cytometric quantification and characterization of the inflammatory cells within the muscle showed that complement did not affect the numbers or types of infiltrating inflammatory cells. Furthermore, disease in

C5-deficient mice did not differ significantly from WT mice, indicating that formation of MAC is not required for disease (Morrison TE and Heise MT, unpublished data).

Follow-up studies evaluating the role of other complement proteins in mediating RRV-induced disease demonstrated that complement receptor 3 (CR3, CD11b/CD18, Mac-1, amb2) contributes to disease (160). CR3 is present on multiple types of immune cells, including monocytes, macrophages, neutrophils, DCs, and T cells, and interacts with the C3 cleavage factor iC3b (259). Mice deficient in CR3/CD11b exhibited reduced RRV-induced disease compared to WT mice, and many aspects of the disease in CR3/CD11b$^{-/-}$ were similar to the disease observed in C3$^{-/-}$ mice. Viral burden and the amount of inflammatory cells within the tissues were equivalent between CR3/CD11b$^{-/-}$ and WT mice, while disease and tissue damage were reduced in CD11b$^{-/-}$ mice.

Ligation of CR3 by iC3b can induce signaling within CR3-bearing cells in a Syk-PI3K mediated pathway and can serve to activate pro-inflammatory effector programs within the cells (50, 132, 157). Interestingly, expression of a subset of pro-inflammatory genes was dependent on both CR3 and C3 following RRV infection (160). The calgranulin proteins S100A8 and S100A9 are secreted as heterodimers from activated leukocytes, and have been implicated in the pathogenesis of inflammatory arthritis (172). Both of these genes are highly expressed in the inflamed quadriceps muscle following RRV infection, and their expression is dependent upon both CR3 and C3 (160). While further investigation is needed to determine if there is a role for these proteins during RRV infection, their complement-dependent expression suggests that the role that complement may have in RRV pathogenesis is at the level of activation of pro-inflammatory effector programs in CR3-bearing cells.

Taken together, these data indicate the complement system can play both a protective and a pathologic role following alphavirus infection. In SINV and VEEV infection, complement appears to be required to neutralize the viruses and help clear virus from the serum, thus limiting spread of the virus into additional tissues. In contrast, following RRV infection, the complement system does not neutralize the virus, but rather contributes to development of disease through activation of CR3-bearing inflammatory cells resulting in the inflammatory tissue destruction and disease. It is not currently clear why complement is protective in certain alphavirus infection but pathologic in another, but further exploration into the mechanisms of complement activation and identification of viral ligands may provide some insight into these processes.

Complement activation pathways.

There are three main activation pathways of complement: the classical, lectin, and alternative pathways. The classical and lectin pathways converge as activation through either pathway leads to the formation of the C3 convertase C4b2b. The classical activation pathway had initially been thought to activate complement only through recognition of IgM and IgG in antibody-antigen immune complexes by the initiator molecule C1q, but recent work has demonstrated that C1q can bind to a number of self and non-self ligands in addition to immunoglobulins (64, 123). Surface binding of C1q to a ligand results in activation of C1r and C1s proteases, and C1s cleaves C4 and C2 to generate the C3 convertase C4b2b (183); the classical pathway and lectin pathways are indistinguishable at this point. The alternative pathway is initiated through binding of factor B (fB) protease to spontaneously hydrolyzed C3 ($C3_{H2O}$). Subsequent cleavage of

C3 within the fB-C3 complex by Factor D generates the alternative C3 convertase, C3bBb, which cleaves C3 and activates the complement cascade.

The lectin activation pathway of complement.

The lectin activation pathway of complement is mediated through the serum proteins mannose binding lectin (MBL) and ficolins (L-, M-, and H-ficolin) that act as pattern recognition receptors (PRRs). Both MBL and the ficolins contain a collagen-like domain in the N-terminus that mediates oligomerization of the structural subunits to form higher order structures required for functional complement activation. MBL has a carbohydrate recognition domain (CRD) in the C-terminus, whereas ficolins have a fibrinogen-like domain that acts in a similar manner to the CRD of MBL (63). The ever-expanding list of MBL ligands will be discussed in further detail in following sections, and the ficolins have been shown to bind to terminal N-acetylglucosamine (GlcNAc) on glycosylated proteins on bacteria as well as apoptotic cells (124, 147, 255). MBL, L-ficolin, and H-ficolin are produced in the liver and circulate within the serum, where as M-ficolin is produced by monocytes and granulocytes (63).

The MBL-associated serine proteases (MASPs) circulate throughout the body in association with the ficolins and MBL. There are three MASP proteins (MASP-1, -2, -3), however, only MASP-2 has been shown to be able to form the C3 convertase C4b2b to activate the complement cascade (192, 226). Interestingly, MASP-1 and MASP-3 have been shown to mediate cleavage of Factor D, which is required for activation of complement through the alternative pathway (9). Once the PRRs have been engaged through the CRD, a conformational change occurs, and allows for the serine proteases to

be able to cleave C4 and C2 to generate the C3 convertase C4b2b, cleavage of C3 and complement activation.

Of note, collectin-11 (CL-11) was recently identified as an additional serum protein that circulates in association with MASP-1 and/or MASP-3 (83). CL-11 bound to several microbial and fungal species including *Escherichia coli*, *Pseudomonas aeruginosa*, and *Candida albicans*. Furthermore, CL-11 bound to influenza A virus and was able to partially inhibit the entry of virus into cells at high concentrations. The ability of CL-11 to activate complement has not yet been demonstrated, but given the microbial substrates, association with MASP-1 and/or MASP-3, and levels circulating in serum, it is likely that CL-11 will join the complement system as a PRR.

Mannose binding lectin (MBL): structure and ligands.

MBL was identified as a serum protein that could recognize and bind to carbohydrate structures (187), and was subsequently found to be able to activate the complement system (105). MBL is produced in primarily in the liver of several vertebrates, and has been associated with complement activation in most organisms (48, 156). There are two human MBL genes, *Mbl1* and *Mbl2*, but only *Mbl2* encodes the functional MBL protein that activates the complement system. Mice and rats have two isoforms of MBL, termed MBL-A and MBL-C, and both appear to be capable of activating the complement system, although they have different circulating levels in resting animals (138). MBL is an acute phase protein, meaning that the expression and production of MBL is elevated following infection or stress (53), and further highlights the important role of MBL in host defense.

The *Mbl2* gene on chromosome 10 encodes the human MBL protein, and the functional protein is composed of multimers of the 32 kDa MBL polypeptide. Each polypeptide has a calcium-dependent carbohydrate recognition domain (CRD) at the C-terminus, and a collagenous region that forms into a triple helix with other two polypeptides to make up one structural subunit of MBL. Each structural subunit maintains a fixed 45Å distance between the three CRDs which allows for binding to the carbohydrate ligands (211). While each subunit can bind to the carbohydrate ligands, the affinity is relatively low, the oligomerized multimers of MBL are able to bind to larger arrays of carbohydrates thus increasing the affinity of binding and allows for activation of complement (106). The importance of 45Å spacing of the CRDs is to allow for specific binding to certain sugars, namely the hydroxyl groups in the hexose structure in N-acetylglucosamine, mannose, glucose, and fucose (102). These sugars are commonly the terminal carbohydrate residue on microbial glycoproteins and not commonly found on mammalian glycoproteins, which favor terminal galactose and sialic acid. The CRDs of MBL do not bind to the hexose structure in galactose or sialic acid therefore preventing binding and activation of complement, which further adds to the specificity of recognition (243).

MBL was originally thought to recognize terminal sugars present on microbial glycosylated proteins, but more recently, several studies have shown that MBL can also bind to sugars on self-antigens such as DNA, RNA, phospholipids, and other altered self-proteins to help mediate phagocytic clearance of apoptotic or necrotic cells (119, 167, 168, 220). The presentation of certain self-antigens, such as DNA and RNA, to MBL present in circulation may be an additional mechanism that is used to alert the innate

immune system to stress and possible infection. MBL is thought to bind to the pentose

sugars present on free DNA and RNA from either apoptotic or necrotic cells to help

facilitate phagocytic clearance (168). Similarly, binding of MBL N-acetylglucosamine on

phospholipids may also serve to enhance recognition and clearance of apoptotic cells

(119, 126). Thus, MBL has an important role in recognition of pathogens as well as

damaged host cells that allows for activation of complement and the innate immune

system.

MBL polymorphisms.

The levels of circulating MBL in healthy human adults varies substantially

between individuals and across the population due to several polymorphisms and

mutations that affect the structure and expression of MBL (reviewed in (47)). The human

MBL2 gene is encoded on chromosome 10 and is composed of four exons: exon 1 and 2

encode the collagenous region of the MBL protein required for oligmerization, exon 3

encodes the neck region, and exon 4 encodes the carbohydrate recognition domain. There

are several mutations that lie within exon 1 (R52C, G54D, and G57E) that all lead to a

functional deficiency of MBL (137, 143, 222). The mutation at codons 52 (D variant)

affects the oligomerization of MBL and prevents formation of the higher order structures

that are required for complement activation through MBL. The mutations at codons 54 (B

variant) and 57 (C variant) lead to distortion of the collagenous helix and prevent high

affinity binding to carbohydrate arrays by MBL. There are also several polymorphisms

that alter the level of expression of MBL. The polymorphisms are located in the promoter

of the gene at -550, -221, and +4 (144, 145). Together with the structural mutations, the

promoter polymorphisms lead to extreme variation within the human populations and serum levels of MBL range from nearly undetectable to 10 µg/ml (47).

The importance of MBL in mediating host protection from a number of bacterial and viral pathogens has been demonstrated by several studies that have evaluated the susceptibility of patients who are functionally deficient in MBL to certain pathogens. Sumiya *et al* found that children with recurrent bacterial infections had genetically lower levels of MBL compared to healthy children (222), and several studies have shown enhanced susceptibility to certain viral infections including heptatitis B virus and HIV (25, 52).

Role of MBL in sterile inflammatory diseases.

Since MBL can bind to both self-antigens such as DNA and phospholipids as well as the glycosylated proteins of pathogens, it is not surprising that MBL, like complement, can be a double edged sword: required for protection from a number of different pathogens, but can also lead to autoimmunity. Indeed, MBL has been associated with pathology in sterile inflammatory diseases such as ischemic reperfusion injury (IRI), and has been implicated in rheumatoid arthritis (RA).

Ischemic reperfusion injury occurs after blood flow is restored to tissues and organs after a period of deprivation. The pathology of disease is characterized by induction of a pro-inflammatory state within the affected tissue and subsequent inflammation that leads to eventual apoptosis, necrosis, and possible permanent tissue damage (76). The complement system has long been known to be involved in development of myocardial IRI through chemotaxis of leukocytes into the tissue (76, 95),

33

and more recently, the lectin pathway has been shown to have a critical role in mediating complement activation following reperfusion (reviewed in (76)). Early in vitro studies demonstrated that the oxidative stress induced by IRI on endothelial cells initiated MBL and subsequent C3 deposition, likely through altered glycosylation of host proteins on the cells (34, 35). Subsequent studies in myocardial, gastrointestinal, and renal reperfusion injury animal models using either antibodies to deplete MBL, or MBL-A^{-/-} MBL-C^{-/-} (MBL-DKO) and MASP-2^{-/-} mice further demonstrated that MBL and the lectin pathway regulated complement activation and subsequent inflammation and damage within the reperfused tissues (112, 205, 237).

Rheumatoid arthritis is an autoimmune disease that is characterized by chronic inflammation within the joints of affected individuals. Autoantibodies are thought to contribute to disease in part through activation of the complement system, but several studies have evaluated the lectin pathway in disease susceptibility and severity in cohorts of RA patients. However, the results from these studies are conflicting as different studies found a correlation of low MBL levels in RA patients with both protection and pathology (80, 109, 110, 198, 228). Thus, the role of MBL in inflammatory arthritis has not been established and remains unclear.

Role of MBL in viral infection: Flaviviruses.

Flaviviruses such as West Nile virus (WNV) and dengue virus (DENV) are mosquito-borne viruses that are a significant cause of disease in humans. The innate immune response is critical for host protection from these viruses, and the complement system has been demonstrated to play an important role in protection (reviewed in (8)).

Mice deficient in C3 are highly susceptible to WNV infection due to a defect in the development of a robust adaptive immune response. Neutralizing antibody responses as well as $CD8^+$ T cell responses were reduced in $C3^{-/-}$ mice, leading to higher viral titers within the CNS of infected mice (149, 150). MBL deficient mice were also more susceptible to WNV infection, and MBL deficient serum showed reduced neutralization of insect derived virus (61, 62).

MBL has also been reported to bind to and neutralize DENV, even in the absence of complement activation (61), and levels of MBL within human serum directly correlated with neutralization of both mosquito and mammalian-derived DENV2 (7), suggesting that MBL has a protective role in DENV infection. However, several studies analyzing the role of MBL in determining disease severity in DENV-infected patients have yielded conflicting results. One study was unable to correlate low levels of MBL with patient progression from dengue fever (DF) to the more severe disease dengue hemorrhagic fever (DHF), yet other studies found that high levels of MBL were associated with DHF, and low levels of MBL protected DHF patients from thrombocytopenia (2, 33, 164). From these studies, it is currently unclear the role of MBL in determining DENV severity, although experimental evidence suggests that MBL contributes to neutralization of DENV and is thus likely to have a protective role following DENV infection.

Role of MBL in viral infection: other viruses.

MBL is thought to contribute to protection from infection by the human immunodeficiency virus (HIV). The HIV gp120 glycoprotein is heavily glycosylated

with N-linked glycans, and several groups have demonstrated that MBL can bind to both lab strains as well as primary isolates of HIV (54, 200). MBL binding to HIV is reported to be important in direct neutralization of the virus by preventing binding to host cells, although studies differ on the extent of neutralization (54, 254).

MBL has also been shown to contribute to host protection of several other viral infections such as herpes simplex virus-2 (HSV-2), Ebola virus, and SARS-coronavirus (65, 107, 111, 257). MBL was found to bind to HSV-2 virions in an ELISA assay, and MBL-DKO mice exhibited enhanced viral titer within the liver compared to WT mice (65). Furthermore, serum levels of MBL in asymptomatic HSV-2 patients were elevated compared to symptomatic patients and those with recurrent infections, suggesting that higher levels of MBL contribute to suppression of virus in human infection (65, 208).

MBL can also mediate direct neutralization of virus infection through blocking of virus receptor interactions with the host cell. Spear and colleagues have found that MBL blocks the interaction between the Ebola and Marburg glycoproteins and the host C-type lectin DC-SIGN, which binds to the viral glycoproteins, resulting in reduced infectivity into cells (111). In addition, MBL contributed to complement dependent neutralization of Ebola and Marburg viruses, and administration of high doses of MBL were able to protect mice from a lethal challenge with Ebola virus (111, 154), indicating a protective role for MBL in filovirus infection. MBL also been shown to bind to SARS-CoV *in vitro*, and was found to inhibit the virus by specifically binding to the N-linked glycan on the tip of the spike protein to block interactions with DC-SIGN (107, 257). Furthermore, enhanced susceptibility to SARS-CoV was found in patients with genotypes conferring

lower levels of MBL compared to patients with genotypes leading to higher amounts of circulating MBL (107).

1.5. The viral N-linked glycans.

Glycosylation is an important post-translational modification.

Glycosylation and other forms of post-translational modifications on proteins have an important, yet understudied and perhaps underappreciated role in protein structure, function, and regulation. On a broader scale, glycosylation of proteins is critical to development and function of many organisms, as mutations or deletions of the glycosyltransferases required for proper glycosylation frequently result in deleterious phenotypes and the inability to glycosylate is lethal (reviewed in (229)). Furthermore, differential glycosylation of proteins can introduce a remarkable amount of variation and diversity to the form and function of any given protein, thus adding another layer of complexity to our already complex and beautiful world.

The term "glycosylation" used in this dissertation refers to the addition of an oligosaccharide, also called a glycan, to a protein at designated sites within the protein by enzymes in the ER and the Golgi. There are generally two types of glycosylation on polypeptides: N-linked and O-linked glycosylation. Asparagine (N)-linked glycosylation is the additional of oligosaccharide at a specific site on the polyprotein indicated by the following sequeon: N-(X)-S/T where X is any amino acid except for proline. About two-thirds of all proteins contain N-linked glycosylation sequences, and about two-thirds of those proteins are actually glycosylated at the indicated site (reviewed in (229)). N-linked glycosylation begins in the lumen of the ER where a base glycan that consists of a N-

aceytlglucosamine (GlcNAc) core and branches of terminal mannose residues is convalently linked to the polyprotein, and is further processed by glycosidases and glycosyltransferases in the Golgi. O-linked glycosylation is commonly found on glycoproteins termed mucins and proteins that are secreted into the mucosa. O-linked glycosylation is characterized by the addition of GlcNAc to serine/threonine residues in the Golgi and does not appear to have any specific sequence that identifies putative sites.

The biological functions of glycans can be broadly categorized into the following roles: structural role, where glycans are required for proper folding of proteins; a role in mediating cell-intrinsic interactions where glycans mediate interactions within the cell organism with glycan-binding proteins; and cell-extrinsic roles which involve the interactions between foreign organisms such as bacteria, viruses, and fungi. The presence of glycans can protect the protein from proteases, antibodies, or premature interactions during synthesis and trafficking. HIV is a notable example where the heavy glycosylation of gp120 can act as a glycan shield, protecting the virus from antibody-mediated neutralization. The cell-extrinsic role of glycans involves recognition and interaction between the glycans and glycan-binding proteins on pathogens and other foreign molecules. These interactions have a major impact on infectious disease, especially since these interactions are required for pathogen entry into a host cell, recognition of a pathogen by the immune system, or affect some other aspect of disease.

N-linked glycosylation.

As the polyprotein is synthesized and translocated into the ER, a base glycan is covalently added at putative N-linked sites by the oligosaccharidetransferase (229). The

base glycan is a fourteen-sugar oligomannose composed of glucose (Glc_3), mannose (Man_9), and N-aceytlglucosamine ($GlcNAc_2$). As the protein moves through the ER and the Golgi, the glycan gets trimmed by glucosidases and mannosidases and then modified by various transferases that add different sugar groups (galactose, GlnNAc, sialic acid) onto the glycan to generate the final glycan structure (215). There are three main types of glycans that are produced: complex, high mannose, and hybrid. While there is a staggering amount of diversity within the three types of glycans, there are defining characteristic of each type. Complex glycans are characterized by the presence of terminal sialic acid residues; high mannose (also can be called oligomannose) glycans have terminal mannose residues; and hybrid glycans have a combination of terminal mannose and sialic acid residues.

Complex glycans can have extensive branching that allows for additional glycan diversity, and the different branching and terminal carbohydrates modifications are dictated in a tissue-specific and cell-lineage dependent manner. The ability to produce complex glycans is due to the presence of specific glycosidases and transferases that are able to trim down the base glycan, and rebuild with different sugars.

High mannose glycans are more typically found on glycosylated proteins produced from invertebrates. While the base glycan is the same glycan as the one found on proteins produced in vertebrate cells, invertebrates do not produce certain glycosidases and transferases and thus are unable to produce complex or hybrid glycans. Glycosylation in bacteria is quite distinct, but plays a similar role in bacterial protein function, interactions, and ultimately pathogenesis.

Innate immune recognition of N-linked glycans.

Given that bacteria, viruses, parasites, and fungi use glycosylation to modify their proteins either for proper folding or interaction with host proteins, it is not surprising that there are several different innate immune receptors that recognize non-self or altered glycans to activate the immune system. Several Toll-like receptors (TLRs) such as TLR4 and TLR2 recognize glycoproteins to activate TLR signaling pathways resulting in initiation of pro-inflammatory programs and activation of adaptive immunity. TLR4 recognizes lipopolysaccharide on bacterial cell walls, and has been shown to recognize glycoproteins from many different viruses as well, including respiratory syncytial virus and MMTV (reviewed in (117)). TLR2 recognizes components of viral glycoproteins as well to stimulate innate immunity (reviewed in (6, 117)). However, to date, viral N-linked glycans present on viral glycoproteins have not been shown to be directly engage TLRs, although given their location on the glycoprotein, it is plausible that they might.

As discussed above, PRRs that activate the complement system such as MBL and ficolin also recognize terminal sugar moities. Furthermore, members of the C-type lectin family of innate immune proteins are carbohydrate-binding proteins, and act as receptors and initiate signaling within myeloid cells (reviewed in (189)). C-type lectins such as DC-SIGN, L-SIGN, SIGN-R1, Dectin-2, Langerin, and mannose receptor recognize high mannose glycans on bacteria, viruses and fungi to modulate the host response (71). Indeed, there have been several studies that demonstrate both protective and pathologic roles for C-type lectins during viral infection. Capture of MBL-opsonsized influenza virus by SIGN-R1 in lymph nodes contribute to development of a protective humoral response by B cells (74). In contrast, another C-type lectin, CLEC5A, has been reported

to contribute to the pathogenesis of flaviviruses such as DENV and Japanese encephalitis virus through induction of pro-inflammatory cytokines and inflammasome activation (30, 31, 250). With regard to alphaviruses, DC-SIGN and L-SIGN have reported to be attachment factors that mediate entry of mosquito-derived virus into dendritic cells (120). The role other members of the C-type lectin family in alphavirus pathogenesis have not been evaluated.

MBL has been shown to directly bind to the N-linked glycans of several viruses discussed in earlier sections. Mosquito-derived WNV and DENV are neutralized by MBL in part through recognition of the high mannose N-linked glycans on the viral E protein on virions leading to complement activation (61). The high mannose and complex glycans on HIV gp120 mediate binding and neutralization by MBL both on the virus and on the infected cell (90), and a single N-linked glycan on the tip of the SARS-CoV spike protein was required for the interaction between the virus and MBL (257). Importantly, all of the described interactions between viruses and MBL indicate that the interaction between viral N-linked glycans and MBL leads to a protective response following viral infection.

The alphavirus N-linked glycans.

Alphaviruses have three to four N-linked glycosylation sites on the envelope glycoproteins. RRV and CHIKV have two E2 N-linked glycans, and one E1 N-linked glycan, whereas SINV has two glycans on E2 and two on E1 (219). The functions of these N-linked glycans appears to differ between the viruses in terms of viability and effects on pathogenesis.

The positions of the SINV and RRV glycans have been mapped by cryo-EM analysis of the structure of the glycoprotein spike (174). Since E1 lies parallel to the virion surface, the E1 glycans are located roughly in between, but below, the E2 glycoprotein spike (174). The glycans at E2 N200 (RRV) and E2 N196 (SINV) are located at the tip of the E2 glycoprotein spike, with the SINV glycan on the top of the "petal" structure, and the RRV glycan on the bottom (174). The locations of the glycans at E2 N262 (RRV) and E2 N318 (SINV) differ slightly. In SINV, the glycan is closer to the lipid bilayer whereas the RRV glycan is in between the glycoprotein spikes. The positions of the E2 glycans on the glycoprotein spike, especially the E2 N200 (RRV) and E2 N196 (SINV) located on the tip of the spike, make the N-linked glycans attractive candidates to interact with host carbohydrate binding proteins.

The oligosaccharide content and type of glycan present at each of the viral glycosylation sites is dependent on the host cell. The glycan composition at each site has been determined for both RRV and SINV and is summarized in Table 1.1 (148, 210). EndoH and PNGase digestion of mutant viruses that lack the glycosylation sites revealed that the RRV E1 N141 and E2 N262 glycans are predominantly complex oligosaccharides while replicating in mammalian cells, whereas the E2 N200 glycan is high mannose (210). EndoH cleaves glycans in between high mannose branches and the GlcNAc core, and PNGase cleaves between GlcNac and the asparagine. Thus, EndoH sensitive glycans are high mannose or hybrid, and EndoH resistant glycans are complex. In mosquito cells, all of the RRV glycans were either high mannose or hybrid glycans, as expected (210).

The composition of oligosaccharides for the SINV glycans were determined by analysis of purification of the E1 and E2 glycoproteins from virus grown in the presence of radiolabeled sugars (148). For SINV replicating in vertebrate cells, the glycans at E1 N139 and E2 N196 are predominantly complex glycans, whereas the glycan at E1 N245 can be either a high mannose or complex glycan and the E2 N318 glycan is predominantly a high mannose oligosaccharide (26, 148). The differences in oligosaccharide composition between the glycans on the same virus when replicating in mammalian cells are generally attributed to the availability of the glycan to glycosidases and glycosyltransferases as the protein moves through the Golgi. Since the base glycan has terminal mannose branches, it is plausible for any given glycan to be inaccessible to a particular glycosylation enzyme due to protein structure and folding (104).

Given the ligand specificity for many carbohydrate-binding proteins such as MBL and many of the C-type lectins, the high mannose and complex glycans on the alphavirus glycoproteins represent possible ligands to interact with host proteins and activate innate immunity. Furthermore, since the E2 glycans are located at the tip of the glycoprotein spike, it is possible that interactions between the glycans and host proteins may modulate alphavirus pathogenesis and disease.

Role of alphavirus glycans in pathogenesis.

To date, the only published studies of the role of the alphavirus N-linked glycans in disease pathogenesis is in the context of SINV infection. Knight *et al.* used previously described mutants of SINV TE12 that have the glycosylation sites mutated from asparagine to a glutamine at each site and evaluated the effect of loss of each glycan in

cells and in a mouse model of SINV encephalomyelitis (122). Loss of either of the E1 glycans generally reduced infectivity and replication within BHK-21 cells and consequently, virulence in mice compared to SINV WT. Interestingly, loss of either of the E2 glycans had the opposite effect and had increased replication within BHK-21 cells, virulence in mice, and delayed clearance from the CNS. This increased replication was due to enhanced binding of the E2 glycan mutants to HS compared to SINV WT (122). Since sialic acid is negatively charged, removal of the glycan likely allowed for tighter binding to the negatively charged HS, thus enhancing infectivity and disease. RRV T48 does not efficiently bind to HS (92), and so it is unclear if loss of the RRV glycans would lead to enhanced disease.

The alphavirus N-linked glycans also interface with the host immune system. In particular, the RRV E2 glycans have been shown to be important in induction of type I IFN production from dendritic cells (210). Mosquito cell derived RRV, which has high mannose and hybrid glycans, failed to induce type I IFN from myeloid dendritic cells compared to mammalian cell derived virus (209). One of the differences between mammalian and mosquito-derived virus is differential glycosylation of proteins, suggesting a possibility that the N-linked glycans may play a role in type I IFN induction. Indeed, infection of mDCs with RRV mutants that lack both E2 N-linked glycosylation sites show reduced type I IFN production compared to RRV WT without altering infectivity into the cells (210). Interestingly, it appeared that the presence of both of the E2 glycans were required for type I IFN induction from mDCs, and suggests that perhaps the combination of a high mannose and a complex glycan presented together that activate the innate immune response.

The studies described above indicate that the alphavirus N-linked glycans can interact with host proteins, and in the case of RRV, the glycans can modulate the innate immune response and are therefore likely to have an impact on disease pathogenesis. However, to date, the role of the N-linked glycans in RRV pathogenesis have not been evaluated.

1.6. Dissertation Objectives.

The objectives of this dissertation are to identify additional host and viral factors that contribute to arthritic alphavirus pathogenesis. The host inflammatory response is critical in the development of RRV-induced disease and some host factors that are important in mediating disease have been identified. Inflammatory macrophage and macrophage products are central in mediating damage within the skeletal muscle leading to disease (94, 134, 135, 193). Furthermore, the host complement system has a critical role in RRV pathogenesis through activation of CR3-bearing inflammatory cells that infiltrate into the skeletal muscle and joints following infection (158, 160). However, it is unknown how the complement system is activated following RRV infection.

The complement system is activated through three main pathways: the classical, the lectin, and the alternative pathways. Given that the complement system plays a critical role in RRV pathogenesis, we first sought to determine which pathway of complement was required for RRV-induced disease. We evaluated the role of each of the three main pathways using mice deficient in the various initiator molecules in RRV pathogenesis, and found that the MBL pathway of complement was essential to development of disease. We characterized RRV-induced disease in MBL-deficient mice,

and found that MBL was required for complement activation and subsequent disease following RRV infection, indicating a previously undescribed pathologic role for MBL in viral infection (79). Furthermore, analysis of samples from RRV patients showed a correlation between higher levels of circulating MBL and severity of disease (79).

Given the ligand specificity of MBL for carbohydrates that can be found on N-linked glycans, we next investigated whether viral N-linked glycans were required for RRV-induced disease through activation of the host complement system. Indeed, the RRV E2 N-linked glycans were required for development of RRV-induced disease, as a virus that lacks both E2 glycans caused mild RRV-induced disease in mice compared to a wild-type virus and is similar to the RRV-induced disease observed in MBL and complement deficient mice. Consistent with our hypothesis that the E2 glycans mediates disease through activation of the lectin pathway of complement, the E2 glycans were required for MBL deposition onto infected cells and within infected tissues, leading to decreased complement activation and C3 deposition. Together, these studies provide a model of RRV pathogenesis where the RRV E2 glycans activate the complement system through MBL to cause disease.

The results of this dissertation identify a critical role for the both MBL and the RRV E2 N-linked glycans in mediating severe RRV-induced disease through activation of the host complement system. Furthermore, these studies describe novel roles for both MBL and the alphavirus N-linked glycans in mediating pathology and disease in viral infection, and are among the first sets of studies to explore and evaluate the role of interaction between host carbohydrate binding proteins of the innate immune system and the viral N-linked glycans.

Aims:

1. Does the mannose-binding lectin pathway of complement contribute to severe RRV-induced disease?

2. Do the RRV E2 N-linked glycans contribute to severe RRV-induced disease?

Figure 1.1: Life cycle of alphaviruses.
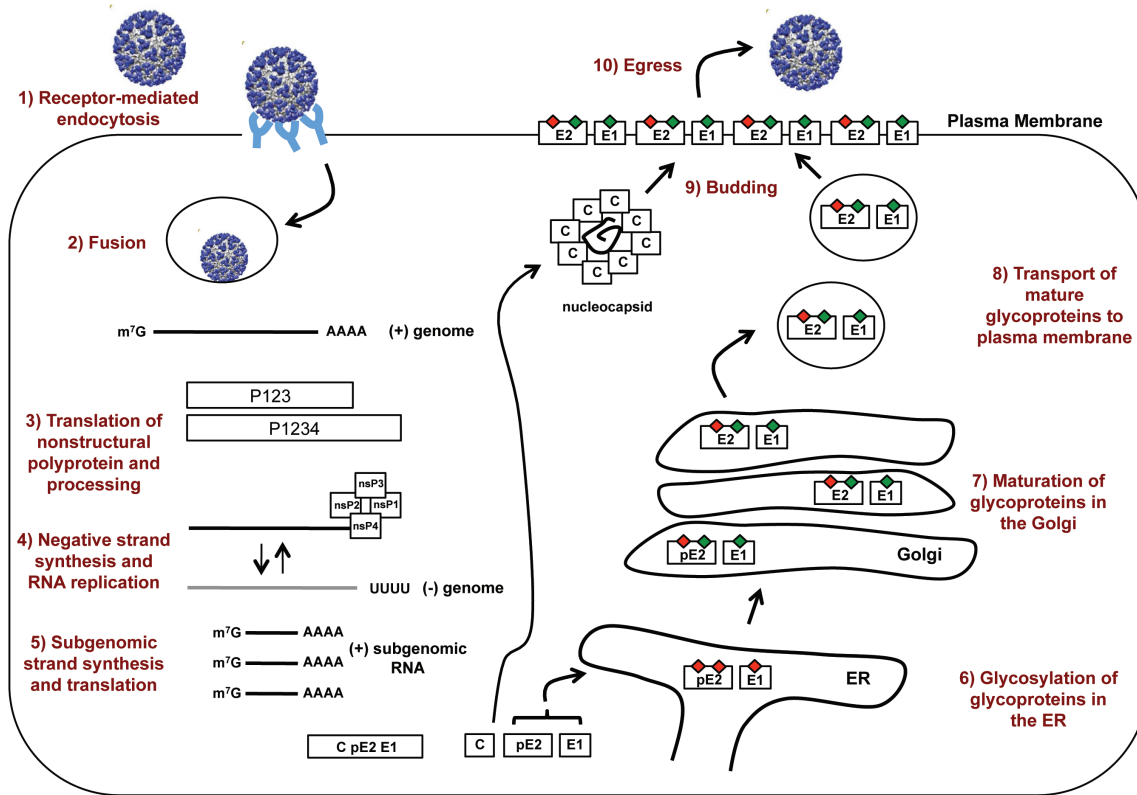
Figure 1.1: Life cycle of alphaviruses.

Details of each step are discussed within the text. N-linked glycans are represented as red and green diamonds. C: capsid; ER: endoplasmic reticulum. Figure adapted from Li *et al* and Jose *et al* with permissions from Nature Publishing Group and Future Medicine, respectively (113, 133).

Figure 1.2: The host complement system.
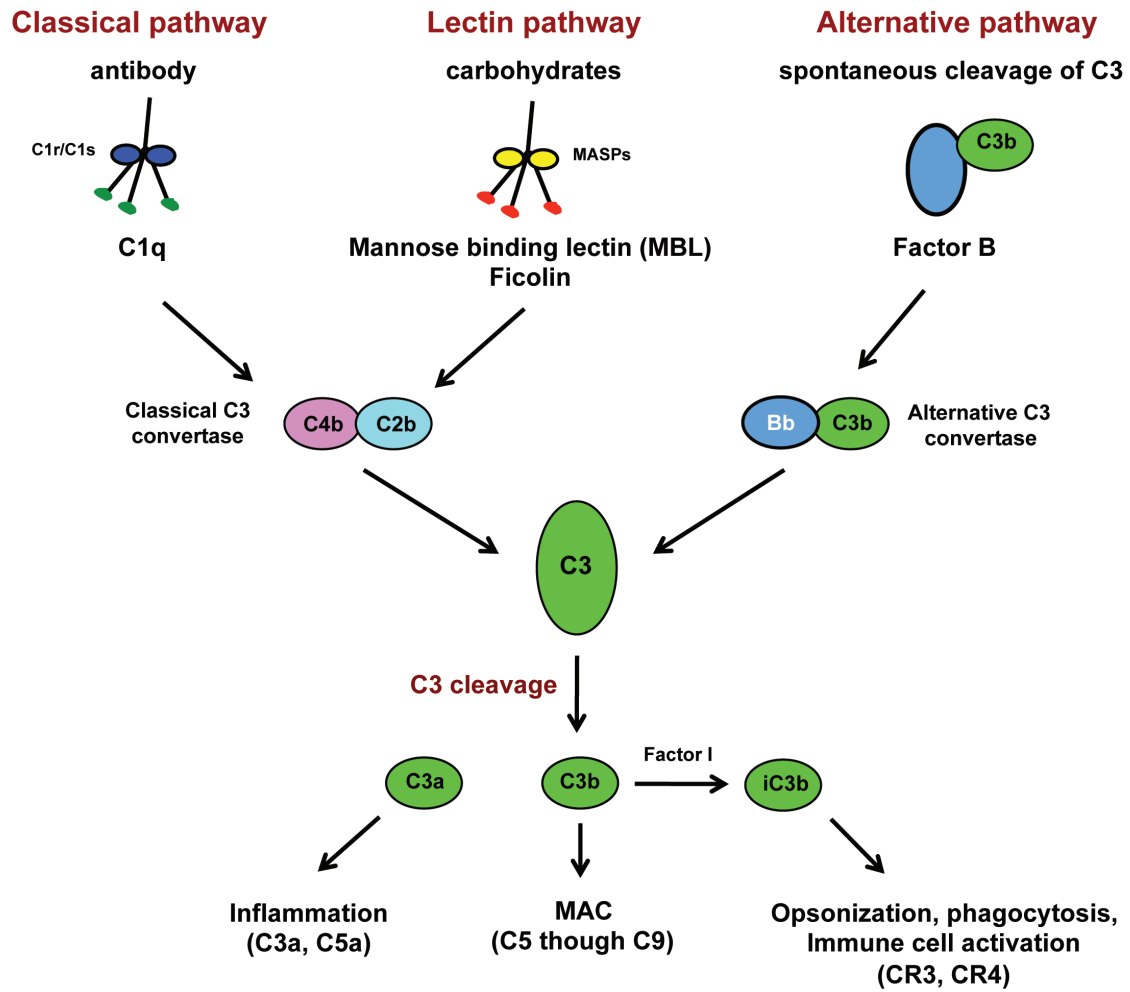
Figure 1.2: The host complement system.

Cartoon schematic of the three main activation pathways of the host complement system. Additional details of ligands and stepwise discussion of the complement cascade are outlined in the text. Briefly, the classical pathway (top left) is activated though C1q recognition of antibodies in immune complexes; the lectin pathway (top middle) is activated through MBL and ficolin recognition of carbohydrates; and the alternative pathway (top right) is activated through spontaneous cleavage of C3. Activation through the classical and lectin pathways results in formation of the classical C3 convertase C4b2b (middle left), and activation through the alternative pathway produces the alternative C3 convertase BbC3b (middle right). The C3 convertases cleave C3 into C3a, C3b, and subsequently C3b is cleaved by factor I to generate iC3b. Effector functions of each of the cleavage products are outlined at the bottom, and are discussed in greater detail in the text.

Table 1.1: N-linked glycans on alphaviruses.

Virus	Glycan position	Cell type	Type of Glycan	Ref.
RRV	E2 N200	Mammalian	high mannose	(210)
	E2 N262	Mammalian	complex	(210)
	E1 N141	Mammalian	complex	(210)
	E2 N200	Mosquito	high mannose/paucimannose	(210)
	E2 N262	Mosquito	high mannose/paucimannose	(210)
	E1 N141	Mosquito	high mannose/paucimannose	(210)
SINV	E2 N196	Mammalian	complex	(26, 148)
	E2 N318	Mammalian	high mannose	(26, 148)
	E1 N139	Mammalian	complex	(148)
	E1 N245	Mammalian	high mannose/complex	(148)

CHAPTER TWO:

MANNOSE BINDING LECTIN IS REQUIRED FOR ALPHAVIRUS-INDUCED ARTHRITIS/MYOSITIS

2.1 Summary

Mosquito-borne alphaviruses such as chikungunya virus and Ross River virus (RRV) are emerging pathogens capable of causing large-scale epidemics of virus-induced arthritis and myositis. The pathology of RRV-induced disease in both humans and mice is associated with induction of the host inflammatory response within the muscle and joints, and prior studies have demonstrated that the host complement system contributes to development of disease. In this study, we have used a mouse model of RRV-induced disease to identify and characterize which complement activation pathways mediate disease progression after infection, and we have identified the mannose binding lectin (MBL) pathway, but not the classical or alternative complement activation pathways, as essential for development of RRV-induced disease. MBL deposition was enhanced in RRV infected muscle tissue from wild type mice and RRV infected MBL deficient mice exhibited reduced disease, tissue damage, and complement deposition compared to wild-type mice. In contrast, mice deficient for key components of the classical or alternative complement activation pathways still developed severe RRV-induced disease. Further characterization of MBL deficient mice demonstrated that similar to $C3^{-/-}$ mice, viral

replication and inflammatory cell recruitment were equivalent to wild type animals, suggesting that RRV-mediated induction of complement dependent immune pathology is largely MBL dependent. Consistent with these findings, human patients diagnosed with RRV disease had elevated serum MBL levels compared to healthy controls, and MBL levels in the serum and synovial fluid correlated with severity of disease. These findings demonstrate a role for MBL in promoting RRV-induced disease in both mice and humans and suggest that the MBL pathway of complement activation may be an effective target for therapeutic intervention for humans suffering from RRV-induced arthritis and myositis.

2.2 Introduction

Arthritogenic alphaviruses, such as Ross River virus (RRV) and chikungunya virus (CHIKV), are mosquito-borne viruses that cause severe polyarthritis and myositis in humans. RRV causes annual disease outbreaks in Australia and has caused sporadic epidemics of debilitating polyarthritis, including one outbreak involving over 60,000 people in Oceania (86). RRV is transmitted to humans primarily by the *Aedes* and *Culex* species of mosquitoes that generally populate marsh areas, and CHIKV transmission has been traditionally mediated by the urban *Aedes aegypti*, though the virus has recently adapted for efficient transmission by the widely distributed *Aedes albopictus* species (227), leading to an increased risk for CHIKV spread into new areas, as illustrated by recent outbreaks in Italy and southern France (181). The expansion of CHIKV into an additional mosquito vector and the subsequent epidemic has highlighted the ability of the

arthritic alphaviruses to move into new geographic areas and cause large-scale outbreaks of acute and persistent arthralgia and myalgia in humans.

RRV-induced arthritic disease presents predominantly as painful stiffness, inflammation, and swelling in peripheral joints that can last months after initial infection and the host inflammatory response is thought to play a major role in disease pathogenesis. Inflammatory monocytes constitute the bulk of leukocytes isolated in synovial aspirates from RRV-infected patients (55, 91), and macrophage-cytotoxic drugs have been shown to drastically reduce disease progression and severity in mice (134, 135). In addition, mice lacking C3, the central complement factor that is essential for complement activation, exhibit reduced RRV-induced disease and tissue destruction (158), implicating a role for complement in development of the disease. Consistent with studies in mice, synovial aspirates from patients with RRV-induced arthritis have been shown to contain increased levels of the C3 cleavage product C3a (158). Although macrophage recruitment to infected tissues is markedly increased after RRV infection, the role played by complement is independent of inflammatory cell recruitment. Rather, tissue destruction and disease progression requires complement receptor 3 (CR3), suggesting that complement interactions with CR3 on inflammatory cells promote tissue destruction in RRV-infected tissues (160). However, it is currently unclear how the complement system is activated following RRV infection.

There are three main activation pathways of the complement cascade; the classical, alternative, and lectin dependent pathways, that all converge on factor C3 and lead to activation of complement effector functions (reviewed in (183)). The classical pathway is initiated by C1q interactions with antigen-bound complexes of IgG and IgM,

and the proteases C1r and C1s cleave C4 and C2 to generate the C3 convertase C4b2b. Binding of factor B (fB) and spontaneously hydrolyzed C3 initiates the alternative pathway, and fB binding to C3b leads to formation of the alternative C3 convertase C3bBb that can amplify complement activation. In the lectin pathway, mannose binding lectin (MBL) or the ficolins bind to carbohydrate moieties on foreign bodies, such as viruses, or to host cells and apoptotic cells, and the MBL-associated serine proteases (MASPs) cleave C4 and C2 to form the C3 convertase C4b2b. Cleavage and processing of C3 by the C3 convertases produce several C3-derived components that are potent activators of the immune system. One such component is iC3b, which is a ligand for several complement receptors, such as CR3. Binding of iC3b to CR3 on cells such as monocytes/macrophages, neutrophils, and NK cells, results in activation of these cells, leading to enhanced phagocytosis and cytotoxic activity against iC3b-opsonized cells (183).

MBL is a soluble C-type lectin that can initiate the complement cascade through binding of the carbohydrate recognition domains (CRD) to cell-surface sugars expressed on bacteria and viruses and some endogenous host ligands (reviewed in (223)). The complement system is notorious for having both a protective and pathologic role and frequently leads to additional tissue injury and damage once activated. Similarly, MBL appears to be able to have the ability to protect as well as harm the host cells. In the context of sterile inflammatory diseases such as myocardial and gastrointestinal ischemic reperfusion injury, MBL and the lectin pathway mediate development of disease through complement-mediated regulation of pro-inflammatory cytokines and inflammation, leading to exacerbated pathology and tissue injury (89, 112, 205, 237). In contrast to the

pathologic role of MBL in sterile inflammatory diseases, MBL is thought to primarily

play a protective role in response to infectious pathogens. MBL has been shown to be

essential for host protection from many different viral and bacterial infections either

through direct binding to pathogens or by limiting spread through complement effector

functions. MBL has been shown to bind directly to many different viruses, including

human immunodeficiency virus (HIV), Ebola virus, and arboviruses such as dengue virus

and West Nile virus (WNV), and MBL can either directly neutralize these viruses

through activation of complement or interfere with their binding to host cells (reviewed

in (217)). Furthermore, studies using mice deficient in both MBL genes (MBL-A$^{-/-}$ and

MBL-C$^{-/-}$; MBL-DKO) have revealed that MBL can have a protective role during WNV

and herpes simplex virus infections (61, 62, 65). Though MBL neutralizes flaviviruses,

such as WNV and dengue virus (61), and plays a protective role during WNV infection

(62), these same studies found no detectable interactions between MBL and alphaviruses,

suggesting that MBL does not play a protective role during alphavirus infection.

However, the role of MBL role in the pathogenesis of alphavirus-induced

arthritis/myositis has not been evaluated.

The goal of this study was to further assess the role of the host complement

system in the pathogenesis of alphavirus-induced inflammatory disease and to determine

which complement activation pathways are required for virus-induced disease. In a

mouse model of RRV-induced arthritis and myositis, mice deficient in either the classical

or alternative pathways developed severe disease, while mice deficient in both genes of

MBL (MBL-DKO) were resistant to disease, suggesting that MBL plays a major role in

RRV-induced disease. Similar to previous findings with C3$^{-/-}$ mice (158), RRV-infected

MBL-DKO mice had similar levels of viral burden and inflammation compared to wild-type (WT) but exhibited significantly less complement deposition, tissue damage, and disease. Further analysis found that MBL levels are enhanced in RRV infected tissues and that MBL binds to RRV infected cells, suggesting that RRV infection leads to MBL deposition and subsequent complement activation. Importantly, studies in human patients suffering from RRV-induced disease found that levels of MBL were elevated in the serum of RRV-infected patients compared to healthy controls. In addition, serum and synovial fluid MBL levels correlated with the severity of RRV disease, while no differences were observed in classical or alternative pathway activation, suggesting that MBL contributes to RRV-induced disease in human populations.

2.3 Materials and Methods

Ethics Statement. Some of the studies described in this manuscript did involve human samples. For human serum samples, all serum samples had been submitted for diagnostic testing with written and oral informed patient consent at CIDMLS, Westmead Hospital and The Royal Melbourne Hospital (Melbourne, Australia). Samples were de-identified by the testing laboratory before being used in the research project. Synovial samples were collected from adult patients (age range, 30–45 years) residing in the Murray-Goulburn Valley (Victoria, Australia) who had acute cases of RRV-induced polyarthritis in accordance with human subjects protocols approved by the Royal Melbourne Hospital Human Ethics Committee. All individuals received and completed written informed consent forms prior to collection of materials. Mouse studies were performed in strict accordance with the recommendations in the Guide for the Care and Use of Laboratory

Animals of the National Institutes of Health. All mouse studies were performed at the University of North Carolina (Animal Welfare Assurance # A3410-01) using protocols approved by the UNC Institutional Animal Care and Use Committee (IACUC). All studies were performed in a manner designed to minimize pain and suffering in infected animals, and any animals that exhibited severe disease signs was euthanized immediately in accordance with IACUC approved endpoints.

Viruses and cells. The viral stocks used in this study were generated from the infectious clone of the T48 strain of RRV (pRR64), kindly provided by Richard Kuhn (Purdue University) as described in (161). Briefly, viral RNA was generated through *in vitro* transcription of SacI-linearized pRR64 using the mMessage mMachine SP6 kit (Ambion) and electroportated into BHK-21 cells (ATCC). Viral titer was determined by plaque assay on BHK-21 cells. BHK-21 cells were grown in α-MEM (Gibco) supplemented with 10% donor calf serum (DCS), 10% tryptose phosphate, L-glutamine, penicillin, and streptomycin. C2C12 cells were grown in DMEM (Gibco) supplemented with 20% fetal bovine serum (FBS), L-glutamine, penicillin, and streptomycin prior to differentiating. To differeniate cells into myotubes, confluent C2C12 cells were maintained in DMEM supplemented with 2% horse serum, L-glutamine, penicillin, and streptomycin.

Mice. All mice used in this study were maintained and bred in house at the University of North Carolina (UNC) in accordance with UNC Institutional Animal Care and Use Committee guidelines. C57BL/6 and MBL-DKO mice were purchased from The Jackson Laboratories (Bar Harbor, ME); $C1q^{-/-}$ mice were a generous gift from Dr. Marina Botto

(Imperial College London, UK); fB$^{-/-}$ mice were generously provided by Dr. Charles

Jennette (UNC). While RRV is classified as a biosafety level-2 agent, due to the exotic

nature of the virus, all animal studies were performed in a biosafety level-3 facility.

Twenty-four day old mice were inoculated with 10^3 PFU of RRV in diluent (phosphate

buffered saline supplemented with 1% DCS) into the left rear footpad. Mice were

weighed daily and assigned a clinical score based on hind limb weakness and altered gait

on the following scale: 0= no disease; 1=mild loss of hind limb grip; 2=moderate loss of

hind limb grip; 3=severe loss of hind limb grip; 4= no hind limb grip and mild inability to

right; 5=no hind limb grip and complete inability to right; 6=moribund.

Viral burden analysis. Mice were infected with RRV as described above, and at

indicated times post infection mice were sacrificed, perfused with 1X PBS, and indicated

tissues were dissected out, weighed, and homogenized with glass beads in diluent. Viral

titer within infected tissues were determined by plaque assay on BHK-21 cells from

tissue homogenates.

In situ **hybridization**. Mice were infected with RRV as described above, and at indicated

times post infection mice were sacrificed, perfused with 4% paraformaldehyde (PFA), pH

7.3. Tissues were paraffin embedded and 5µm sections were generated and in situ

hybridization was performed as previously described (161) using an RRV-specific or

EBER-specific ^{35}S-labeled RNA probe.

Histological analysis. At desired times post infection, mice were sacrificed and perfused with 4% paraformaldehyde (PFA), pH 7.3. Tissues were paraffin embedded and 5μm sections were generated and stained with hematoxylin and eosin (H&E) to examine tissue pathology and inflammation. Sections were visualized by bright field light microscopy (Olympus BX61).

Evans blue dye uptake analysis. At 10 days post infection mice were injected with 1% Evans blue dye in PBS into the peritoneal cavity (50μl/10g mouse weight). At 6 hours post injection, mice were sacrificed and perfused with 4% PFA. Quadriceps muscle tissues were embedded in optimal cutting temperature compound (OCT) and frozen in an isopentane histobath, 5μm sections were generated, mounted with ProLong Gold with DAPI (Invitrogen) and sections were analyzed by fluorescence microscopy (Olympus BX61).

Immunohistochemistry. At 7 dpi, mice were sacrificed and perfused with 4% PFA. Quadriceps muscles were removed, paraffin embedded, and 5μm sections were generated. Sections were deparaffinized in xylene, rehydrated through an ethanol gradient, and probed with a goat anti-mouse C3 polyclonal antibody (1:500 Cappel) using the Vectastain ABC-AP kit (Vector Labs, CA) and Vector Blue Alkaline phosphatase substrate kit (Vector Labs, CA) according to the manufacturers' instructions. Sections were counterstained with Gill's hematoxylin.

Immunoblot analysis. At indicated times post infection, mock-infected and RRV-infected mice were sacrificed, and perfused with 1X PBS. Quadriceps muscles were removed and homogenized in radioimmunoprecipitation lysis buffer (RIPA; 50μM Tris pH 8.0, 150mM NaCl; 1% NP-40, 0.5% deoxycholate, 0.1% SDS and 1X complete protease inhibitor cocktail (Roche)) by glass beads. Protein concentration was determined by Bradford protein assay and 25-30μg of protein was run onto a 10% SDS-PAGE gel. Protein was transferred onto a PVDF membrane, and membranes were blocked in 5% milk, 0.1% Tween-20 in PBS. Membranes were probed with goat anti-mouse MBL-A (1:1000 R&D Systems), goat anti-mouse MBL-C (1:1000 R&D Systems), goat anti-mouse C3 polyclonal antibody (1:1000 Cappel), mouse anti-RRV (1:1000 ATCC), or goat anti-mouse actin polyclonal antibody (1:500 SCBT), washed with PBS containing 0.1% Tween-20 and incubated with rabbit anti-goat antibody or sheep anti-mouse antibody conjugated to horseradish peroxidase (1: 10, 000 Sigma). Membranes were washed again and protein visualized by ECL (Amersham) according to manufacturer's instructions. Densitometry was performed using ImageJ software (NIH).

MBL deposition onto C2C12 cells. Differentiated C2C12 cells were either mock-infected or infected at an approximate MOI of 20 with RRV. At 24 hpi, culture medium was removed and cells were incubated in differentiation medium containing either 10% serum from WT or MBL-DKO mice for an additional 30 minutes. Cells were washed and harvested in RIPA lysis buffer, and cell lysates were analyzed by immunoblot analysis.

Enzyme Linked Immunosorbent Assay (ELISA). High binding ELISA plates were coated overnight at 4°C with either 10μg/ml mannan (Sigma Aldrich, St. Louis, MO), 5 x 10^6 PFU of either mammalian (BHK-21 cells) or mosquito (C6/36 cells) derived virus, or mock supernatant from either BHK-21 or C6/36 cells in 1X carbonate buffer. Wells were washed with three times with 1X PBS, and subsequently incubated for one hour at room temperature in serum from WT mice at 1:20 dilution in gelatin veronal buffer with calcium and magnesium (Sigma Aldrich, St. Louis, MO). Wells were washed three times with 1X PBS, and incubated in primary antibody against either mouse MBL-C (1:100 R&D Systems) or against RRV (1:200 ATCC). Wells were washed three times with 1X PBS + 0.1% Tween 20 and then incubated in the appropriate HRP-conjugated secondary antibody, and developed using TMB substrate (Sigma Aldrich). The OD_{450nm} was measured and recorded.

Analysis of infiltrating inflammatory cells by flow cytometry. To determine the composition of the inflammatory cell infiltrates within the quadriceps muscle, at indicated times post infection mice were sacrificed and perfused with 1X PBS. Both quadriceps muscles were removed, minced, and digested with RPMI containing 10% fetal bovine serum (FBS), 15mM HEPES, 2.5mg/ml collagenase A (Roche), 1.7mg DNase I (Roche) for 2 hours at 37ºC with shaking. Cells were strained through a 40μm strainer and washed twice with wash buffer (HBSS containing 1% sodium azide and 1% FBS) and total viable cells were determined by trypan blue exclusion. To stain cells for flow cytometry, cells were incubated with anti mouse FcγRII/III (2.4G2; BD Pharmingen) and stained with combinations of the following antibodies: fluorescein

isothiocyanate (FITC)-conjugated anti-mouse CD3, phycoerythrin (PE)-conjugated anti-NK1.1, PE-Cy5 anti-CD45 (leukocyte common antigen), PE-Cy7 anti-F4/80, Allophycocyanin (APC)-conjugated anti-CD49b, eF450-conjugated anti-CD11b, APC anti-major histocompatibility complex class II antigens (MHC II), and eF780-conjugated anti-CD45 (B220) (eBiosciences, San Diego, CA), FITC anti-Ly-6G, and PE anti-SigLecF (BD-Pharmingen, San Diego, CA), and PE-Texas Red-conjugated anti-CD45 (B220), and PE-Texas Red anti-CD11c (Molecular Bioprobes, Invitrogen). Cells were fixed with 2% PFA (pH 7.3) and analyzed on a CyAn flow cytometer (Becton Dickinson), and data was analyzed using Summit software.

Gene expression. At 7 dpi following RRV infection, mice were sacrificed and perfused with 1X PBS. Quadriceps muscles were removed and homogenized in Trizol (Invitrogen) using glass beads. RNA was extracted using Invitrogen PureLink RNA purification kit, and mRNA expression of indicated genes was measured by quantitative real-time PCR. Raw data values were normalized to 18S rRNA levels.

Patient samples. Convalescent serum samples from five patients presenting with acute, serologically confirmed (seroconversion by neutralization, IgM and IgG) RRV-infection and thirteen samples from healthy individuals were provided by CIDMLS, Westmead Hospital (Sydney, Australia). All serum samples had been submitted for diagnostic testing with informed patient consent at CIDMLS, Westmead Hospital and The Royal Melbourne Hospital (Melbourne, Australia). Samples were de-identified by the testing laboratory before being used in the research project. Needle biopsy was performed to

collect synovial fluid samples from adult patients (age range, 30–45 years) residing in the

Murray-Goulburn Valley (Victoria, Australia) who had acute cases of RRV-induced

polyarthritis. Samples were collected and prepared aseptically in the laboratories of

Echuca Hospital (Murray-Goulburn Valley; Victoria, Australia) and The Royal

Melbourne Hospital and was performed in accordance with The Royal Melbourne

Hospital Human Ethics Committee. Severe RRV-induced disease was defined as a patient

presenting with intense swelling, severe joint pain and myalgia affecting both the knee

joints and joints of the fingers. Mild RRV-induced disease was defined as a patient

presenting with minor swelling, localized in the knees, and no additional symptoms. For

osteoarthritis samples, synovial fluid aspirates were obtained from 5 patients with

osteoarthritis from the John James Hospital (Canberra, Australia). Sample collection was

performed in accordance with the AustralianCapital Territory Health Community Care

Human Research Ethics committee. Samples were obtained at the time that knee joint

arthroplasty was performed, and joints were aspirated before arthrotomy. The diagnosis

given to patients was primary osteoarthritis with no evidence of an inflammatory

arthropathy. These samples were de-identified prior to analysis.

Levels of MBL in serum and synovial fluid were determined using a

commercially available ELISA kit according to the manufacturer's instructions (R&D

Systems). Levels of C4a in the synovial fluid was determined using BD OptEIA (BD).

Bb levels were determined using Microvue Bb Plus (Quidel). The levels of the C1q-C4

complex were determined as described in (249).

Statistical analysis. Clinical scores and percent of starting weight at 10 dpi between C1q$^{-/-}$, fB$^{-/-}$, MBL-DKO, and wild-type mice were analyzed for statistically significant differences by Mann-Whitney analysis with multiple comparisons corrections (clinical scores; $p<0.01$ is considered significant), and by one-way ANOVA with Bonferroni's correction (percent of starting weight; $p<0.05$ is considered significant). Viral burden, total number of infiltrating cells, and gene expression data at each time point between wild-type and MBL-DKO mice was analyzed for statistically significant differences by Mann-Whitney analysis or t-test ($p<0.05$ is considered significant). Levels of MBL, C4a, C1q-C4 complexes, and Bb in serum and synovial fluid from human patients were analyzed by Mann-Whitney analysis for statistical significance ($p<0.05$ is considered significant). Statistical analyses were performed using GraphPad Prism 5.

2.4 Results

The MBL pathway is essential for RRV-induced disease and inflammatory tissue destruction.

Complement activation products are elevated in the synovial fluid of persons suffering from RRV-induced arthritis and complement activation is required for virus-induced arthritis/myositis in a mouse model (158, 160, 161). Although other alphaviruses, such as the neurovirulent Sindbis virus, have been shown to activate complement via both the classical and alternative pathways (99), the pathway(s) leading to complement activation by arthritic alphaviruses is currently unknown. Therefore, mice deficient in key components of the classical ($C1q^{-/-}$), alternative (factor B, $fB^{-/-}$), or lectin ($MBL-A/C^{-/-}$, MBL-DKO) pathways were assessed for their susceptibility to RRV-induced disease. $C1q^{-/-}$, $fB^{-/-}$, MBL-DKO, or WT C57BL/6 mice were inoculated with RRV in the footpad and assessed for weight loss and scored for hind limb function as previously described (161). RRV-infected WT mice showed signs of hind-limb weakness by 5 days post infection (dpi) and developed severe hind-limb weakness by 7 dpi through 10 dpi (Figure 2.1). RRV causes disease independently of B cells and antibody (161), suggesting that the classical pathway does not contribute to disease during RRV infection. Consistent with this, $C1q^{-/-}$ mice exhibited severe disease signs and hind-limb weakness similar to WT animals (Figure 2.1A). Likewise, $fB^{-/-}$ mice developed severe RRV-induced disease (Figure 2.1A), demonstrating that the alternative pathway of complement activation is not required for RRV-induced disease, though it is important to note that RRV-infected $fB^{-/-}$ mice tended to develop more severe disease compared to WT mice, suggesting that the alternative pathway is activated and may actually play a protective

67

role during RRV infection. In contrast to C1q$^{-/-}$ and fB$^{-/-}$ mice, MBL-DKO mice infected

with RRV developed mild hind-limb weakness and exhibited reduced weight loss

compared to WT mice (Figure 2.1, A and B). Mock-infected WT and MBL-DKO mice

did not differ in weight gain and showed no signs of disease throughout the course of

infection (data not shown). While we cannot rule out a minor contribution of the classical

and alternative activation pathways or activation of the lectin pathway through ficolins in

development of RRV disease, this data demonstrates that the lectin pathway initiated by

MBL plays an essential role in driving RRV-induced disease.

MBL contributes to damage within quadriceps muscle.

Following infection of WT C57BL/6 mice, RRV replicates to high levels within

both the joints and skeletal muscle and elicits an inflammatory infiltrate into these tissues

(161). Following the onset of inflammatory cell infiltration, wild type mice develop

severe destructive myositis, which is a major aspect of virus-induced disease in this

mouse model, and we have previously shown that muscle cell killing and disease is

dependent upon both C3 activation and CR3 (158, 160). Therefore, to confirm the role of

MBL in driving RRV-induced disease, inflammatory pathology was assessed within the

quadriceps muscles of RRV-infected fB$^{-/-}$, C1q$^{-/-}$, MBL-DKO, or WT mice by H&E

staining of paraffin embedded sections. At 10 dpi, a time point of peak RRV disease, we

observed similar inflammation and tissue pathology in fB$^{-/-}$, C1q$^{-/-}$, and WT mice (Figure

2.2A). Inflammatory cells are present in the quadriceps muscles of infected mice from all

strains, as indicated by the solid arrowheads. We observed tissue damage in the

quadriceps muscles in fB$^{-/-}$, C1q$^{-/-}$, and WT mice as evidenced by the degeneration of the

fibrous architecture of the skeletal muscle. In contrast, RRV infected MBL-DKO mice maintained the architecture of the skeletal muscle with very little tissue damage, despite the presence of inflammatory cells (Figure 2.2A), which was strikingly similar to previous results demonstrating an essential role for C3 in RRV-induced disease (158). To confirm that MBL-DKO mice have decreased tissue damage following RRV infection compared to WT mice, we used Evans Blue dye (EBD) uptake to detect areas of damage. Consistent with the clinical scores and histological analyses at 10 dpi, RRV-infected WT mice had abundant EBD positive muscle fibers within the quadriceps muscle whereas EBD positive cells were rare in RRV-infected MBL-DKO mice (Figure 2.2B), further demonstrating that MBL is required for the induction of tissue damage during RRV-induced disease.

RRV infection induces MBL deposition onto tissues and cells.

To determine if MBL is deposited onto tissues following RRV infection, we evaluated tissue homogenates of quadriceps muscle from RRV-infected WT mice at 7 dpi for levels of MBL by immunoblot analysis. We observed an increase in the amount of MBL in the quadriceps muscle of infected mice compared to that of mock-infected mice (Figure 2.3A), indicating that RRV infection results in elevated amounts of MBL within target tissues. Given the enhanced MBL within RRV infected muscle tissue, we next evaluated whether MBL would directly bind to RRV or RRV infected cells. Studies with two other alphaviruses, CHIKV and Sindbis virus, found no evidence for interactions with MBL, while mosquito derived West Nile virus was efficiently bound and neutralized by MBL (61). Consistent with these findings, we were unable to detect direct binding

between MBL and either mammalian cell or mosquito cell derived RRV virions by

ELISA (Figure 2.4A-B) and we also found no evidence for MBL-mediated neutralization

of RRV (Figure 2.4C). Given the lack of detectable interactions between MBL and the

RRV virion, we assessed whether MBL bound to RRV-infected cells. Differentiated

C2C12 murine skeletal muscle cells were infected with RRV for 24 hours and then

incubated with medium containing either C57BL/6 wild-type serum or MBL-DKO serum

for 30 minutes. Cell lysates were harvested and analyzed for presence of MBL-C by

immunoblot analysis. As shown in Figure 2.3B, the amount of MBL-C deposition was

enhanced in cells infected with RRV compared to mock infected cells, indicating that

RRV infection results in increased MBL binding to cells. No deposition of MBL was

detected onto cells incubated with MBL-DKO serum, indicating the specificity of

detection. Therefore, though MBL does not appear to interact with the RRV virion, RRV

infection does lead to MBL deposition on infected cells.

*Complement deposition and activation is reduced in RRV-infected MBL-DKO compared
to WT mice.*

MBL, but not the alternatively or classical complement activation pathways, was

required for RRV-induced disease and tissue pathology (Figures 2.1 and 2.2), and the

phenotype in MBL-DKO mice is strikingly similar to C3$^{-/-}$ mice, suggesting that MBL

plays a major role in driving complement activation during RRV infection. Therefore,

we directly assessed whether MBL was required for RRV-dependent complement

deposition. Western blot analysis of skeletal muscle from wild type or MBL-DKO mice

indicated that C3 levels, including the α and β chains of C3 were present at reduced

levels in the skeletal muscle of RRV infected MBL-DKO mice compared to wild type

mice (Figure 2.5). However, since inflammatory macrophages produce C3 (20), western

blot analysis was not able to clearly differentiate between complement deposition within

the tissue and de novo production of complement by the infiltrating inflammatory cells in

both wild type and MBL-DKO animals. Therefore, we directly assessed the impact of

MBL deficiency on complement deposition within the RRV infected muscle by

performing immunohistochemistry on quadriceps muscle from WT and MBL-DKO mice

using an anti-mouse C3 antibody. Abundant C3 staining localized to damaged skeletal

muscle at 7 dpi in WT mice while C3 staining was substantially reduced in muscle from

RRV-infected MBL-DKO mice (Figure 2.6A). Importantly, we observed comparable C3

staining between RRV-infected C1q^{-/-}, fB^{-/-}, and WT mice (Figure 2.6B), suggesting that

neither C1q nor fB are required for C3 deposition on muscle tissue following RRV

infection. Therefore, these results suggest that MBL is the major mediator of complement

activation and deposition within RRV infected muscle tissue.

Viral replication is unaffected in the muscle tissue of MBL-DKO mice.

Prior studies with C3^{-/-} and CR3^{-/-} mice demonstrated that complement activation

and CR3-dependent signaling is essential for RRV-induced disease and tissue destruction,

but complement deficiency had no effect on viral burden or tropism. To determine

whether this was also the case in MBL-DKO mice, we evaluated WT and MBL-DKO

mice for viral load within the quadriceps muscles, ankle joints, and serum. As shown in

Figure 2.7A, MBL-DKO mice exhibited no significant difference in the amount of

infectious virus in the quadriceps muscle through days 7 and 10 dpi, which represent the

71

times when RRV-induced muscle destruction peaks. Furthermore, analysis of the viral distribution within wild type and MBL-DKO animals by in situ hybridization found no differences in the localization of RRV specific signal between the two mouse strains. (Figure 2.7D). Therefore, the differences in RRV-induced tissue destruction (Figure 2.2A-B) or C3 deposition (Figure 2.6) within the RRV infected muscle of MBL-DKO mice cannot be explained by differences in viral replication.

In addition to evaluating viral titers within the skeletal muscle, we also assessed viral loads within the serum and ankle joints. Viral titers within the ankle joints were similar between MBL-DKO and WT mice through 7 dpi (Figure 2.7B), though we did observe a small, but statistically significant decrease in viral titer within the ankle joints of MBL-DKO mice compared to wild type mice at day 10 post infection. MBL-DKO mice had higher amounts of virus in the serum at 1 dpi compared to WT mice (Figure 2.7C), indicating that MBL may play some role in initial control of viremia. However, virus was cleared from the serum of infected animals at similar rates in both WT and MBL-DKO mice (Figure 2.7C), suggesting that MBL does not play a major role in serum clearance of RRV or direct neutralization of virus in the serum. The impact of this initial increase in serum viremia in MBL-DKO mice on downstream disease through antibody production is unclear, although it is important to note that both RAG-1$^{-/-}$ and μMT mice develop disease similar to WT mice (158), indicating that the antibody response is not required for development of disease.

MBL deficiency does not affect inflammatory cell recruitment, but alters expression of inflammatory mediators within the RRV-infected muscle.

Prior studies demonstrated that complement activation drives inflammatory tissue destruction, but does not regulate inflammatory cell recruitment during RRV infection (158). However, as MBL may regulate the host inflammatory response independently of its effects on complement activation, we quantified and analyzed the inflammatory cell populations within the muscle of WT and MBL-DKO animals at 7 and 10 dpi, which are the times of peak inflammation in WT mice (161). Consistent with prior findings in $C3^{-/-}$ mice, RRV infected MBL-DKO mice exhibited no statistically significant differences in either total number of leukocytes (Figure 2.8A) or the composition of the inflammatory infiltrates at either 7 or 10 dpi (Figure 2.8B). Representative flow cytometry plots of the various cell types are shown in Figure S2.1. The total numbers of $CD4^+$ T cells, $CD8^+$ T cells, and NK cells at both 7 and 10 dpi were not significantly different between RRV-infected WT and MBL-DKO mice (Figure 2.8B). Given the role of inflammatory macrophage in development of RRV-induced disease (135), we compared total numbers of cells with staining characteristics of inflammatory macrophages ($F4/80^+$ $CD11b^+$ $Gr-1^{lo}$ $B220^-$) at both 7 and 10 dpi, and observed no difference at 7 dpi, and interestingly, a significant increase in numbers of these cells in RRV-infected MBL-DKO mice at 10 dpi. While we cannot rule out the possibility that minor populations of inflammatory cells are differentially regulated by MBL, these data suggest that MBL does not affect the major populations of inflammatory infiltrates recruited to the skeletal muscle following RRV infection.

Although inflammatory cell recruitment was largely unaffected by either MBL or C3 deficiency (158) we have previously shown CR3 is also required for RRV-induced disease and that a subset of inflammatory genes expressed in the inflamed muscle of RRV-infected mice are dependent upon both C3 and CR3, including the calgranulins S100A8 and S100A9, IL-6 and the enzyme arginase I (ArgI) (160). Therefore, to determine if MBL affected expression of these genes in the same manner as C3 and CR3, expression levels were assessed in the quadriceps muscle from both WT and MBL-DKO mice at 7 dpi. As shown in Figure 2.9, RRV-infected WT mice exhibited significantly higher expression of S100A8 and S100A9 compared to RRV-infected MBL-DKO mice, indicating that expression of these genes is also regulated by MBL during RRV infection. Interestingly, the S100A8/S100A9 complex has been associated with inflammatory arthritis (reviewed in (172)) however, the role of these proteins in RRV disease requires further investigation. Expression of TNFα and IL-1β, which were shown to be C3-independent (160), were also unaffected in MBL-DKO mice (Figure 2.9). Expression of IL-6 and Arg I, which we have previously shown to be C3 and CR3-dependent, were unaffected in MBL-DKO mice (IL-6) or slightly reduced (Arg I) (Figure 2.9). Expression of these genes may reflect residual complement activation in the absence of MBL (Figure S3), though this requires further study. Interestingly, expression of IL-10, which is largely C3-independent following RRV infection (160), was dependent on MBL and suggests that MBL may be interacting with pathways other than the complement system to mediate IL-10 expression (Figure 2.9).

Levels of MBL are elevated in RRV patients.

Prior studies have shown that the C3 cleavage product C3a is elevated in synovial fluid of RRV polyarthritis patients (158). To determine if circulating levels of MBL are elevated in RRV-infected patients, we compared serum MBL levels from patients during convalescence to serum MBL levels in RRV-seronegative controls. As shown in Figure 2.10A, RRV patients had significantly higher levels of circulating MBL compared to healthy controls. Since MBL levels are highly variable in human populations, we also assessed serum and synovial fluid MBL levels in a small cohort of patients clinically characterized as having severe or mild RRV-induced polyarthritis. MBL levels correlated with severity of RRV disease (Figure 2.10B), with higher levels of MBL observed in patients classified as having severe disease. Severity of disease also correlated with increased levels of C4a in the synovial fluid (Figure 2.10C), which could result from complement activation through either the lectin or classical pathway. However, analysis of the level of C1q-C4 complexes formed within the synovial fluid, an activation marker of the classical pathway (249), showed no difference between patients with severe or mild disease (Figure 2.10C), suggesting that the higher C4a levels in severe RRV disease was primarily due to activation through the lectin pathway. In addition, we did not observe a difference in levels of Bb, an activation marker of the alternative pathway (Figure 2.10C), further supporting the hypothesis that the MBL pathway primarily mediates complement activation following RRV infection. Importantly, when we assessed MBL levels in a cohort of patients suffering from non-inflammatory osteoarthritis, we found no evidence for elevated MBL levels (mean MBL levels of 57.8 $\pm$ 24.8 ng/ml [n=5 patients with severe osteoarthritis]) compared to MBL levels of 485 $\pm$

163.7 ng/ml in patients with severe RRV induced disease and 218.5 ± 82.4 ng/ml within

the synovial fluid of patients with mild RRV-induced disease, suggesting that elevated

levels of MBL are not simply the result of arthritis symptoms within the joints. Although

additional studies with a larger cohort of patients are required to determine whether MBL

levels associate with the severity of RRV-induced arthritis, and whether this effect

reflects a causal role for MBL in human disease, these results, combined with the

knockout mouse studies strongly suggest that the MBL pathway of complement

activation plays a major role in the pathogenesis of RRV-induced inflammatory disease.

2.5 Discussion

Alphaviruses such as CHIKV and RRV represent significant emerging disease threats that cause large-scale outbreaks of severe chronic and persistent arthralgia/myalgia in human populations. Though alphavirus-induced arthralgia and myalgia is often debilitating, the mechanisms by which these viruses cause arthritis/arthralgia are not fully understood. Previous studies have shown that inflammatory macrophages play a major role in the pathogenesis of both RRV and CHIKV (68, 135), that the host complement cascade is essential for the induction of muscle destruction by these inflammatory cells during RRV infection, and that this process is dependent on complement receptor 3 (CR3) (158, 160). The data presented here demonstrate that RRV infection results in the deposition of MBL within RRV infected tissues, and that MBL, but not the alternative or classical complement activation pathways, was essential for RRV induced complement activation and subsequent inflammatory tissue destruction and disease. Consistent with this, humans suffering from severe RRV disease exhibited increased levels of MBL, but not markers of the classical or alternative complement activation pathways in their synovial fluid. Therefore, these studies demonstrate that MBL plays a key role in promoting the pathogenesis of alphavirus-induced inflammatory disease, and suggest that MBL may represent a target for therapeutic intervention in the treatment of alphavirus-induced arthritis/myositis.

MBL has generally been associated with a protective role during viral infection, either through its ability to neutralize viruses directly or via the downstream activation of complement. In the context of arbovirus infection, MBL contributes to direct neutralization of mosquito-derived West Nile virus and both mammalian and mosquito-

derived dengue virus through interactions between MBL and viral N-linked glycans (7, 61), and MBL contributes to protection from West Nile virus-induced disease in vivo (62). Though the host complement cascade has been shown to play a protective role during neurotropic alphavirus infection (23, 98, 99) these processes are dependent upon either the classical or alternative complement activation pathways (99). Furthermore, though Fuchs, et al., found that MBL bound and neutralized WNV virions, they found no evidence for MBL interactions with two alphaviruses, CHIKV and Sindbis virus (61), which is supported by our inability to demonstrate direct binding or neutralization of RRV virions by MBL. Therefore, our findings demonstrate a novel role for MBL in the pathogenesis of alphavirus-induced arthritis/myositis and indicate that this pathway, which plays a protective role against many viral infections, is actually a major driver of RRV-induced tissue pathology and disease.

In addition to its prominent role in the pathogenesis of RRV-induced disease, the complement cascade is linked to a number of host autoimmune inflammatory disorders, including rheumatoid arthritis (reviewed in (103)). However, the role of MBL in these processes is less clear. Though MBL has been shown to contribute to ischemic injury in mouse models of cardiac or intestinal reperfusion injury (89, 112, 205, 237), MBL has not been directly linked to inflammatory arthritis. There are conflicting reports associating MBL polymorphisms with rheumatoid arthritis in humans (80, 109, 110, 198, 228), however in mouse models of collagen-induced arthritis, which serves as a model of RA, MBL is dispensable for complement activation and arthritis induction (10, 11). Therefore, MBL appears to be playing a unique role in the pathogenesis of RRV-induced

arthritis/myositis that is not shared with other arthritic syndromes, though further comparisons between these different disease states are needed to clarify this issue.

The studies presented here demonstrate that MBL-dependent complement activation promotes RRV-induced disease and raises several questions relating to the mechanism of RRV activation of complement, the role of MBL polymorphisms in determining disease severity, and the therapeutic potential of MBL inhibition to treat RRV-infected patients. The CRD of MBL recognizes terminal carbohydrates, such as mannose and glucose, which can be found on glycosylated proteins in bacteria and viruses. The RRV glycoproteins contain three N-linked glycosylation sites that are glycosylated with a combination of high mannose and complex glycans (210) and may serve as ligands for MBL, leading to complement activation. While we did not observe direct binding of MBL to virions, we did observe an increase in the amount of MBL deposited onto infected tissues and on virally infected cells (Figure 2.3), indicating that some aspect of RRV infection induces MBL deposition and complement activation. Alphaviruses bud from the plasma membrane of infected cells and the viral glycoproteins are prominently exposed on the surface of the cell. Therefore, it is possible that MBL is recognizing and binding to viral glycoproteins on infected tissues during viral egress, resulting in complement activation directly onto the tissue rather than binding to free virus. Alternatively, viral infection may lead to the modification of host cell N-linked glycans or other cellular components, thereby promoting MBL deposition and complement activation; however, both of these possibilities require further investigation.

Given the central role of MBL in development of severe RRV-induced disease, specific inhibition of the MBL activation pathway of the complement system in RRV-

patients may be a strategy to alleviate disease. Current therapy involves administration of

non-steroidal anti-inflammatory drugs, and given the role that complement plays in

mediating severe RRV-induced disease, treatment with complement inhibitors may

provide an attractive alternative to nonspecific anti-inflammatory drugs. However,

prolonged inhibition of the complement system can leave patients susceptible to other

infectious diseases, especially as treatment of disease symptoms may require several

months for some individuals (163). Our results suggest that a more focused approach

targeting MBL may prove effective in limiting RRV-induced arthralgia/myalgia, while

limiting the general immune suppression associated with complement inhibition.

Inhibitors targeting the MBL pathway of complement through inhibition of MASP-2 are

in development (14), and may be useful in treatment of RRV-induced disease in humans.

In addition to raising the possibility of targeting MBL in the treatment of RRV or

other alphavirus-induced arthraligias/myalgias, these studies raise the issue of whether

polymorphisms in MBL affect susceptibility to RRV-induced disease. Common genetic

polymorphisms within the promoter region and exon 1 of the human *Mbl2* gene lead to

variations in serum MBL levels or functional deficiency of MBL (reviewed in (51)).

Human patients with severe RRV disease have higher levels of MBL within the synovial

fluid and serum; however, it is unclear if levels of MBL are elevated in response to

severe RRV infection or if naturally higher levels of MBL contribute to the development

of severe disease. Preliminary analysis of a small cohort of RRV patients does not

associate *Mbl2* polymorphisms with severity of RRV disease (S. Mahalingam, B. Piraino,

B. Cameron, L. Herrero, and A. Lloyd, unpublished data), however a larger cohort of

RRV-infected individuals must be analyzed before we can conclude whether MBL

polymorphisms associate with RRV-induced disease severity or if up-regulation of MBL in response to viral infection contributes to disease pathogenesis in humans.

In summary, the data presented in this study demonstrate the role for MBL in promoting severe disease following RRV infection through complement activation and subsequent destruction of RRV infected tissue. Numerous studies have shown a protective role for MBL and the complement system in response to a diverse set of viruses. Our results demonstrate a novel role of MBL following viral infection in which MBL contributes to development of severe disease, and these findings suggest that MBL may be a therapeutic target for treatment in humans suffering from RRV-induced polyarthritis or other alphavirus-induced arthritides.

2.6 Acknowledgements

Figure 2.1: MBL is required for development of severe RRV-induced disease and tissue damage.

A.
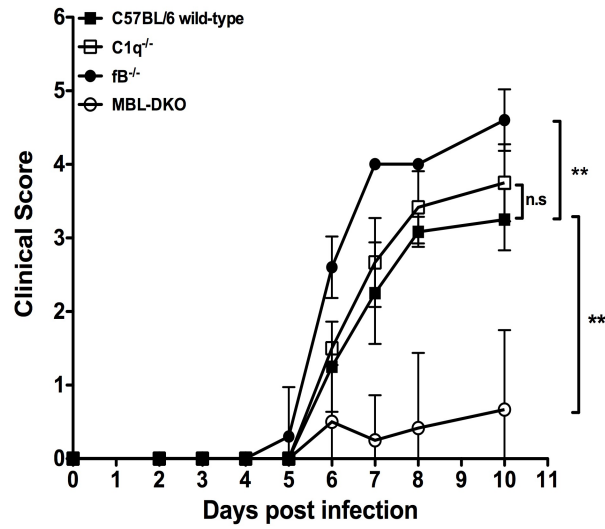
B.

Figure 2.1 MBL is required for development of severe RRV-induced disease and tissue damage.

(A-B) Twenty-four day old WT C57BL/6 (solid square, n=6), C1q$^{-/-}$ (open square, n=6), fB$^{-/-}$ (solid circle, n=5), or MBL-DKO (open circle, n=6) mice were infected with RRV, scored for hind limb function based on a scale described in the Materials and Methods **(A)**, and assessed for weight loss **(B)**. Each data point represents the arithmetic mean ±SD and is representative of at least three independent experiments. We performed a Mann-Whitney analysis with multiple comparison corrections (p<0.01 was considered significant) on clinical scores at 10 dpi and a one-way ANOVA analysis with Bonferroni's correction on percent of starting weight at 10 dpi (p<0.05 was considered significant) to determine significance between the various knock-out lines compared to WT **p<0.01; *** p<0.001; n.s. not significant.

Figure 2.2: MBL is required for development of severe RRV-induced pathology and tissue damage within skeletal muscle.

A.
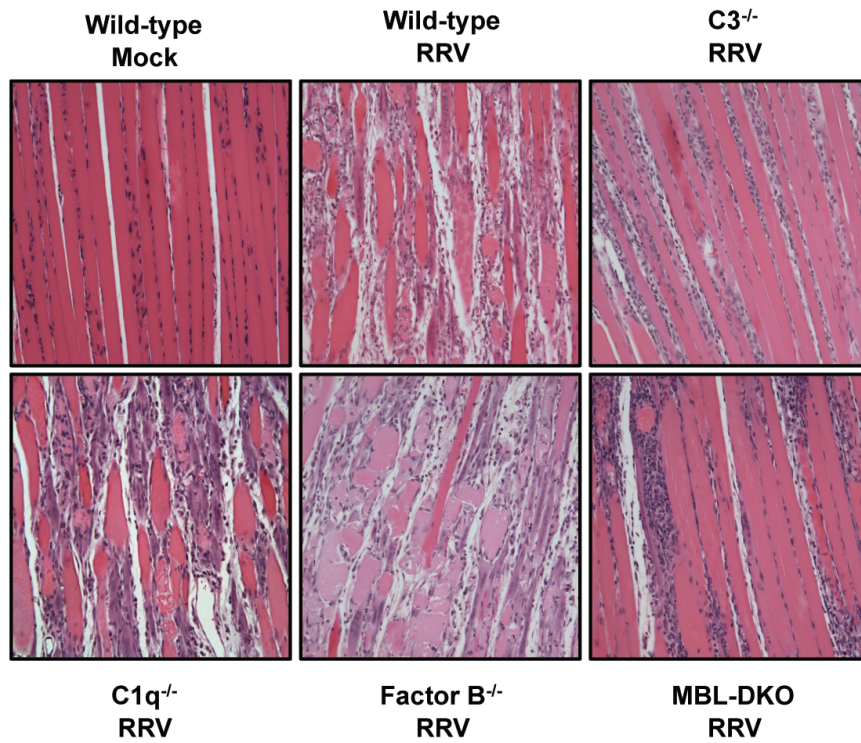
B.
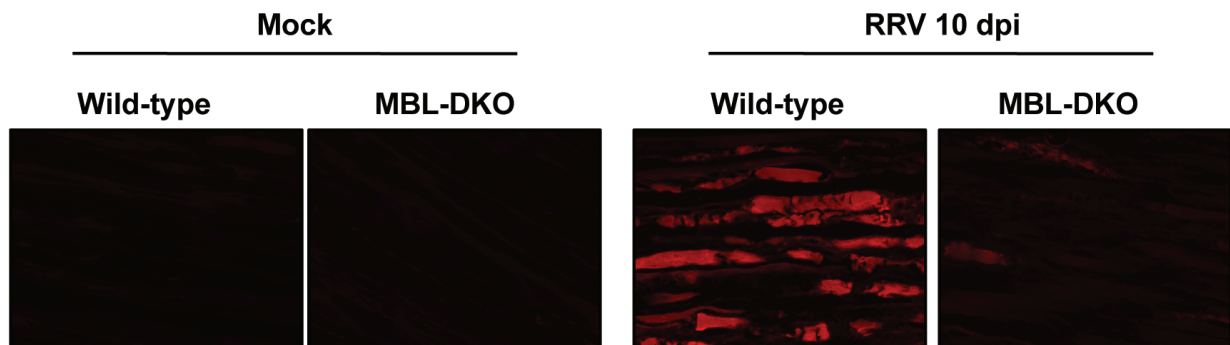
Figure 2.2 MBL is required for development of severe RRV-induced pathology and tissue damage within skeletal muscle.

(A) Twenty-four day old WT C57BL/6, C1q$^{-/-}$, fB$^{-/-}$, or MBL-DKO mice were infected with RRV. Tissue pathology and inflammation was examined at 10 dpi by H&E staining of paraffin embedded sections of quadriceps muscle. A representative section from each knockout strain is shown. A section from RRV-infected C3$^{-/-}$ is shown for comparison.

(B) To assess damage within the muscle, mock or RRV-infected WT or MBL-DKO mice were injected with EBD at 10 dpi, and frozen sections were generated. EBD positive muscle fibers were identified by fluorescence microscopy. Representative sections of mock- and RRV-infected mice are shown and are representative of two independent experiments.

Figure 2.3: RRV infection induces MBL deposition onto cells

A.
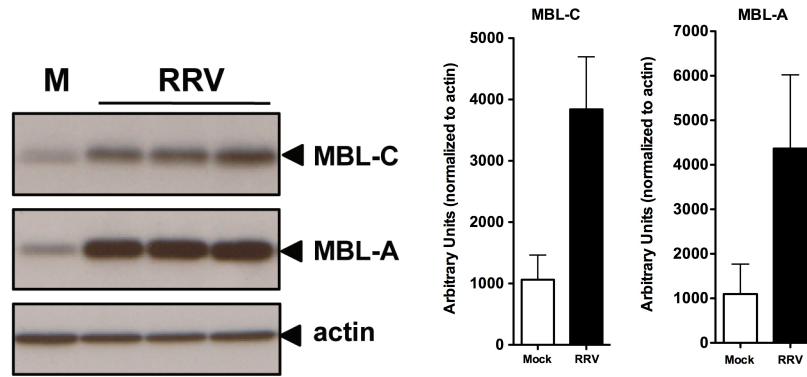
B.
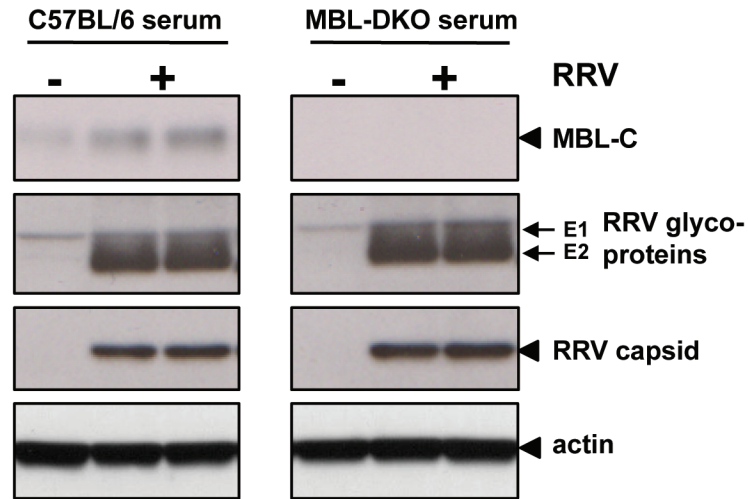
Figure 2.3 RRV infection induces MBL deposition onto cells

(A) To determine if MBL levels are elevated within the quadriceps muscles of RRV-infected wild-type animals, homogenized quadriceps muscles from either mock- or RRV-infected WT mice at 7 dpi were analyzed by immunoblot analysis using anti-mouse MBL-A, anti-mouse MBL-C, or anti-mouse actin antibodies. Each lane represents an individual mouse and is representative of at least three independent experiments. Densitometry measurements of bands in immunoblot from three different experiments are graphically depicted as arbitrary units normalized to actin (mock n=4; RRV n=9).

(B) To determine if MBL deposition is enhanced onto RRV-infected cell, differentiated C2C12 murine skeletal muscle cells were infected with RRV, and incubated with either serum from a WT or MBL-DKO mouse for 30 minutes prior to harvesting. Cells were washed, harvested, and lysates were analyzed by immunoblot analysis using anti-mouse MBL-C, anti-RRV, or anti-mouse actin antibodies.

Figure 2.4: MBL does not bind or neutralize RRV virions.

A.
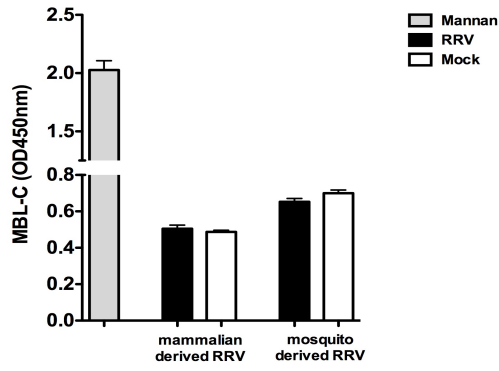
B.
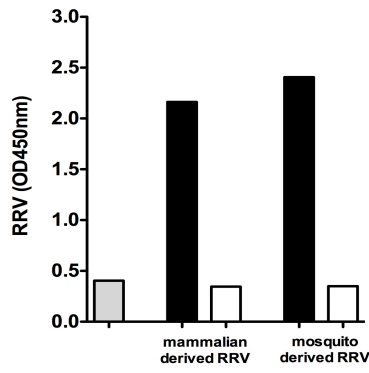
C.
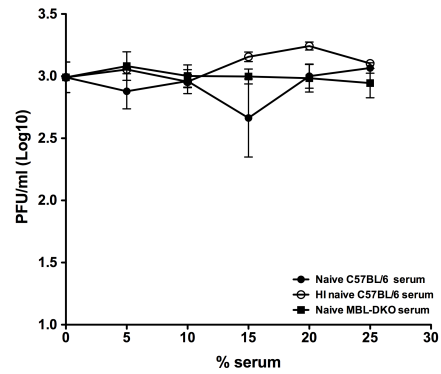
Figure 2.4 MBL does not bind or neutralize RRV virions.

(A-B) To determine if MBL could bind to RRV virions directly, a modified sandwich ELISA was performed. Wells were coated with mannan (grey bar), mammalian or mosquito-derived RRV (solid bar), or mock supernatant (open bar), and were subsequently incubated in WT mouse serum as a source of MBL. **(A)** The amount of MBL deposition within the wells was detected by an antibody against mouse MBL-C using standard ELISA techniques. **(B)** The amount of RRV antigen was detected using an antibody against the RRV structural proteins. Data is expressed as raw OD_{450nm} values normalized to background, and each bar is the arithmetic mean ± SD of three replicates and is representative of two independent experiments.

(C) To determine if RRV could be directly neutralized by complement components within serum, 10^3 PFU of RR64 was incubated with increasing amounts of naïve mouse serum from wild-type (solid circle) or MBL-DKO mice (solid square), or heat-inactivated wild-type serum (open circle) for 1 hour at 37°C. The number of plaques was determined by plaque assay on BHK-21 cells. Each data point represents the arithmetic mean ± SD of three replicates and is representative of three independent experiments.

Figure 2.5: Complement activation within quadriceps muscle is largely dependent on MBL.
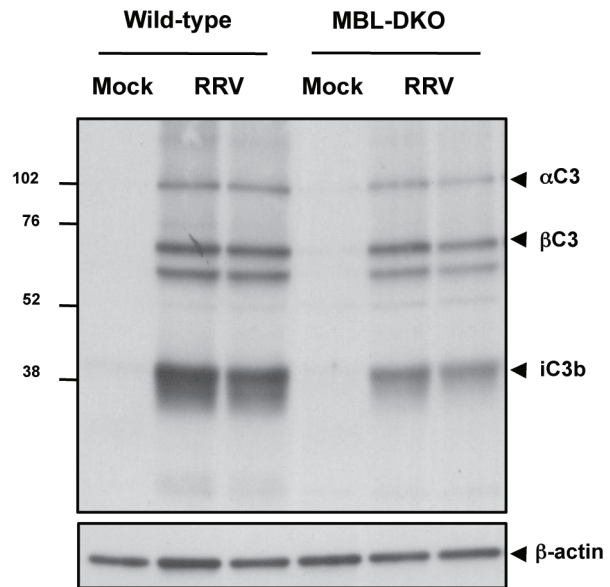
Figure 2.5. Complement activation within quadriceps muscle is largely dependent on MBL.

To determine if complement activation was dependent on MBL, we analyzed homogenized quadriceps muscles from either mock- or RRV-infected WT or MBL-DKO mice 7 dpi by immunoblot analysis using an anti-mouse C3 or anti-mouse actin antibody. C3 cleavage products are indicated with solid arrowheads. Each lane represents an individual mouse, and the western blot is representative of three independent experiments

Figure 2.6: MBL is required for C3 deposition following RRV-infection.

A.
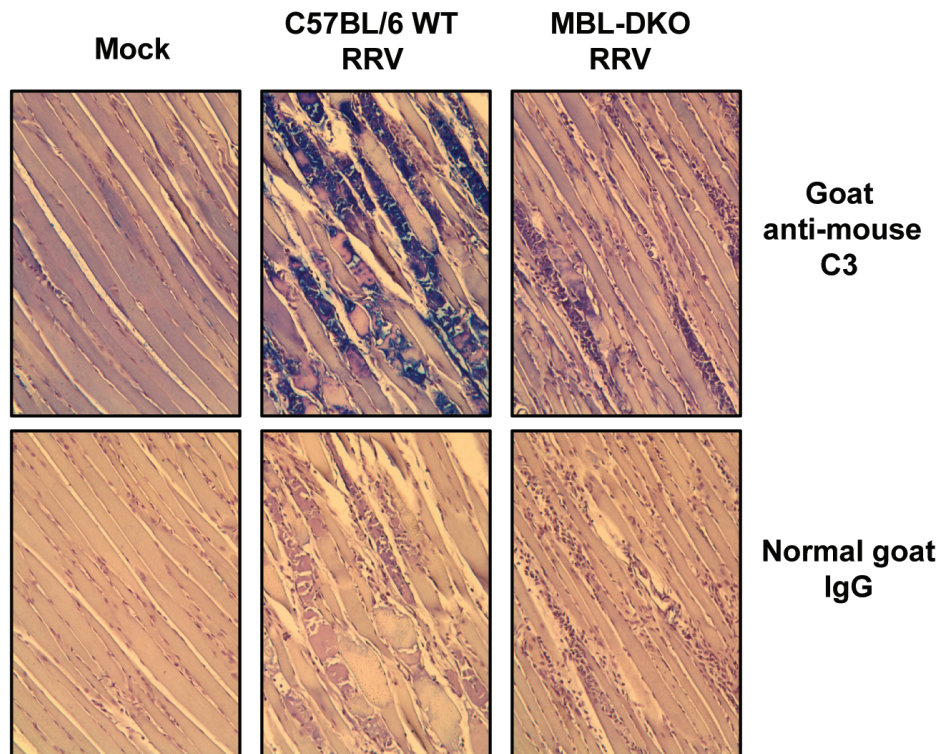
B.
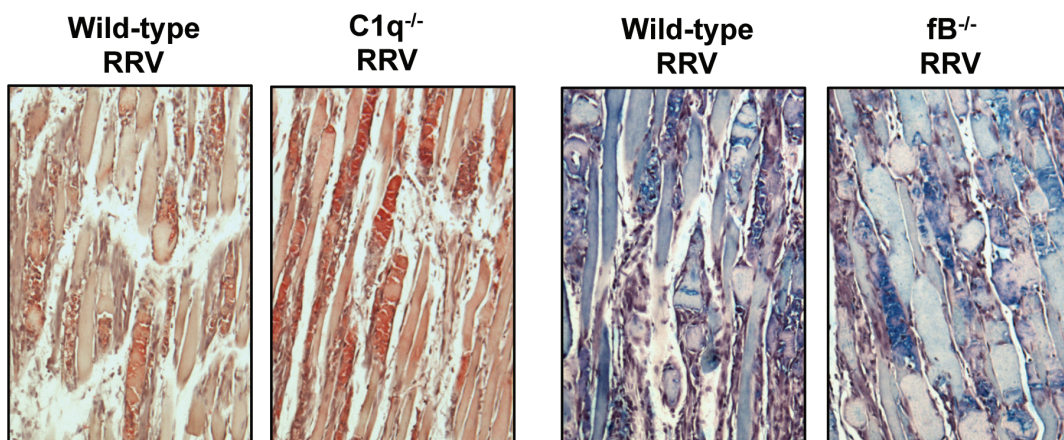
Figure 2.6. MBL is required for C3 deposition following RRV-infection.

(A) C3 deposition was assessed by IHC using an anti-mouse C3 antibody on quadriceps muscle sections from either mock- or RRV-infected WT or MBL-DKO mice at 7 dpi. C3 positive areas are stained in blue. A representative section from each strain is shown and is representative of two independent experiments. No signal was observed in sections incubated with a control goat IgG antibody.

(B) To determine if either the classical or alternative complement activation pathways contribute to C3 deposition following RRV infection, we performed IHC using an anti-mouse C3 on quadriceps muscle sections from RRV-infected wild-type, C1q$^{-/-}$, or fB$^{-/-}$ at 10 dpi. C3 deposition is shown in red for C1q$^{-/-}$ and the wild-type control, and in blue for the fB$^{-/-}$ and wild-type control. 5μm thick paraffin-embedded sections were prepared as described in the Materials and Methods, with the following modification: RRV-infected C1q$^{-/-}$ and wild-type sections were developed using Vector Red Alkaline phosphatase substrate kit (Vector Labs, CA) instead of Vector Blue Alkaline phosphatase substrate kit. A representative section from each strain is shown (n=3 for wild-type mice, n=3 for C1q$^{-/-}$ mice; n= 3 for wild-type mice, n=3 for fB$^{-/-}$ mice)

Figure 2.7: MBL deficiency does not affect viral replication or tropism within infected tissues.

A.
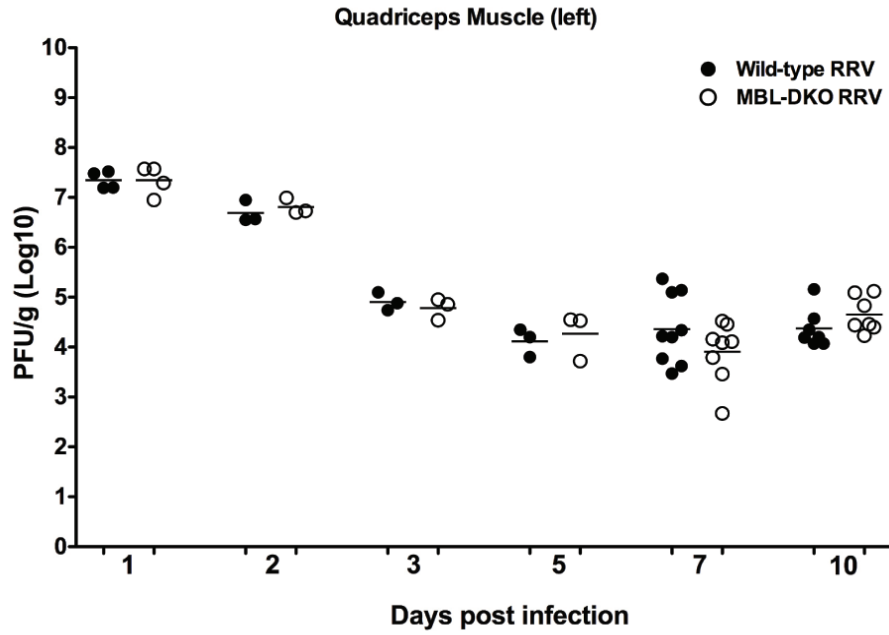
B.
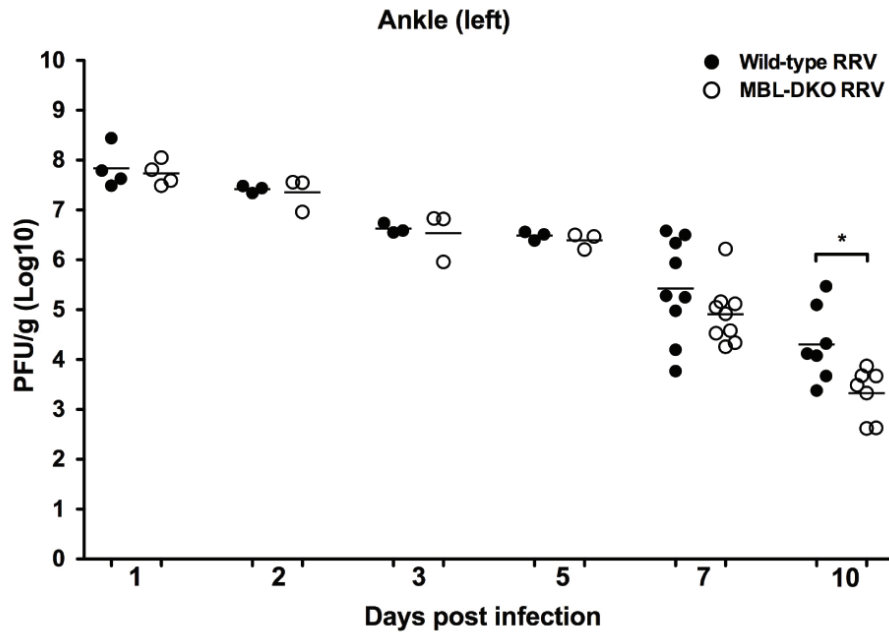
Figure 2.7: MBL deficiency does not affect viral replication or tropism within infected tissues.

C.
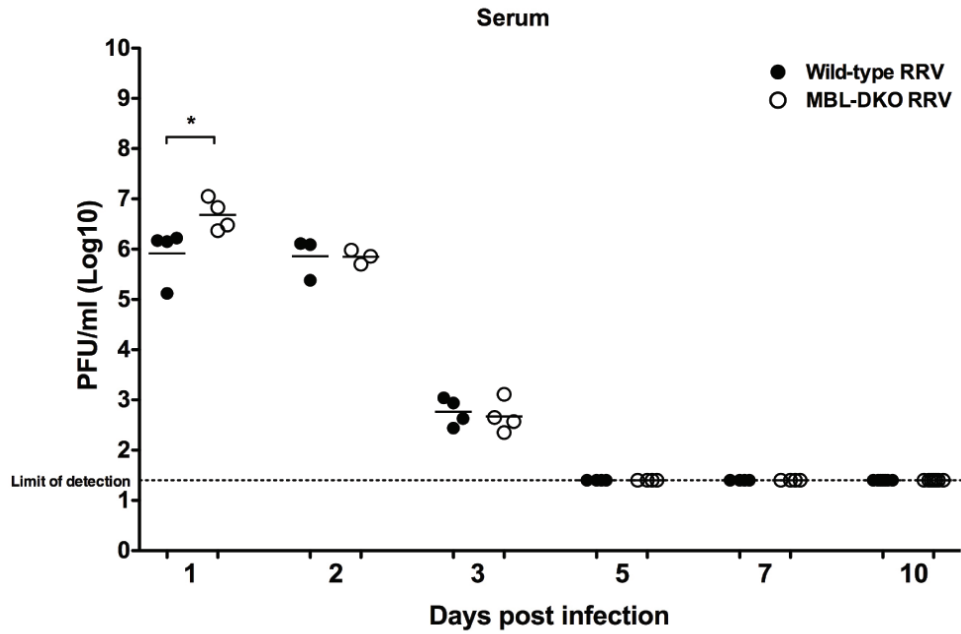
D.
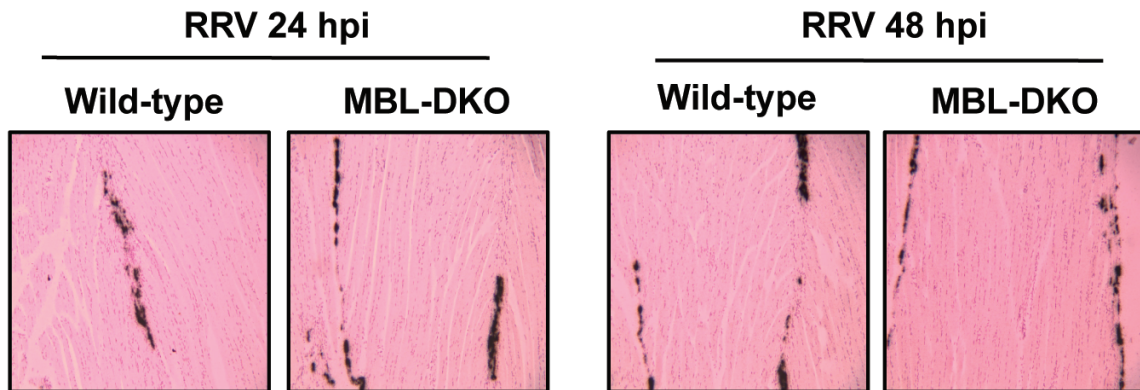
Figure 2.7 MBL deficiency does not affect viral replication or tropism within infected tissues.

(A-C) Quadriceps muscle (A), ankle joints (B), and serum (C) from RRV-infected WT (solid circles, n=3-9/time point) or MBL-DKO (open circles, n=3-8/time point) mice were assayed to determine viral titer at various times post infection. Viral titer was determined by plaque assay on BHK-21 cells. Each data point represents the viral titer from a single animal; data is combined from two independent experiments. *p<0.05 as determined by t-test.

(D) Tropism within the quadriceps muscle tissue was determined by *in situ* hybridization using RRV-specific probe. We did not detect any signal using an EBER-specific probe (data not shown). A representative section from each strain is shown (n=3 for both WT and MBL-DKO mice)

Figure 2.8: MBL deficiency does not affect inflammatory cell recruitment.

A.
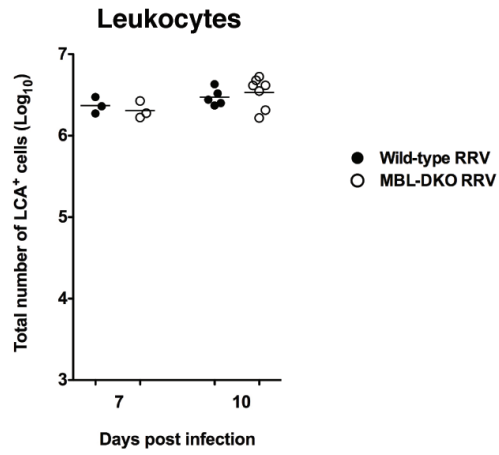
B.
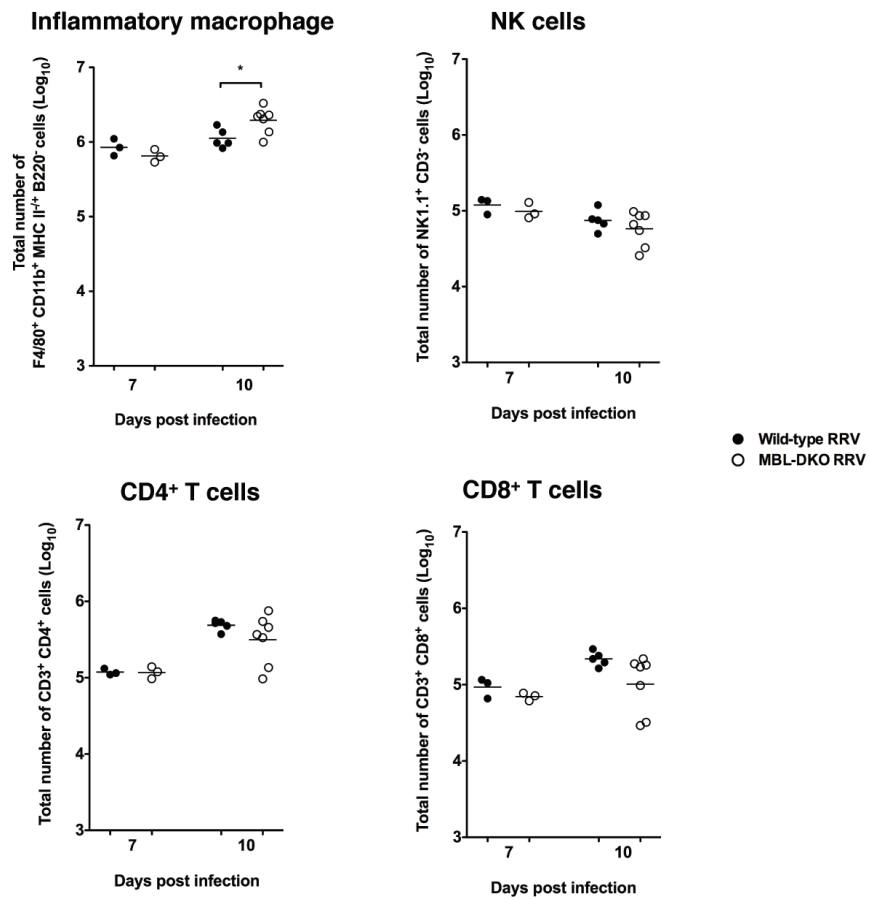
Figure 2.8 MBL deficiency does not affect inflammatory cell recruitment.

(A-B) Leukocytes were isolated from the quadriceps muscle of RRV-infected WT (solid circles, n=3-5/time point) or MBL-DKO (open circles, n=3-7/time point) mice at 7 or 10 dpi. Cells were characterized and quantified by flow cytometry using the markers described in the materials and methods. Total numbers of leukocytes (A) and specific cells types (B) are shown. A single experiment for each time point is shown. *p<0.05 by Mann-Whitney analysis.

Figure 2.9: MBL deficiency alters expression of inflammatory mediators within the RRV infected muscle.
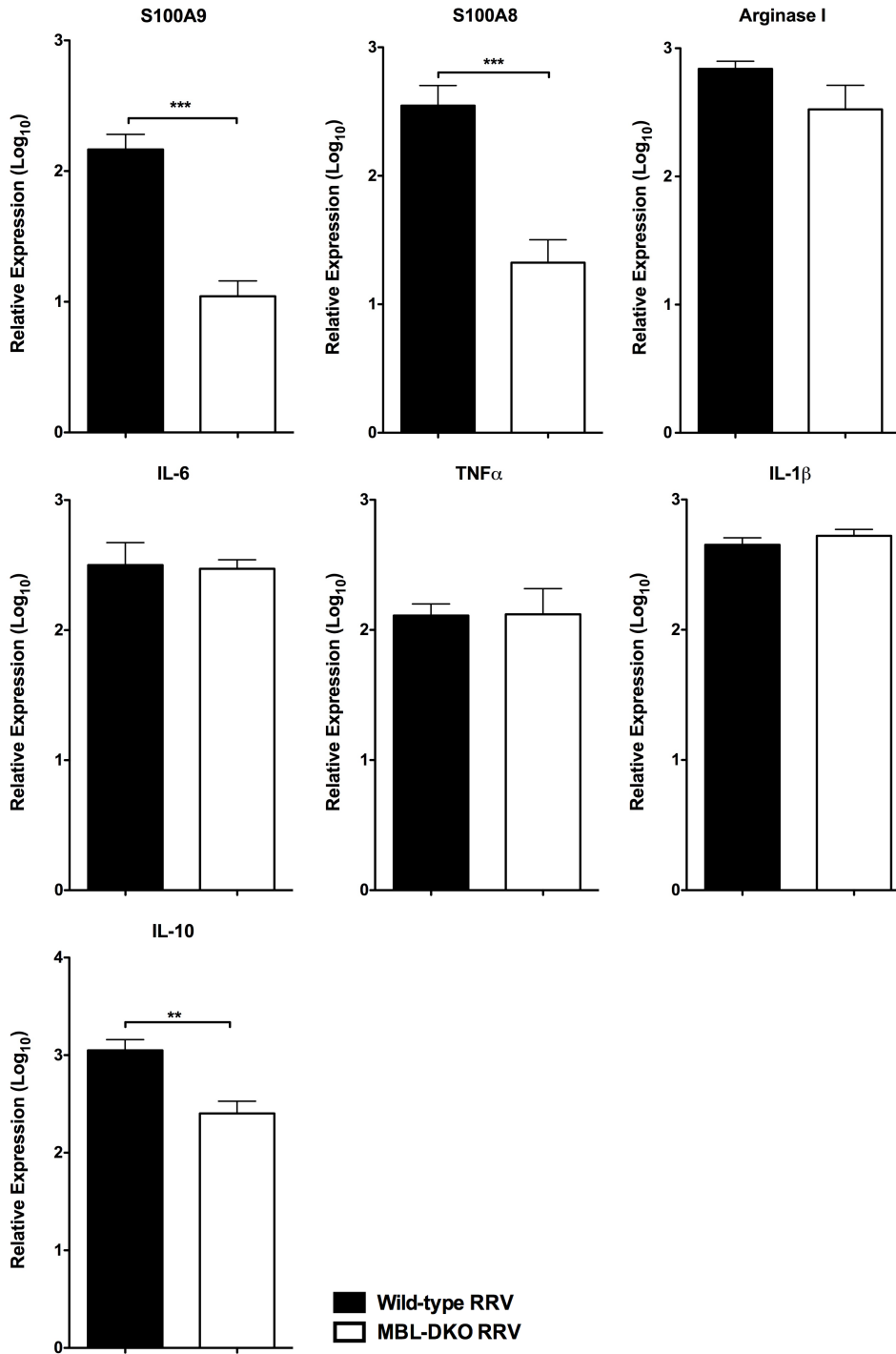
Figure 2.9 MBL deficiency alters expression of inflammatory mediators within the RRV infected muscle.

Relative mRNA expression of C3-dependent inflammatory mediators and cytokines S100A9, S100A8, Arginase I, and IL-6, and C3-independent cytokines TNFα, IL-1β, and IL-10 from quadriceps muscle from RRV-infected WT (solid bar, n=3) or MBL-DKO (open bar, n=3) mice by quantitative real-time PCR. Raw data values were normalized to 18S rRNA levels, log-transformed, and are graphically depicted as fold expression over mock-infected mice. Data from a single experiment is shown, but is representative of two independent experiments. ***$p<0.001$; **$p<0.005$ by t-test.

Figure 2.10: Levels of MBL are elevated in RRV patients.

A.
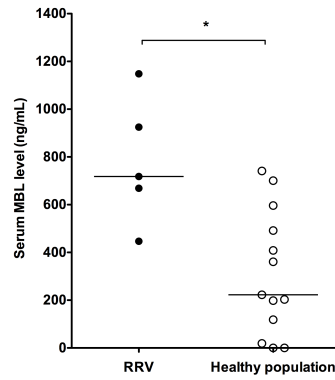
B.
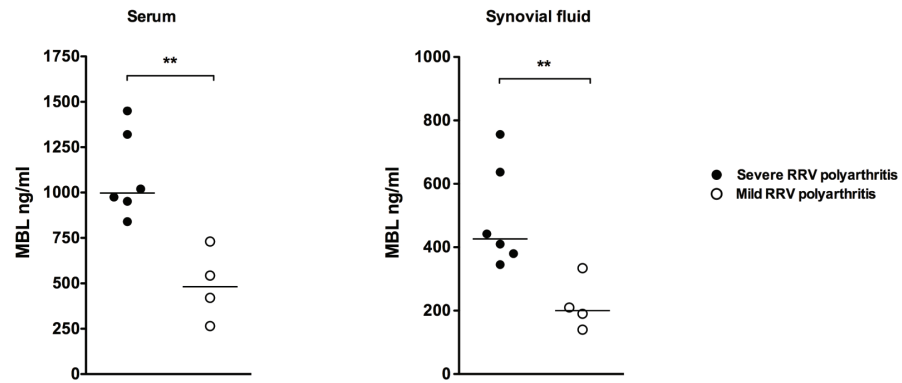
C.
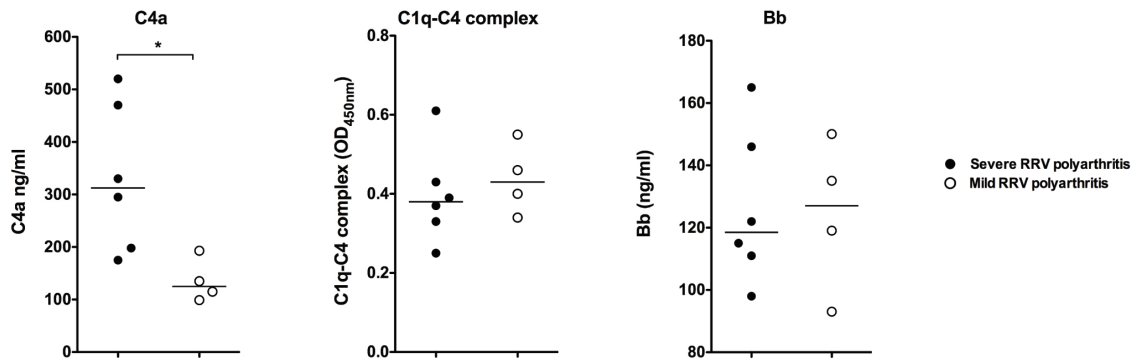
Figure 2.10 Levels of MBL are elevated in RRV patients.

(A) Serum from RRV-infected patients (solid circles, n= 5) or healthy sero-negative controls (open circles, n=13) were analyzed by ELISA for MBL levels. Each data point represents a single individual, and bar represents the median. *$p<0.05$ by Mann-Whitney analysis.

(B) MBL levels within serum and synovial fluid from patients clinically characterized with either severe RRV-induced disease (solid circles, n=6) or mild RRV-induced disease (open circles, n=4) were analyzed by ELISA. Each data point represents a single individual, and the bar represents the median. **$p<0.01$ by Mann-Whitney analysis.

(C) Levels of C4a (left), C1q-C4 complex (middle) and Bb (right) within the synovial fluid from patients described in (B) were analyzed by ELISA. *$p<0.05$ by Mann-Whitney analysis.

Figure S2.1: Representative flow cytometry plots and gating scheme used to characterize inflammatory infiltrates.

A.
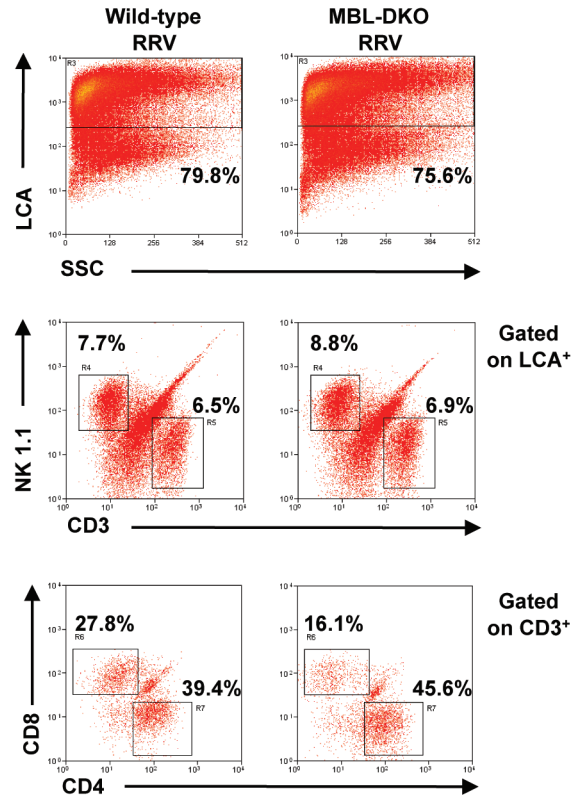
B.
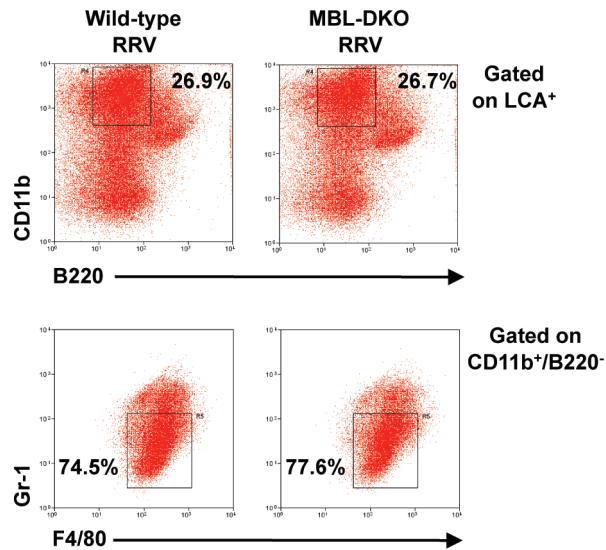
Figure S2.1 Representative flow cytometry plots and gating scheme used to characterize inflammatory infiltrates.

(A) To determine the number of leukocytes, we gated on LCA$^+$ cells. To further distinguish between NK cells and T cells, we analyzed expression of NK1.1 and CD3 on LCA$^+$ lymphocytes. NK1.1$^+$CD3$^-$ were classified as NK cells, and NK1.1$^-$CD3$^+$ cells were classified as T cells. T cells were further classified into CD4$^+$ and CD8$^+$ T cells based on CD4 and CD8 expression. Percentages displayed on plots represent the percentage of cells within the indicated gate. (B) To determine the number of inflammatory macrophage, we first gated on LCA$^+$ cells, followed by analysis of CD11b and B220 expression. Inflammatory macrophage typically stain CD11b$^+$B220$^-$. We distinguished inflammatory macrophage from neutrophils within the CD11b$^+$B220$^-$ population by analyzing F4/80 and Gr-1/Ly-6G expression; inflammatory macrophage were defined as CD11b$^+$B220$^-$F4/80$^+$Gr-1^{lo}. Percentages displayed on plots represent the percentage of cells within the indicated gate.

CHAPTER THREE:

ROSS RIVER VIRUS ENVELOPE N-LINKED GLYCANS CONTRIBUTE TO ALPHAVIRUS-INDUCED ARTHRITIS AND MYOSITIS THROUGH ACTIVATION OF THE HOST COMPLEMENT SYSTEM.

3.1 Summary

Mannose binding lectin (MBL) generally plays a protective role during viral infection, both through the ability to directly neutralize viruses and its role in activating the host complement cascade. However, in the context of alphavirus-induced arthritis and myositis, MBL-mediated complement activation plays a pathologic role by promoting virus-induced inflammatory tissue destruction. To define the mechanisms by which MBL contributes to virus-induced disease following Ross River virus (RRV) infection, studies were performed to identify specific viral factors were involved in promoting MBL-dependent complement activation. Since MBL recognizes and binds to terminal carbohydrates, we hypothesized that one or more of the three N-linked glycosylation sites on the RRV envelope glycoproteins acted as ligands for MBL binding and subsequent complement activation and disease. Using a panel of RRV mutants lacking one or more envelope glycans, we have found that the RRV E2 N-linked glycans were required for MBL binding to infected cells and induction of RRV-induced disease. Animals infected with a virus lacking both N-linked glycans on the E2 glycoprotein (E2 N200;262Q) exhibited reduced disease, significantly less tissue damage, and decreased MBL binding

---

Authors: Bronwyn M. Gunn, Reed S. Shabman, Alan C. Whitmore, Lance K. Blevins, Thomas E. Morrison, and Mark T. Heise

and complement activation compared to animals infected with the wild type virus. These results demonstrate that interactions between MBL and the viral N-linked glycans play a major role in promoting virus induced disease and suggest that targeting these interactions may be of benefit in developing potential therapies in the treatment of alphavirus-induced arthritis.

3.2 Introduction

Arthritic alphaviruses such as RRV and chikungunya virus (CHIKV) are mosquito-borne viruses that cause outbreaks of debilitating infectious arthritis in many regions of the world. These viruses are transmitted to humans primarily by the *Aedes* and *Culex* species of mosquito and have been found to cause epidemics of disease in both urban and rural settings (86). Both RRV and CHIKV share similar disease symptoms that are characterized by debilitating polyarthritis and myositis that frequently results in painful swelling of the peripheral joints. Studies in both humans and mice have identified a critical role for the host inflammatory response in the development of RRV-induced arthritis and immunopathology associated with disease (135, 161). In particular, the host complement system plays a critical role in development of disease and is thought to act not through direct lysis of cells by formation of the terminal complex, but rather through activation of CR3-bearing inflammatory cells to mediate direct damage to the inflamed tissues (158, 160). Furthermore, we recently demonstrated that the lectin pathway, which is one of the three main activation pathways of the complement system, initiated by mannose binding lectin (MBL) mediates activation of complement following RRV infection and contributes to disease without altering tropism and viral burden (79). This

is in contrast with many other viral systems, such as West Nile virus (WNV), Ebola virus, human immunodeficiency virus, and SARS-CoV, where MBL plays a protective role during infection, either through direct inhibition of viral infection or via complement activation (54, 61, 111, 257).

MBL-mediated complement activation is initiated by the recognition of terminal sugars on glycosylated proteins by the CRD of MBL (reviewed in (223)). Though we have previously demonstrated that MBL does not directly bind to free RRV virions, given the ligand specificity of MBL, we hypothesized that MBL might interact with the N-linked glycans on the RRV envelope glycoproteins when they are displayed on the surface of infected cells. The alphavirus glycoproteins E1 and E2 contain three to four N-linked glycosylation sites (Asn - X - Ser/Thr) that are glycosylated with N-linked glycans (219). The RRV pE2 and E1 glycoproteins are synthesized and processed through the ER and then further processed in the Golgi to generate mature E2-E1 heterodimers. The E2-E1 heterodimers self-assemble into trimeric spikes at the plasma membrane, and each budding alphavirus virion incorporates 80 glycoprotein spikes to make up the viral envelope. The E2 glycoprotein is prominently displayed on the surface of the virus and on the surface of infected cells, and for most alphaviruses, two of the N-linked glycans are located on E2. The positions of the RRV E2 glycans on the glycoprotein spike have been mapped: the E2 N200 carbohydrate moiety is located on one side of the tip of the protruding E2 "petal", and the E2 N262 glycan appears to be located between the trimeric spikes (174). Thus, the RRV E2 N-linked glycans are surface exposed and are in a key position to interact with host proteins. The RRV E2 N-linked glycans are glycosylated with a combination of high mannose and complex glycans when produced in mammalian

cells; the glycan at E2 N200 is either a high mannose or hybrid glycan and the E2 N262 position is predominantly glycosylated with a complex glycan (210). The role of these N-linked glycans in arthritic alphavirus pathogenesis to date has not been evaluated.

In this study, we have used a panel of mutant viruses that lack one or both of the two N-linked glycosylation sites on E2 to demonstrate that the E2 N-linked glycans are required for MBL binding to virally infected cells and subsequent induction of virus-induced disease. While RRV infected cells are readily bound by MBL, this activity was lost when the cells were infected with RRV lacking both N-linked glycans on the viral E2 glycoprotein. Furthermore, viruses lacking either E2 N-linked glycosylation site cause reduced RRV disease in mice, while a virus lacking both sites causes very mild disease. Our results supports a model of RRV disease pathogenesis wherein the E2 N-linked glycans promote activation of the lectin complement pathway by MBL, resulting in activation of CR3-bearing inflammatory cells and subsequent damage within inflamed tissues

3.3 Materials and Methods

Viruses and cells. Wild-type RRV is derived from the infectious clone of RRV T48 (pRR64), and the E2 N-linked glycan mutants were generated previously by site directed mutagenesis of N-linked glycosylation sites in E2 in pRR64 (210). The viral stocks used in this study were generated as described in (161). Briefly, viral RNA was generated through *in vitro* transcription of SacI-linearized pRR64 using the mMessage mMachine SP6 kit (Ambion) and electroportated into BHK-21 cells (ATCC). Viral titer was determined by plaque assay on BHK-21 cells. BHK-21 cells were grown in α-MEM

(Gibco) supplemented with 10% donor calf serum (DCS), 10% tryptose phosphate, L-glutamine, penicillin, and streptomycin. Murine myoblast C2C12 cells (ATCC) were grown in DMEM supplemented with 20% FBS, L-glutamine, penicillin, and streptomycin prior to differentiating. To differentiate cells into myotubes, confluent C2C12 cells were maintained in DMEM supplemented with 2% horse serum, L-glutamine, penicillin, and streptomycin for 96 hours. Primary myoblasts from C57BL/6 mice were harvested from limbs of 1-day old mice. Skeletal muscle was dissociated using type I collagenase (Worthington Biochemicals) and grown in DMEM supplemented with 6% FBS, L-glutamine, penicillin, streptomycin, and gentamycin. To differentiate cells, the medium was replaced with DMEM containing 3% FBS.

MBL deposition onto myotubes. Differentiated myotubes (either C2C12 or primary cells from C57BL/6 mice) cells either mock-infected or infected with RRV WT or RRV E2 DM at an approximate MOI of 20. At 18 hpi, culture medium was removed and cells were incubated in medium containing either 10% serum from WT or MBL-DKO mice for an additional 30 minutes. Cells were washed with PBS containing 400mM NaCl and harvested in RIPA lysis buffer. Cell lysates were analyzed by immunoblot analysis as described below.

Immunoblot analysis. At indicated times post infection, mock-infected and RRV-infected mice were sacrificed, and perfused with 1X PBS. Quadriceps muscles were removed and homogenized in radioimmunoprecipitation lysis buffer (RIPA; 50μM Tris pH 8.0, 150mM NaCl; 1% NP-40, 0.5% deoxycholate, 0.1% SDS and 1X complete

protease inhibitor cocktail (Roche)) by glass beads. Protein concentration was determined

by Bradford protein assay and 25-30μg of protein was run onto a 10% SDS-PAGE gel.

Protein was transferred onto a PVDF membrane, and membranes were blocked in 5%

milk, 0.1% Tween-20 in PBS. Membranes were probed with goat anti-mouse MBL-A

(1:1000 R&D Systems), goat anti-mouse MBL-C (1:1000 R&D Systems), goat anti-

mouse C3 polyclonal antibody (1:1000 Cappel), mouse anti-RRV (1:1000 ATCC), or

goat anti-mouse actin polyclonal antibody (1:500 SCBT), washed with PBS containing

0.1% Tween-20 and incubated with rabbit anti-goat antibody or sheep anti-mouse

antibody conjugated to horseradish peroxidase (1: 10, 000 Sigma). Membranes were

washed again and protein visualized by ECL (Amersham) according to manufacturer's

instructions. Densitometry was performed using ImageJ software (NIH).

Immunofluorescence. BHK-21 cells were seeded at 1×10^4 cells/well into an 8-well

chamber slide. Cells were infected at MOI of 1 with either diluent alone (mock), RRV

WT or RRV E2 DM. At 12 hpi medium was removed and cells were incubated in HBSS

with 5mM $CaCl_2$ with or without 10ug/ml rhMBL (R&D Systems) for 30 minutes at

37°C. Cells were washed 3-4 times with PBS, fixed in 1.5% PFA for 15 minutes, washed

and incubated in PBS containing 100mM glycine, followed by incubation in 3% BSA in

PBS with 0.05% Tween 20 containing 10% normal donkey serum. The primary antibody

incubation with anti-MBL-C (SCBT 1:50) and anti-RRV (ATCC 1:1000) for 1 hour at

RT. Wells were washed 3 times with PBS with 0.05% Tween 20 and incubated in

secondary antibody (Alexa Fluor 488-anti mouse 1:1000; Alexa Fluor 594 anti-rabbit

1:1000). Wells were washed in PBS with 0.05% Tween 20 three times and mounted

(ProLong Gold with DAPI, Invitrogen) and imaged by fluorescence microscopy
(Olympus BX61). Images were processed using ImageJ (NIH).

Mice. All mice used in this study were maintained and bred in house at the University of
North Carolina (UNC) in accordance with UNC Institutional Animal Care and Use
Committee guidelines. Mouse studies were performed in strict accordance with the
recommendations in the Guide for the Care and Use of Laboratory Animals of the
National Institutes of Health. All mouse studies were performed at the University of
North Carolina (Animal Welfare Assurance # A3410-01) using protocols approved by the
UNC Institutional Animal Care and Use Committee (IACUC). All studies were
performed in a manner designed to minimize pain and suffering in infected animals, and
any animals that exhibited severe disease signs was euthanized immediately in
accordance with IACUC approved endpoints. C57BL/6 mice were purchased from The
Jackson Laboratories (Bar Harbor, ME) and bred at UNC.

Infection of mice with RRV. While RRV is classified as a biosafety level-2 agent, due
to the exotic nature of the virus, all animal studies were performed in a biosafety level-3
facility. Twenty-four day old mice were inoculated with 10^3 PFU of RRV strain in
diluent (phosphate buffered saline supplemented with 1% DCS) into the left rear footpad.
Mice were weighed daily and assigned a clinical score based on hind limb weakness and
altered gait on the following scale: 0= no disease; 1=mild loss of hind limb grip;
2=moderate loss of hind limb grip; 3=severe loss of hind limb grip; 4= no hind limb grip
and mild inability to right; 5=no hind limb grip and complete inability to right;

6=moribund.

Viral burden analysis. Mice were infected with RRV as described above, and at indicated times post infection mice were sacrificed, perfused with 1X PBS, and indicated tissues were dissected and removed, weighed, and homogenized with glass beads in diluent. Viral titer within infected tissues were determined by plaque assay on BHK-21 cells from tissue homogenates.

Quantitation of RRV genomes. Mice were infected with RRV as described above, and at indicated times post infection, mice were sacrificed, perfused with 1X PBS, and the quadriceps muscle were dissected and removed, and homogenized with glass beads in Trizol (Invitrogen). Total RNA was extracted using Pure Link RNA purification kit (Invitrogen), and cDNA was generated from 1μg of RNA using Superscript III reverse transcriptase. RRV genomes were amplified using a tagged RRV specific primer by quantitative RT-PCR, and absolute numbers of RRV genomes were determined using a standard curve of serial dilutions ranging from 10^8 to 10^0 copies of RRV genomes.

Histological analysis. At desired times post infection, mice were sacrificed and perfused with 4% paraformaldehyde (PFA), pH 7.3. Tissues were paraffin embedded and 5μm sections were generated and stained with hematoxylin and eosin (H&E) to examine tissue pathology and inflammation. Sections were visualized by bright field light microscopy (Olympus BX61).

Evans blue dye uptake analysis. At 10 days post infection mice were injected with 1%

Evans blue dye in PBS into the peritoneal cavity (50µl/10g mouse weight). At 6 hours

post injection, mice were sacrificed and perfused with 4% PFA. Quadriceps muscle

tissues were embedded in optimal cutting temperature compound (OCT) and frozen in an

isopentane histobath, 5µm sections were generated, mounted with ProLong Gold with

DAPI (Invitrogen) and sections were analyzed by fluorescence microscopy (Olympus

BX61).

Immunohistochemistry. At 7 dpi, mice were sacrificed and perfused with 4% PFA.

Quadriceps muscles were removed, paraffin embedded, and 5µm sections were generated.

Sections were deparaffinized in xylene, rehydrated through an ethanol gradient, and

probed with a goat anti-mouse C3 polyclonal antibody (1:500 Cappel) using the

Vectastain ABC-AP kit (Vector Labs, CA) and Vector Blue Alkaline phosphatase

substrate kit (Vector Labs, CA) according to the manufacturers' instructions. Sections

were counterstained with Gill's hematoxylin.

Analysis of infiltrating inflammatory cells by flow cytometry. To determine the

composition of the inflammatory cell infiltrates within the quadriceps muscle, at

indicated times post infection mice were sacrificed and perfused with 1X PBS. Both

quadriceps muscles were removed, minced, and digested with RPMI containing 10%

fetal bovine serum (FBS), 15mM HEPES, 2.5mg/ml collagenase A (Roche), 1.7mg

DNase I (Roche) for 2 hours at 37ºC with shaking. Cells were strained through a 40µm

strainer and washed twice with wash buffer (HBSS containing 1% sodium azide and 1%

FBS) and total viable cells were determined by trypan blue exclusion. To stain cells for flow cytometry, cells were incubated with anti-mouse FcγRII/III (2.4G2; BD Pharmingen) and stained with combinations of the following antibodies: fluorescein isothiocyanate (FITC)-conjugated anti-mouse CD3, phycoerythrin (PE)-conjugated anti-NK1.1, PE-Cy5 anti-CD45 (leukocyte common antigen), PE-Cy7 anti-F4/80, Allophycocyanin (APC)-conjugated anti-CD49b, eF450-conjugated anti-CD11b, APC anti-major histocompatibility complex class II antigens (MHC II), and eF780-conjugated anti-CD45 (B220) (eBiosciences, San Diego, CA), FITC anti-Ly-6G, and PE anti-SigLecF (BD-Pharmingen, San Diego, CA), and PE-Texas Red-conjugated anti-CD45 (B220), and PE-Texas Red anti-CD11c (Molecular Bioprobes, Invitrogen). Cells were fixed with 2% PFA (pH 7.3) and analyzed on a CyAn flow cytometer (Becton Dickinson), and data was analyzed using Summit software.

Gene expression. At 7 dpi following RRV infection, mice were sacrificed and perfused with 1X PBS. Quadriceps muscles were removed and homogenized in Trizol (Invitrogen) using glass beads. RNA was extracted using Invitrogen PureLink RNA purification kit, and cDNA was generated using Superscript III reverse transcriptase. Expression of indicated genes was measured by quantitative real-time PCR. Raw data values were normalized to 18S rRNA levels.

Statistical analysis. Clinical scores and percent of starting weight at 10 dpi between WT RRV and the glycan mutants were analyzed for statistically significant differences by Mann-Whitney analysis. Viral burden, total number of infiltrating cells, and gene

114

expression data at each time point between the different virus strains was analyzed for statistically significant differences either Mann-Whiney analysis, one-way ANOVA, or t-test ($p<0.05$ is considered significant). Statistical analyses were performed using GraphPad Prism 5.

3.4 Results

RRV E2 N-linked glycans contribute to MBL deposition onto infected cells.

We have previously shown that MBL deposition is enhanced on cells following RRV infection, suggesting that some aspect of viral infection induces MBL binding to infected cells (79). Given the ligand specificity of MBL, we hypothesized that the RRV E2 N-linked glycans mediate MBL binding to infected cells, resulting in MBL deposition and subsequent complement activation. Although MBL did not directly bind to RRV virion particles, we reasoned that the glycoproteins might be in a slightly different conformation when they were displayed on the cell surface compared to the virion, and that this might allow MBL to bind the N-linked glycans on the viral glycoproteins located on the surface of infected cells. While both E1 and E2 contain N-linked glycosylation sites, we were primarily interested in evaluating the role of the E2 N-linked glycans due to their highly exposed location on the glycoprotein spike.

To test whether the RRV E2 N-linked glycans contributed to binding of MBL to infected cells, we used a previously generated panel of mutant viruses lacking one or both of the E2 glycans: RRV E2 N200Q, E2 N262Q, and E2 N200;262Q (E2 DM) (210). Differentiated C2C12 myotubes or primary C57BL/6 murine myotubes, which are derived from skeletal muscle, were infected with either wild-type RRV (RRV WT) or the

glycan mutants for 18 hours. Infected cells were then incubated in medium containing

serum from either naïve C57BL/6 or MBL-DKO mice for 30 minutes as a source of MBL.

Cells were then extensively washed to remove unbound MBL and free virus, and cell

lysates were analyzed by immunoblot for levels of MBL. Consistent with our hypothesis,

we observed a significant decrease in MBL deposition onto RRV E2 DM-infected C2C12

cells compared to RRV WT-infected cells (Figure 3.1A), despite similar levels of viral

replication (Figure 3.1B). Similar results were observed in primary C57BL/6 myotubes

(Figure 3.1C-D). We did not observe MBL deposition in cells incubated with MBL-DKO

serum, demonstrating both the specificity of the MBL western blots and indicating that

we were detecting only exogenously added MBL in the assay, rather than modulation of

MBL production by the different viruses within the infected cells. Interestingly, infection

with the viruses lacking each glycan individually showed comparable MBL deposition

levels to RRV WT (Figure 3.2A-B), indicating that both N-linked glycans contribute to

MBL deposition onto RRV-infected cells. To confirm the western blot analysis and

demonstrate that MBL was binding to virally infected cells in a viral glycan dependent

manner, we evaluated MBL deposition by fluorescence microscopy. BHK-21 cells were

infected with either diluent alone (mock-infected), RRV WT or RRV E2 DM for 12

hours, and subsequently incubated with 10μg/ml of recombinant human MBL for 30

minutes. Cells were washed extensively, fixed, stained without permeabilization to only

detect surface localization of MBL (Texas Red) and RRV structural proteins (FITC), and

imaged by fluorescence microscopy. As shown in Figure 3.3, we observed enhanced

deposition of MBL onto RRV-infected cells compared to mock-infected cells. Within the

RRV WT-infected culture, we only observed deposition onto the infected cells and not

onto uninfected cells (indicated by white arrowhead), indicating that viral infection

within the cell induces MBL deposition. Levels of MBL were reduced on cells infected

with E2 DM compared to WT, despite comparable levels of RRV antigen between WT

and E2 DM infection. Taken together, these data support the hypothesis that MBL

recognizes and binds to the E2 N-linked glycans on the surface of infected cells.

The RRV E2 N-linked glycans contribute to severe disease.

Given that the E2 N-linked glycans were required for MBL binding to infected

cells, and since MBL is required for RRV-induced disease (79), we hypothesized that the

E2 glycans were also required for development of RRV-induced disease. Wild-type

C57BL/6 mice were infected with either RRV WT or the panel of glycan mutant viruses,

and mice were weighed and assigned a clinical score as previously described (161).

Consistent with our previous studies, RRV WT-infected mice began to develop severe

disease characterized by hind-limb dysfunction by 5 dpi, with peak disease severity from

7 to 10 dpi (Figure 3.4A), and had reduced weight gain compared to mock-infected mice

(Figure 3.4B). Mice infected with viruses lacking either one of the E2 glycosylation sites

(E2 N200Q Figure 3.4A, top; E2 N262Q Figure 3.4A, middle) developed hind-limb

dysfunction with approximately the same kinetics as WT-infected mice, but the peak

disease severity was reduced in these mice compared to WT-infected mice. In addition,

these mice had reduced weight loss compared to WT-infected mice (Figure 3.4B). These

data suggest that each individual E2 glycan contributes to the severity of RRV-induced

disease. Interestingly, mice infected with the virus lacking both of the E2 glycans (RRV

E2 DM) developed a very mild disease with little to no hind-limb dysfunction, and

117

continued to gain weight throughout the course of infection (Figure 3.4A-B, bottom). Notably, the disease in the E2 DM-infected mice was remarkably similar to the disease induced in MBL-DKO and complement deficient mice (79, 158). Taken together, these data indicate while each of the E2 glycans contribute to disease severity individually, both of the E2 N-linked glycans are required for development of maximal disease, and suggests that the N-linked glycans have a key role in mediating RRV pathogenesis.

RRV lacking one or both E2 N-linked glycans are attenuated for inflammatory pathology and tissue damage within quadriceps muscle.

Infiltration of inflammatory cells into the skeletal muscle is a characteristic of RRV-induced disease, and much of the disease observed following RRV infection is due to the pathology mediated by inflammatory infiltrates. To assess the role of the E2 glycans in mediating inflammatory pathology following RRV infection, we analyzed H&E stained quadriceps muscle sections from mice infected with either RRV WT or the RRV glycan mutants at 10 days post infection. As expected, we observed severe inflammatory pathology in the quadriceps of RRV WT-infected mice, as evidenced by the destruction of the fibrous architecture of the skeletal muscle and the presence of infiltrating cells (Figure 3.5A). We observed the presence of infiltrating cells in the quadriceps muscle of mice infected with any of E2 glycan mutant viruses. However, consistent with the disease scores, the quadriceps muscles of mice infected with either E2 N200Q or E2 N262Q had moderate tissue damage that was reduced compared to RRV WT-infected mice, as indicated by the presence of intact muscle fibers (Figure 3.5A). In

118

contrast, mice infected with RRV E2 DM had intact skeletal muscle fibers with minimal

tissue damage despite the presence of infiltrating cells (Figure 3.5A).

To further confirm that mice infected with the RRV glycan mutants had reduced

tissue damage we administered Evans blue dye (EBD) into either RRV WT or glycan

mutant-infected mice at 10 dpi to visualize damaged muscle fibers within the quadriceps

muscle. EBD is excluded from healthy cells, but taken up by cells with permeabilized

membranes and is easily visualized by fluorescent microscopy due to its' fluorescent

properties; thus, EBD positive tissues indicate tissue damage. As shown in Figure 3.5B,

we observed abundant EBD positive muscle fibers in quadriceps muscle from RRV WT-

infected mice. Consistent with the reduced clinical scores and pathology in mice infected

with the glycan mutants, there were fewer EBD positive fibers observed in mice infected

with either of the single E2 glycans mutants compared to RRV WT-infected mice.

Furthermore, EBD positive muscle fibers were rare in mice infected with E2 DM,

suggesting that both glycans are required for tissue damage.

RRV glycan mutants retain ability to replicate in vivo.

Although the RRV E2 N-linked glycans are dispensable for replication in cell

culture (210), it is possible that the glycans might be required for efficient viral

replication and dissemination *in vivo*. Therefore, we evaluated the viral titer within the

quadriceps muscle and the ankle joints from either RRV WT, or glycan mutant-infected

mice at multiple times points post-infection by plaque assay. There was no difference in

viral titer within the quadriceps and ankle joints at 1 dpi between any of the viruses,

suggesting that the E2 glycans are not required for initial dissemination to and replication

119

within target tissues (Figure 3.6 A-B). Overall, all of the glycan mutant viruses replicated at or near to wild-type levels in target tissues, although there were some differences in titer observed at intermediate time points. At 3 dpi, we observed reduced viral titer within the quadriceps muscle in mice infected with E2 N200Q and E2 DM compared to WT (Figure 3.6A). The E2 N262Q virus did not show any difference in titer compared to RRV WT at any time post-infection in either the ankle or the quadriceps muscle. At 5 dpi, only the RRV E2 DM titer is reduced in the quadriceps muscle compared to RRV WT, but importantly, at time points of severe disease, 7 and 10 dpi, no difference was observed in the quadriceps muscle between any of the viruses (Figure 3.6A). Similar results were observed in the ankle joints, although there were significant differences in titer at day 5 in the ankle joint between RRV E2 DM and RRV WT, but these differences were not sustained at time points of peak disease severity (7 or 10 dpi) (Figure 3.6B).

In order to confirm the plaque assay results, we also performed quantitative real time RT-PCR to determine the absolute numbers of RRV genomes per µg of RNA within the quadriceps muscle between WT and E2 DM virus at 3 and 5 dpi. We did not observe any differences in the number of RRV genomes between the two viruses at 3 dpi (Figure 3.7A). This suggests that the overall levels of viral replication within the tissues are equivalent between the wild type and mutant virus at this time point. However, consistent with reduced viral titer at 5 dpi, we observed a similar decrease in viral RNA at 5 dpi in the quadriceps muscle between WT and E2 DM (Figure 3.7B). Taken together, these data indicate that the loss of the glycans does not overall affect the ability of the virus disseminate to and replicate within target tissues, however the E2 DM does show reduced replication at intermediate times in the infection process.

The RRV E2 glycan mutants and WT RRV induce equivalent inflammatory responses.

RRV infection induces an inflammatory response that results in infiltration of inflammatory cells into target tissues such as the quadriceps muscle, subsequently leading to tissue damage (161). Prior studies demonstrated that even though RRV-infected C3$^{-/-}$ and MBL-DKO mice were resistant to virus-induced disease, virus induced inflammatory cell recruitment was unaffected in these mice (79, 158). Therefore, we evaluated the E2 glycan mutants to determine whether the virus induced disease process was similar to that observed in C3 or MBL deficient animals by quantifying and characterized inflammatory cell populations from quadriceps muscle of mice infected with the wild type or each of the mutant viruses by flow cytometry. At 10 dpi, which is a time point of peak inflammation within tissues, we did not observe any differences in the total magnitude nor the composition of the inflammatory cell population between RRV WT and the glycan mutants (Figure 3.8). Total numbers of leukocytes (as defined by LCA^{+} staining) in the quadriceps muscle were equivalent between mice in all groups (Figure 3.8), indicating that the E2 N-linked glycans do not affect infiltration of inflammatory cells into skeletal muscle. Furthermore, the numbers of inflammatory macrophage, which are thought to drive much of the tissue damage during RRV infection (135), and other cell types including CD4^{+} and CD8^{+} T cells, NK cells, and neutrophils, were equivalent between WT and the glycan mutants (Figure 3.8). These data suggest that loss of the E2 glycans does not significantly affect the induction of the infiltration or composition of the inflammatory cells into the quadriceps muscle following RRV infection.

The RRV E2 N-linked glycans contribute to complement activation in quadriceps muscle.

We have previously shown that complement activation following RRV infection is mediated primarily through MBL (79). Given that we observed a decrease in MBL deposition within RRV E2 DM-infected cultures, and since the disease phenotype induced by E2 DM in WT mice was strikingly similar to the disease induced by WT RRV in MBL-DKO mice, we hypothesized that the presence of the E2 glycans contribute to MBL deposition and complement activation in the quadriceps muscle following infection. MBL-mediated complement activation is initiated by the recognition of terminal sugars on glycosylated proteins by the CRD of MBL. Binding of MBL to the ligand leads to formation of the C3 convertase C2a4b by the MASPs, resulting in localized C3 deposition. The C3 convertase cleaves and processes C3 into smaller components, and is indicative of complement activation. One such component is iC3b, which opsonizes targeted cells and interacts with CR3 to mediate phagocytic uptake by CR3-bearing cells (50).

MBL levels are elevated within quadriceps muscle of RRV-infected mice at 7 dpi compared to mock-infected mice (79) and MBL deposition onto infected cells is dependent on the E2 glycans (Figures 3.1 and 3.3). Thus, if the RRV E2 glycans mediate complement activation through interactions with MBL, we would expect to see reduced amounts of MBL in mice infected with RRV E2 DM compared to RRV WT-infected mice. To test this, we infected mice with either RRV WT or RRV E2 DM and harvested quadriceps muscle at 7 dpi and analyzed the muscle homogenates by western blot for MBL-C levels. As shown in Figure 3.9A, RRV WT-infected mice had elevated levels of MBL-C in the quadriceps at 7 dpi compared to mock-infected mice, and importantly, we

observed reduced levels of MBL in RRV E2 DM-infected mice compared to RRV WT-infected mice, suggesting that the RRV E2 glycans are required for MBL deposition within infected tissues.

To determine if the reduced levels of MBL within the quadriceps muscle of RRV E2 DM infected mice correlated with reduced complement activation, we analyzed quadriceps muscle homogenates from RRV WT or RRV E2 DM-infected mice for levels of C3 cleavage products by western blot. Consistent with our hypothesis, we observed reduced levels of both the alpha and beta chain of C3 in E2 DM-infected mice compared to RRV WT-infected mice (Figure 3.9B), indicating that the E2 glycans are required for C3 deposition onto infected tissues. Furthermore, the levels of the C3 cleavage product iC3b was significantly reduced in E2 DM-infected mice compared to WT-infected mice (Figure 3.9B), indicating that the RRV E2 glycans are also required for complement activation following RRV infection.

As western blot analysis of C3 present in quadriceps muscle tissue does not distinguish between C3 produced by infiltrating inflammatory monocytes and C3 that is deposited onto infected tissues, we wanted to further confirm that the RRV E2 glycans are required for C3 deposition onto skeletal muscle following infection by IHC staining of C3 on skeletal muscle sections. We infected mice with either RRV WT or E2 DM, and generated sections of the quadriceps muscle at 7 dpi. Consistent with results in Figure 3.9B, we observed a reduction in C3 deposition onto the skeletal muscle from mice infected with RRV E2 DM compared to RRV WT (Figure 3.10).

Prior studies indicate that MBL and the complement system induce expression of a subset of inflammatory mediators commonly associated with inflammatory arthritis

following RRV infection through CR3 dependent signaling (79, 160). Given that the

RRV E2 N-linked glycans contribute to complement activation, we hypothesized that

expression of these inflammatory mediators is also dependent on the glycans. To test this,

we infected mice with either RRV WT or RRV E2 DM, harvested quadriceps muscles at

7 dpi, and analyzed mRNA expression of various genes by quantitative real-time PCR.

Expression of the pro-inflammatory calgranulin proteins S100A8 and S100A9 was

diminished in MBL-DKO, C3$^{-/-}$, and CR3$^{-/-}$ mice following RRV infection (79, 160). As

shown in Figure 3.11, we observed significantly higher expression of S100A8 and

S100A9 in the quadriceps muscle of RRV WT-infected mice compared to RRV E2 DM-

infected mice at 7 dpi, suggesting that expression of these genes was also dependent on

the RRV glycans. Furthermore, expression of Arginase I and IL-6, whose expression is

complement dependent, was also dependent on the E2 glycans (Figure 3.11). These data

are consistent with the hypothesis that the RRV E2 N-linked glycans contribute for

complement activation following infection, as they are required for expression of the

same subset of genes that are complement dependent.

Expression of the pro-inflammatory cytokine TNFα that is MBL, C3, and CR3-

independent following infection was unchanged between RRV WT and RRV E2 DM-

infected mice (Figure 3.11). However, expression of other C3-independent cytokines IL-

1β and IL-10 was dependent on the presence of the viral N-linked glycans. IL-1β

expression is induced upon Toll-like receptor engagement (44), and may suggest that the

viral N-linked glycans are interacting with TLRs to mediate IL-1β induction.

Interestingly, IL-10 expression was dependent on MBL following RRV infection (79),

further supporting the hypothesis that the E2 glycans interact with MBL. Taken together,

these data suggest that the RRV E2 N-linked glycans regulate expression of a similar subset of pro-inflammatory genes as MBL, C3, and CR3, and further supporting the hypothesis that the RRV E2 glycans activate the host complement system through MBL.

3.5 Discussion

Mosquito-borne alphaviruses such as RRV and CHIKV are emerging viruses that are a significant cause of explosive outbreaks of infectious arthritis in humans. The host complement system through the mannose binding lectin pathway plays a critical role in mediating development of disease and tissue damage through activation of inflammatory cells that infiltrate into the muscle and joints following infection (158, 160). In this study, we demonstrate that the RRV envelope N-linked glycans are a viral ligand for MBL, and that this interaction contributes to activation of complement and induction of severe virus-induced disease.

The N-linked glycans on the alphavirus glycoproteins have been implicated in a number of viral processes. The E1 glycan is embedded and the E1 glycoproteins mediates membrane fusion of the alphaviruses (125, 174), and loss of any of these sites has been shown to attenuate both Sindbis virus and Ross River virus replication in mammalian cells (174, 210). Therefore, given the impact of the RRV E1 mutation on viral replication, which would have affected our ability to interpret results in vivo, we did not evaluate this virus within our study. The E2 glycans, on the other hand, are relatively surface exposed and in the case of RRV, do not significantly affect replication within cell culture (174, 210). The alphavirus E2 glycoprotein is thought to be involved in receptor binding, but there has been no direct evidence to suggest that the N-linked glycans mediate receptor interaction (125). Studies using glycan mutants of a cell-culture adapted SINV found that loss of the SINV E2 glycans actually enhanced binding of virus to mammalian cells, due to a loss of negative charge of sialic acid, which is the terminal carbohydrate of complex glycans, allowing for tighter binding to heparan sulfate (122). Consequently, SINV

lacking either of the E2 glycans displayed enhanced virulence, disease, and viral titer in a mouse model of encephalomyelitis (122). The fact that we did not see a corresponding enhancement of virulence with the RRV N-linked glycan mutants likely reflects the central role that virus-induced MBL binding and complement activation plays in the pathogenesis of RRV-induced disease (79, 158, 160). Furthermore, unlike the TE12 strain of Sindbis, which binds heparin sulfate and where the enhanced virulence of N-linked glycan mutants has been linked to effects on heparin sulfate binding, the wild type T48 strain of RRV used in our studies does not efficiently use heparan sulfate as an attachment factor to bind to mammalian cells (92).

The results presented in this study clearly demonstrate that viral N-linked glycans promote MBL binding to RRV infected cells and that MBL deposition and subsequent complement activation is reduced in tissues from animal infected with the N-linked glycan double mutant (Figures 3.1, 3.3 and 3.10). Given the central role that MBL, complement activation, and subsequent inflammatory cell activation plays in the pathogenesis of RRV-induced disease (79), it is likely that the major mechanism of attenuation for the E2 DM virus is through the lack of MBL activation. However, given that the E2 DM virus did show reduced levels of replication at intermediate times post infection (Figure 3.6), we cannot rule out the possibility that at least some of the impact on virus-induced disease with the E2 DM virus is due to this transient reduction in viral load. However, it is important to point out that the decrease in viral load on days 3 and 5 post infection did not affect the recruitment of inflammatory cells into the sites of viral replication (Figure 3.8), and that viral loads were indistinguishable on day 7 post infection, which is a time when severe disease is readily apparent with the wild type virus

(Figure 3.6). It is also possible that in addition to their effects on MBL, which are crucial for disease, that the viral N-linked glycans are also regulating other aspects of the disease process. This possibility is supported by the fact that both of the single mutant viruses, which are still capable of promoting MBL binding, were partially attenuated for virus-induced disease. Therefore it will be important to evaluate whether one or both of the viral N-linked glycans is mediating other interactions, such as interactions with C-type lectin receptors, that might also affect virus-induced disease.

The interaction between MBL and viral N-linked glycans has been demonstrated in a number of other virus systems including HIV, SARS-CoV, and WNV (54, 61, 90, 107, 257). In these systems, MBL recognizes and binds to high mannose glycans on the envelope glycoproteins, and leads either to direct neutralization of virus, or aids in inhibiting virus infection by prevent or abrogating attachment and entrance into entering host cells. In contrast to the protective role of MBL for other viruses, MBL clearly plays a pathologic role during RRV infection and these studies provide new insights into the role of viral N-linked glycans in driving this pathologic process. Furthermore, studies with other viruses have demonstrated that the interaction between MBL and the virus particle is important for MBL-mediated neutralization (61, 111, 257). In contrast to those studies, we have several lines of evidence that demonstrate MBL interacts with RRV-infected cells through the E2 N-linked glycans on the surface of the infected cell rather than with the virion particle. First, MBL deposition onto infected cells in vitro and within infected tissues in vivo are elevated compared to mock-infected (79). Second, MBL deposition is reduced in cells and tissues infected with E2 DM RRV compared to WT RRV independent of viral replication, indicating that the E2 glycans mediate MBL

128

binding. Finally, we observed MBL deposition onto RRV-infected cell only, which was reduced in RRV E2 DM-infected cells. To our knowledge, this is the first demonstration where the interaction between the viral N-linked glycans and MBL on the surface of infected cells contributes to pathology and disease.

In addition to providing new insights into the pathogenesis of alphavirus-induced arthritis, these findings suggest that targeting interactions between the viral N-linked glycans and MBL may have therapeutic potential for treating RRV induced arthritis. Blocking the ability of MBL to interact with the viral N-linked glycans or inhibiting downstream proteases, such as MASP proteins that mediate subsequent complement activation, could prevent the severe pathology associated with RRV induced disease and other arthralgia associated alphaviruses, while keeping the protective aspects of the host innate immune response intact. Furthermore, given that the viral N-linked glycan mutants are attenuated for disease, but not replication, it may be possible to incorporate N-linked glycan mutants into live attenuated alphavirus vaccines.

In summary, we have demonstrated that the interaction between the host innate immune protein MBL and the RRV E2 N-linked glycans contribute to the pathogenesis of RRV-induced arthritis and myositis through activation of the host complement system. Our data suggests that specifically targeting the interaction between the RRV E2 N-linked glycans and MBL through the use of MBL inhibitors may be an effective therapeutic strategy in the treatment of RRV and other virus-induced inflammatory diseases.

3.6 Acknowledgements

Figure 3.1: The RRV E2 N-linked glycans contribute to MBL deposition onto infected cells.

A.
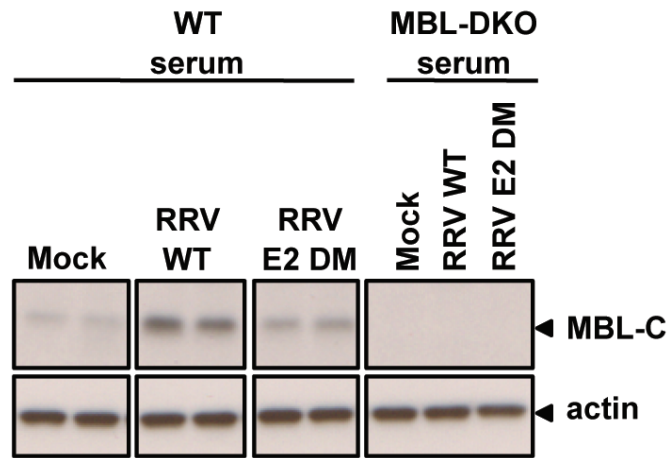
B.
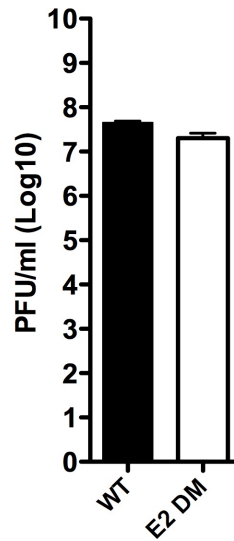
Figure 3.1: The RRV E2 N-linked glycans contribute to MBL deposition onto infected cells.

C.
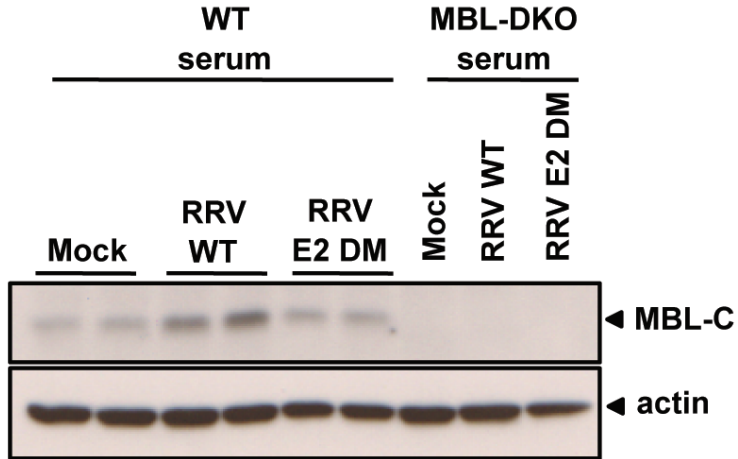
D.
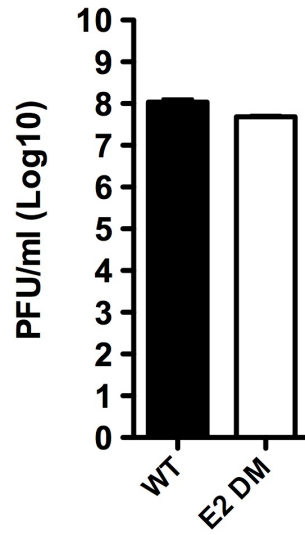
Figure 3.1 The RRV E2 N-linked glycans contribute to MBL deposition onto infected cells.

(A) To determine if the RRV E2 N-linked glycans were required for MBL deposition onto infected cells, C2C12 myotubes were infected with either RRV WT or RRV E2 DM at an MOI of 20 for 18 hours, and subsequently incubated with either serum from a WT or MBL-DKO mouse for 30 minutes prior to harvesting. Cells were washed, harvested, and lysates were analyzed by immunoblot analysis using anti-mouse MBL-C, or anti-mouse actin antibodies. Western blots of MBL-C and actin are shown.

(B) Infected cell culture supernatants from **(A)** were assayed to determine viral titer at 18 hpi between RRV WT (solid bar) and RRV E2 DM (open bar). Viral titer was determined by plaque assay on BHK-21 cells, and the bar represents the arithmetic mean ± SD of three replicates.

(C) Primary C57BL/6 myotube cultures were infected with either RRV WT or RRV E2 DM at an MOI of 20 for 18 hours, and subsequently incubated with either serum from a WT or MBL-DKO mouse for 30 minutes prior to harvesting. Cells were washed, harvested, and lysates were analyzed by immunoblot analysis using anti-mouse MBL-C, or anti-mouse actin antibodies. Western blots of MBL-C and actin are shown.

(D) Infected cell culture supernatants from **(C)** were assayed to determine viral titer at 18 hpi between RRV WT (solid bar) and RRV E2 DM (open bar). Viral titer was determined by plaque assay on BHK-21 cells, and the bar represents the arithmetic mean ± SD of three replicates.

Figure 3.2: Each E2 glycan contributes to MBL deposition onto infected cells

A.
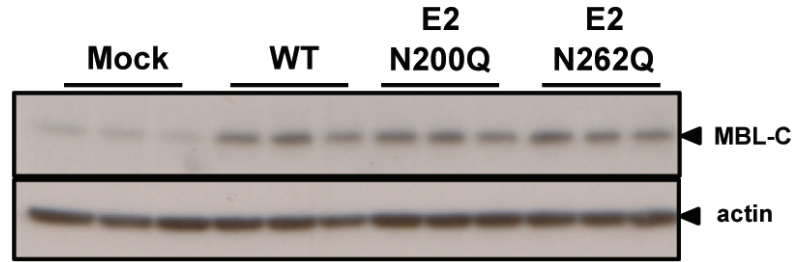
B.
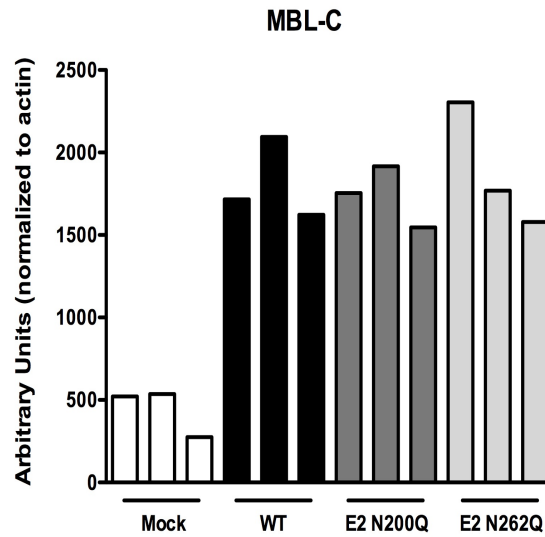
Figure 3.2: Each E2 glycan contributes to MBL deposition onto infected cells

(A-B) To determine if each individual E2 N-linked glycan was required for MBL deposition onto infected cells, C2C12 myotubes were infected with either RRV WT, E2 N200Q, or E2 N262Q at an MOI of 20 for 18 hours, and subsequently incubated with either serum from a WT or MBL-DKO mouse for 30 minutes prior to harvesting. Cells were washed, harvested, and lysates were analyzed by immunoblot analysis using anti-mouse MBL-C, or anti-mouse actin antibodies. Western blots of MBL-C and actin are shown **(A)** and densitometry measurements of bands in immunoblot from three different experiments are graphically depicted as arbitrary units normalized to actin **(B).**

Figure 3.3: RRV E2 glycans contribute to MBL deposition onto infected cells.
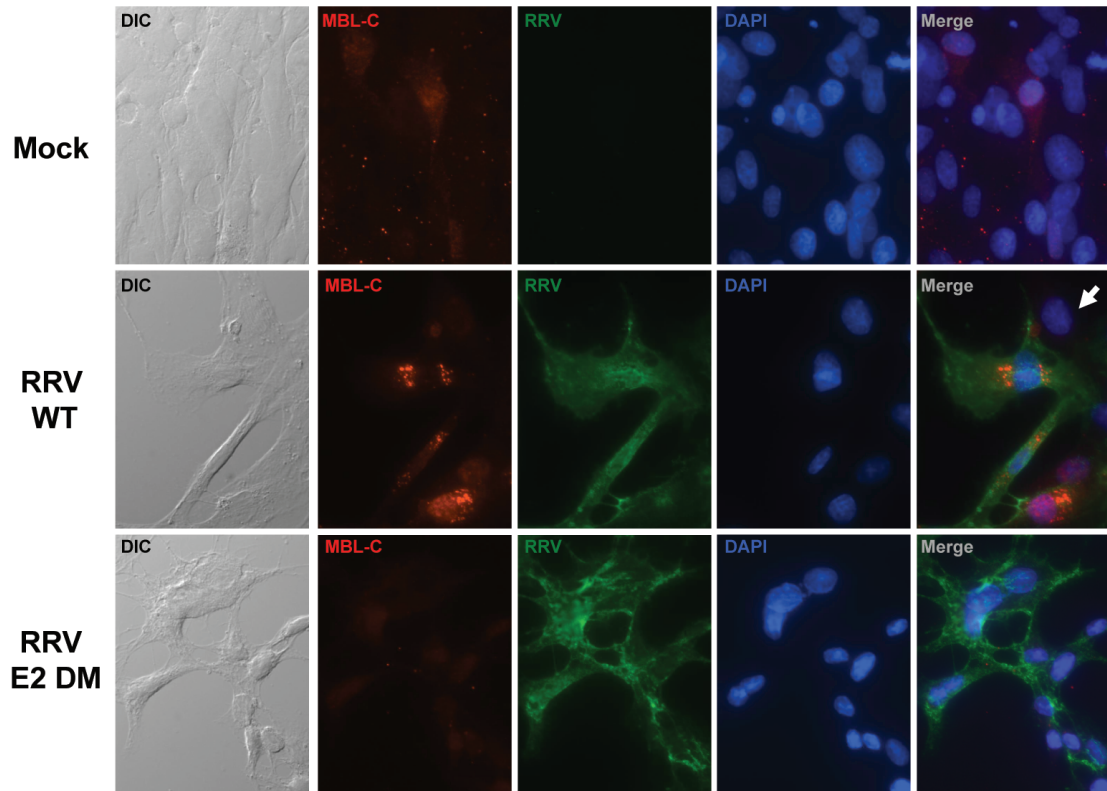
Figure 3.3: RRV E2 glycans contribute to MBL deposition onto infected cells.

To determine if the E2 glycans regulated MBL deposition onto RRV-infected cells,

immunofluorescence staining of BHK-21 cells infected with either diluent (mock, top

row), RRV WT (middle row) or RRV E2 DM (bottom row) at an MOI of 1 for 12 hours.

Cells were subsequently incubated with 10µg/ml rhMBL-C for 30 minutes, washed, fixed,

and stained for MBL-C, RRV antigen, and DAPI. Individual panels from left: DIC,

MBL-C (red), RRV antigen (green), DAPI (blue), and merge. White arrow indicated

uninfected cell. No MBL-C binding was observed in cells incubated without 10µg/ml of

MBL-C (data not shown).

Figure 3.4 The RRV E2 N-linked glycans contribute to severe disease.

A.
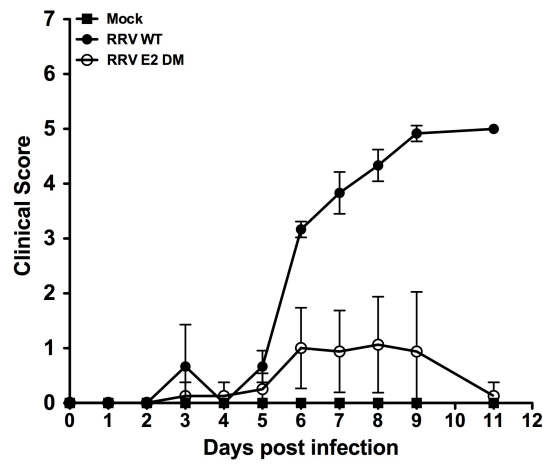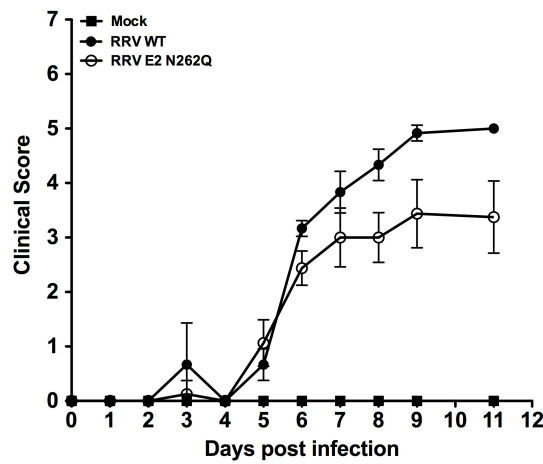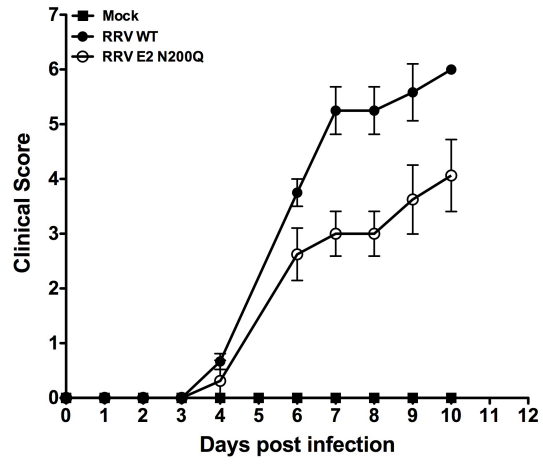
Figure 3.4 The RRV E2 N-linked glycans contribute to severe disease.

B.
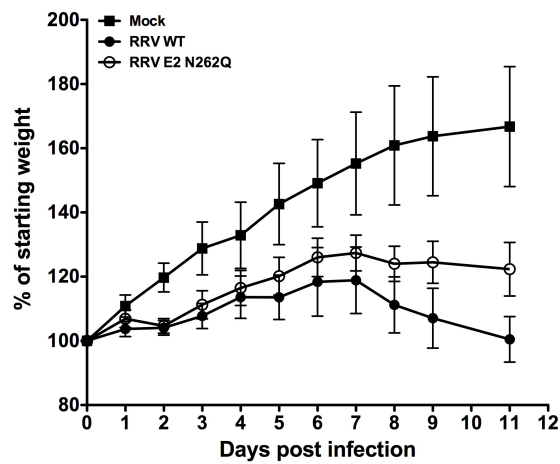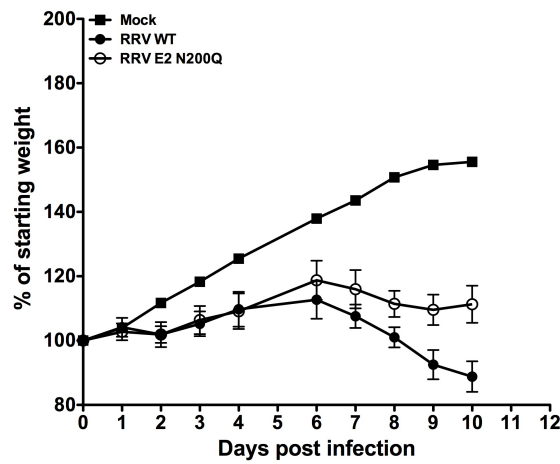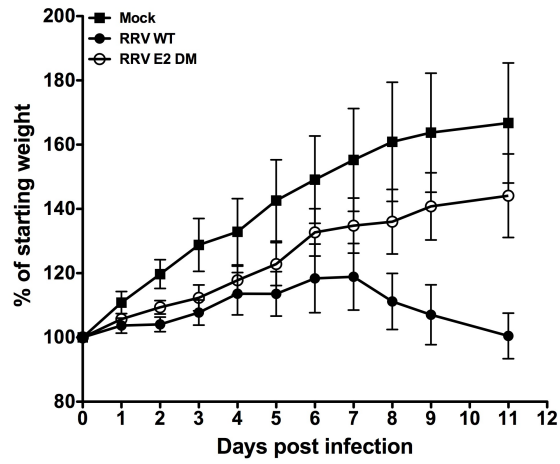
Figure 3.4: The RRV E2 N-linked glycans contribute to severe disease.

(A-B) Twenty-four day old C57BL/6 were either mock-infected, or infected with either RRV WT or a RRV glycan mutant. Mice were assigned a clinical score **(A)** and assessed for weight loss **(B)** as described in the Materials and Methods. Mice infected with RRV WT were compared directly to mice infected with E2 N200Q (top graphs), E2 N262Q (middle graphs) or E2 DM (bottom graphs). Each data point represents the arithmetic mean ± SD and is representative of at least three independent experiments.

Figure 3.5: The RRV E2 N-linked glycans contribute to pathology and tissue damage.
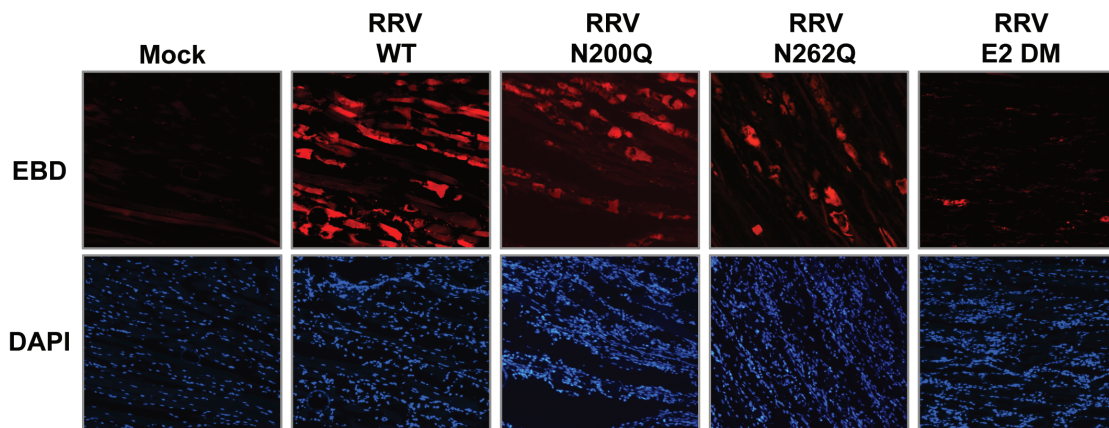
A.

Mock   RRV WT

RRV E2 N200Q   RRV E2 N262Q   RRV E2 DM

B.

Figure 3.5: The RRV E2 N-linked glycans contribute to pathology and tissue damage.

(A-B) Twenty-four day old WT C57BL/6 mice were infected with either RRV WT, E2 N200Q, E2 N262Q, or E2 DM.

(A) Tissue pathology and inflammation was examined at 10 dpi by H&E staining of paraffin embedded sections of quadriceps muscle from either RRV WT or the glycn mutants. A representative section from mice infected with each virus strain is shown.

(B) To assess damage within the muscle, mice infected with either RRV WT or the RRV glycan mutants were injected with EBD at 10 dpi, and frozen sections were generated. EBD positive muscle fibers were identified by fluorescence microscopy. Representative sections of each virus strain are shown.

Figure 3.6: RRV lacking E2 N-linked glycans retain ability to replicate *in vivo*

A.

B.

Figure 3.6: RRV lacking E2 N-linked glycans retain ability to replicate *in vivo*

Quadriceps muscle (A) and ankle joints (B) from mice infected with RRV WT (solid circles, n=4-15/time point), RRV E2 N200Q (open circles, n=3-6/time point), RRV E2 N262Q (solid squares, n=3-5/time point) or RRV E2 DM (open square, n=3-8/time point) were assayed to determine viral titer at various times post infection. Viral titer was determined by plaque assay on BHK-21 cells. $**p<0.01$ $***p<0.005$ as determined by one-way ANOVA analysis with Bonferroni's Multiple Comparison test of glycan mutant compared to RRV WT.

Figure 3.7: Amounts of RRV genomes in quadriceps muscle are equivalent at 3 dpi but not 5 dpi between RRV WT and E2 DM.

A.
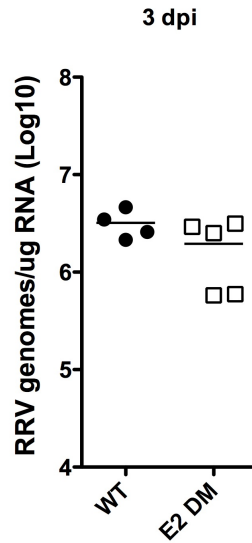
B.
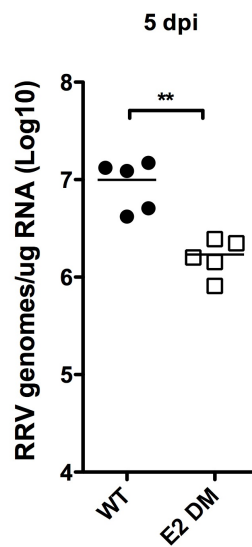
Figure 3.7: Amounts of RRV genomes in quadriceps muscle are equivalent at 3 dpi but not 5 dpi between RRV WT and E2 DM.

(A-B) Mice were infected with either RRV WT or E2 DM to determine absolute numbers of RRV genomes per μg of RNA between RRV WT and E2 DM at 3 dpi (A) and 5 dpi (B). At indicated times post infection, quadriceps muscle were harvested, RNA was isolated and absolute numbers of RRV genomes between RRV WT (solid circles) or E2 DM (open squares) were quantified by quantitative RT-PCR. **p<0.01 by t-test.

Figure 3.8: The RRV E2 glycan mutants and WT RRV induce equivalent inflammatory responses.
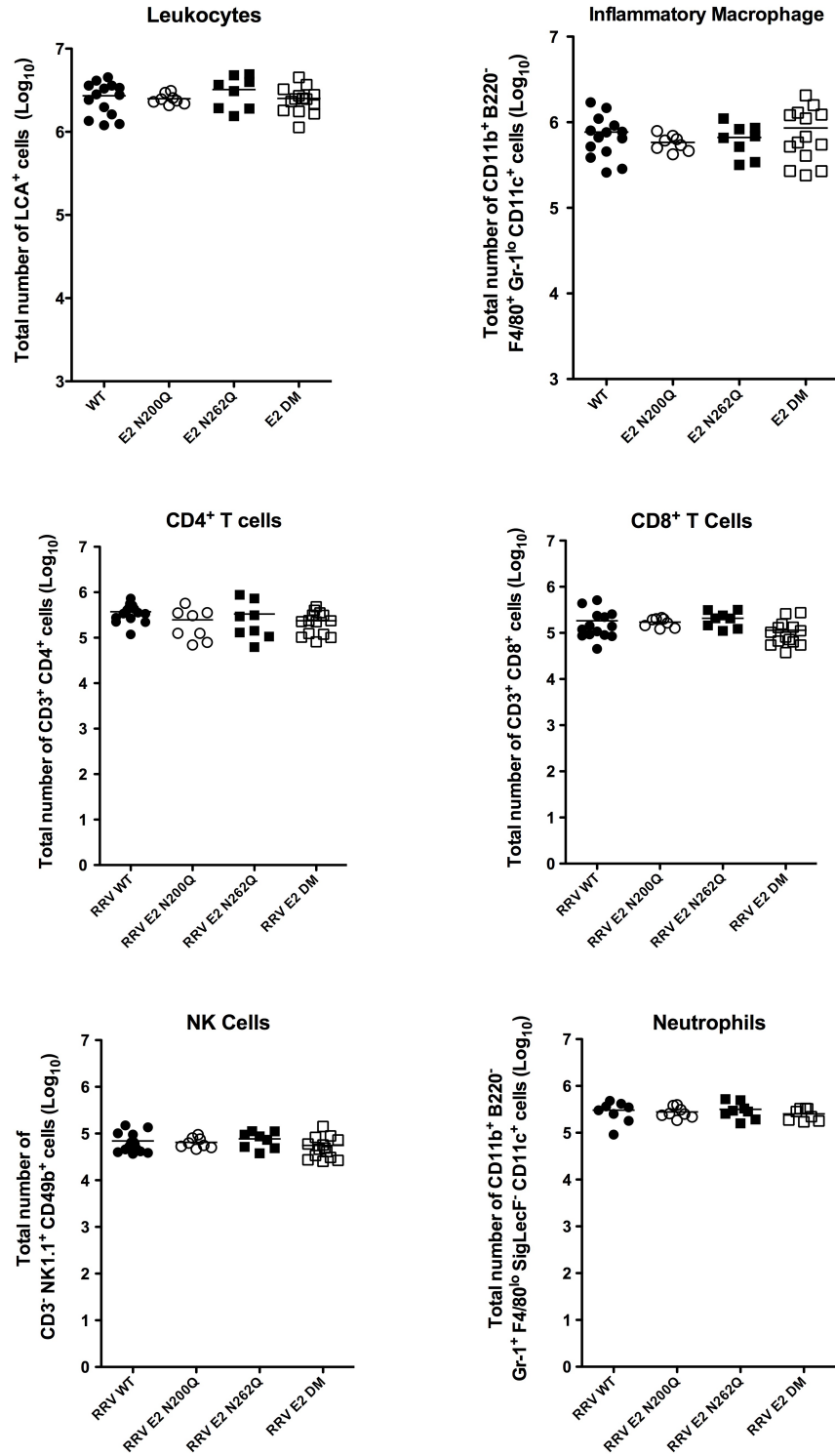
Figure 3.8: The RRV E2 glycan mutants and WT RRV induce equivalent inflammatory responses.

Leukocytes were isolated from the quadriceps muscle of mice infected with either RRV WT (solid circles, n=8-16), RRV E2 N200Q (open circles, n=8), RRV E2 N262Q (solid square, n=8) or RRV E2 DM (open square, n=8-16) mice at 10 dpi. Cells were characterized and quantified by flow cytometry using the markers described in the Materials and Methods. Total numbers of leukocytes, inflammatory macrophage and other inflammatory cell types are shown. Each data point represents a single animal, and data presented in the figure are combined from three independent experiments. *p<0.05 by one-way ANOVA with Bonferroni's Multiple Comparison post-test.

Figure 3.9: The RRV E2 N-linked glycans contribute to MBL deposition and complement activation in quadriceps muscle.

A.
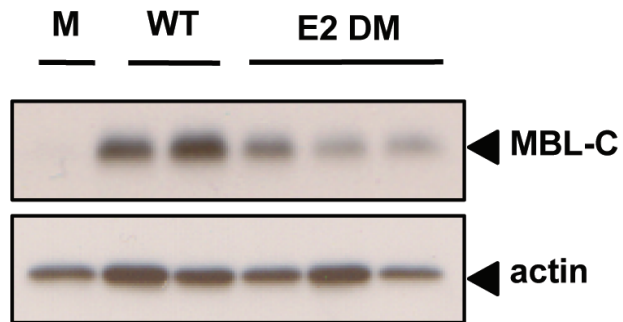
B.
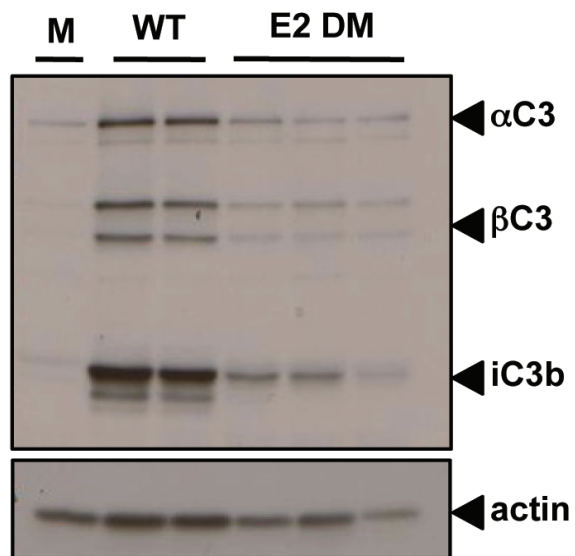
Figure 3.9: The RRV E2 N-linked glycans contribute to MBL deposition and complement activation in quadriceps muscle.

(A) Quadriceps muscle homogenates from mock-infected mice or mice infected with either RRV WT or RRV E2 DM were analyzed by immunoblot analysis at 7 dpi to determine relative levels of MBL. Each lane represents an individual mouse.

(B) To determine if complement activation differed between mice infected with RRV WT or RRV E2 DM, we analyzed homogenized quadriceps muscles from either mock-infected or infected mice at 7 dpi by immunoblot analysis using an anti-mouse C3 or anti-mouse actin antibody. C3 cleavage products are indicated with solid arrowheads. Each lane represents an individual mouse.

Figure 3.10: The RRV E2 glycans contribute to complement deposition in quadriceps muscle
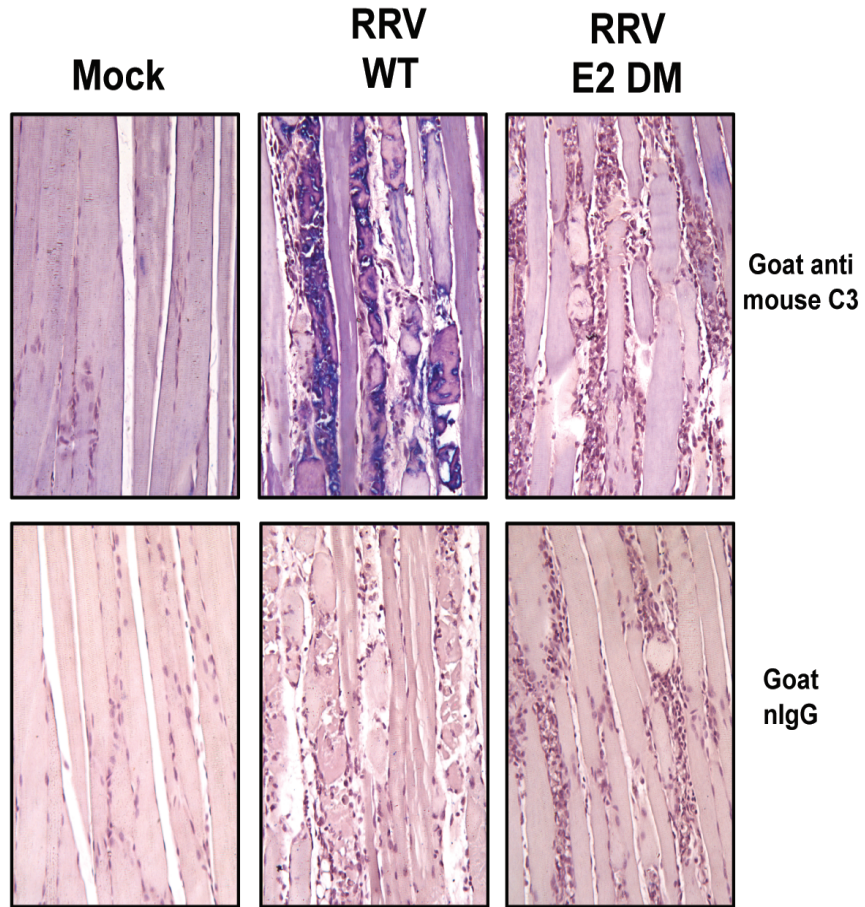
Figure 3.10: The RRV E2 glycans contribute to complement deposition in quadriceps muscle

C3 deposition was assessed by IHC using an anti-mouse C3 antibody on quadriceps muscle sections from mock-infected mice or mice infected with either RRV WT or RRV E2 DM at 7 dpi. C3 positive areas are stained in blue. A representative section from each strain is shown.

Figure 3.11: RRV E2 glycans contribute to expression of complement dependent pro-inflammatory genes

Figure 3.11: RRV E2 glycans contriute to expression of complement dependent pro-inflammatory genes

Relative mRNA expression of C3-dependent inflammatory mediators and cytokines S100A9, S100A8, Arginase I, and IL-6, and C3-independent cytokines TNFα, IL-1β, and IL-10 from quadriceps muscle from mice infected with either RRV WT (solid bar, n=7) or E2 DM (open bar, n=8) mice by quantitative real-time PCR. Raw data values were normalized to 18S rRNA levels, log-transformed, and are graphically depicted as fold expression over mock-infected mice. Data from a single experiment is shown, but is representative of two independent experiments. ***p<0.001; **p<0.005 *p<0.05 by t-test.

CHAPTER FOUR:

DISCUSSION AND FUTURE DIRECTIONS

Arthritic alphaviruses such as Ross River virus and chikungunya virus are a

significant cause of epidemics of infectious arthritis in various areas around the world.

Patients infected with these viruses experience debilitating polyarthritis, arthalgia and

myalgia in peripheral joints that can last from weeks to months. Studies in a mouse model

of RRV-induced disease have demonstrated the central role of the host inflammatory

response in mediating disease following viral infection. In particular, inflammatory

macrophages and macrophage products are thought to drive disease through direct

damage to inflamed tissues. The host complement system, which is a component of the

innate immune system, plays a critical role in regulating activation of the inflammatory

cells through CR3-dependent mechanisms (158, 160). However, the precise mechanisms

and viral ligands that activate complement following RRV infection are not known.

4.1 MBL and the RRV E2 N-linked glycans contribute to RRV-induced disease

through activation of the host complement system.

MBL contributes to development of severe RRV-induced disease

To further investigate how RRV activated the complement system, we first sought

to determine which activation pathway(s) are involved in complement activation

following RRV infection using mice deficient in the different initiator molecules of the

three main complement activation pathways. We found that the lectin pathway of complement, specifically mediated by mannose binding lectin, was the activation pathway required for development of RRV-induced disease (Figure 2.1, (79)), and mice deficient in the classical pathway initiator molecule C1q or the alternative pathway molecule factor B developed disease similar to WT mice, indicating that neither the classical or alternative pathways were involved in development of disease. Interestingly, these results are consistent with human data that failed to find evidence of immune complexes, which activate complement through the classical pathway, in the synovial fluid of patients suffering from RRV-induced polyarthritis (57, 58).

We characterized the disease in mice deficient in both mouse isoforms of MBL (MBL-DKO) and found that the disease was very similar to both C3 and CR3 deficient mice. Viral burden within the ankle joints and skeletal muscle did not differ between WT and MBL-DKO mice (Figure 2.7), indicating that similar to C3, MBL is not required for infection or clearance of virus. This is in contrast to the role that MBL has in other arboviral systems where MBL contributes to direct neutralization of virions (7, 61). Virus-induced inflammation is equivalent between MBL-DKO and WT mice, suggesting that MBL does not regulate infiltration of cells into the skeletal muscle (Figure 2.8).

To determine if MBL regulated complement activation following RRV infection, we analyzed deposition of C3 onto quadriceps muscle from WT or MBL-DKO mice. Consistent with our hypothesis, MBL-DKO mice had dramatically reduced amounts of C3 within the inflamed skeletal muscle compared to WT mice, and consequently had decreased levels of C3 cleavage products such as iC3b. Analysis of complement dependent expression of pro-inflammatory genes such as the calgranulins S100A8 and

S100A9 also showed dependence on MBL, as their expression was reduced in MBL-DKO mice following RRV infection.

The C3 cleavage product C3a was found to be elevated in RRV patients compared to osteoarthritis patients, suggesting that complement was activated following RRV infection in humans (158). We observed elevated levels of MBL within the quadriceps muscle as well as in the serum of RRV-infected mice (79). Similarly, we found elevated levels of MBL in the serum of RRV patients compared to healthy controls (79), suggesting that MBL may have a role in human RRV-induced disease. Circulating levels of MBL with the serum levels can rise following bacterial or viral infection since MBL is an acute phase protein (53), and thus might be up-regulated following RRV infection.

The results presented in this study demonstrate a pathologic role for MBL in RRV-induced disease and presents a possible avenue for therapeutic intervention for patients suffering from RRV-induced disease. Current treatment of RRV-induced disease is merely palliative and patients are often prescribed NSAIDS and rest. A therapeutic that that specifically targets the lectin pathway of complement may be an effective approach to limit disease pathology and alleviate symptoms caused by RRV infection. Pharmacological inhibitors of the lectin pathway, which primarily target and inhibit MASP activity, are currently in development, and may be of some use in treatment of RRV-induced disease in humans (14).

The role of MBL polymorphisms in severity of RRV-induced disease.

MBL is a highly polymorphic protein in the human population and polymorphisms in the promoter region of the human *Mbl2* gene affect expression and

production of MBL, leading to a wide range of "normal" baseline MBL levels across the human population (47). Given that elevated levels of MBL correlated with severity of RRV-induced polyarthritis in humans, it is tempting to speculate that people with MBL polymorphisms conferring higher levels of circulating MBL may be at greater risk of developing more severe disease in response to RRV infection. Conversely, humans with MBL polymorphisms conferring lower levels of MBL may be protected from developing severe RRV-induced disease. A small subset of nine patients suffering from RRV-induced disease has been genotyped to determine if any MBL polymorphism associated with severity of disease. Overall, there was no association within this very small subset of patients with severity of polyarthritis (79). However, there was a significant association with the polymorphism at -550 in the *Mbl2* promoter region, which confers higher levels of circulating MBL with neurocognitive impairment (S. Mahalingam, B. Piraino, B. Cameron, L. Herrero, and A. Lloyd, unpublished data). While we cannot draw any concrete conclusions from such a small data set, the implications from these data is people with genotypes conferring higher levels of MBL might be at greater risk for developing severe atypical symptoms of RRV-induced disease. Additional studies that include a larger cohort of patients are really needed to further address the role of MBL polymorphisms in determining severity of RRV-induced disease in humans. Ideally, such a study would include patients exhibiting a wide range of disease severity, including those who are asymptomatic but have serological evidence of RRV infection.

Another possible approach to studying the role of MBL polymorphisms in determining severity of RRV-induced disease may be to use a panel of genetically diverse mice called the Collaborative Cross (CC). The CC is composed of a panel of

recombinant inbred mouse lines that have been generated through interbreeding of eight different mouse lines (C57BL/6J, A/J, 129s1/SvImJ, NZO/HILtJ, NOD/ShiLtJ, WSB/EiJ, PWK/PhJ, and CAST/EiJ) (37). The genotypes and single nucleotide polymorphisms present in the CC lines that have been generated through this system represent greater than 90% of common mouse genetic diversity, and is currently being used to model genetic variation in the human population (186). In particular, our lab has been involved in initial studies evaluating the effect of host genetics on susceptibility or protection to infectious diseases (Ferris MT *et al*, manuscript under review). Furthermore, the CC provides a powerful tool to be able to evaluate the role of host genetics on viral pathogenesis (21, 170). Given the single nucleotide polymorphisms found specifically in *Mbl2* and expression differences across the CC founder lines, it is likely that this system will better allow us to understand the role of MBL polymorphisms in mediating disease (118).

Liu *et al* determined the baseline circulating MBL levels in various commonly used laboratory mouse strains including some of the founder lines of the CC, and found that levels of MBL-A ranged from 5.7µg/ml to 9.4µg/ml and levels of MBL-C ranged from 25µg/ml to 91µg/ml (138). The range in MBL levels between the different mouse strains suggests that there may be some genetic basis conferring differential MBL expression and production. However, not much, if anything, is known about the MBL polymorphisms in mice or if they are similar to the human *Mbl2* polymorphisms.

As a preliminary foray into exploring the possibility of using the CC to evaluate the role of host genetics, particularly MBL, on RRV pathogenesis, we were interested in determining if levels of MBL differed within the founder lines of CC. We performed a

western blot analysis of relative amounts of MBL-C present in the serum of both male and female naïve mice from each of the founder lines (Figure 4.1). Interestingly, we observed a wide range of MBL-C levels across the founder lines as well as between males and females within some of the lines. Of note, C57BL/6J mice, which we have used as our standard model to study RRV pathogenesis, appeared to have moderate to high levels of MBL and develop severe RRV disease, whereas other mouse lines, such as the 129s1/SvImJ line, had very low levels of MBL, and develop very mild RRV-induced disease, despite similar viral burden within target tissues (Gunn BM, Lotstein AR, and Heise MT, unpublished data). However, other strains of mice such as PWK/PhJ, who appear to have comparable levels of MBL to the C57BL/6J mice, developed mild disease, and suggests that levels of MBL is unlikely to be the sole determinant of disease severity following RRV infection. However, while these data are by no means conclusive or indicative of the role of lower levels of MBL protecting from disease, they suggest that the CC may be a useful tool to experimentally address questions relating to polymorphisms of MBL as well as the role of host genetics on RRV pathogenesis.

The RRV E2 N-linked glycans contribute to severe RRV-induced disease through activation of the host complement system.

Since MBL recognizes high mannose carbohydrates, we hypothesized that MBL may be recognizing the viral N-linked glycans present on the surface of infected cells. MBL does not bind directly to SINV or CHIKV virion particles (61), and we were unable to demonstrate direct interaction between either mammalian-derived or mosquito-derived RRV virions (79). However, since alphaviruses bud from the plasma membrane of

infected cells and the N-linked glycans are also present on the mature RRV glycoprotein spikes, we reasoned that it might be possible that MBL was recognizing the arrays of E2 glycans on the infected cell rather than on the virion. In support of this hypothesis, RRV infection resulted in elevated levels of MBL within the quadriceps muscles of infected mice as well as onto infected cells (Figure 2.3, (79)). To determine if the E2 glycans regulated MBL deposition onto infected cells, we used a virus that had been genetically mutated to lack the E2 glycosylation sites and evaluate deposition of MBL onto infected cells between the E2 glycan mutant and WT virus. Consistent with our hypothesis, the E2 glycan mutant-infected cells had reduced MBL deposition compared to WT virus as determined by western blot as well as by immunofluorescence despite similar levels of virus replication and output in both assays. These data together indicate that the E2 glycans present on the infected cell regulate extracellular deposition of MBL onto infected cells.

We next evaluated the role of the RRV N-linked glycans in RRV pathogenesis. Interestingly, mice infected with viruses that lacked either of the two E2 glycans showed reduced disease compared to WT virus; however, the single E2 glycan mutant-infected mice still exhibited some level of disease. In contrast, mice infected with a virus that lacks both of the E2 glycans E2 N200;262Q (E2 DM), exhibited dramatically reduced disease compared to WT mice. Further analysis of the pathology induced by RRV E2 DM compared to RRV WT showed striking similarity to the disease induced in MBL-DKO, C3^{-/-}, and CR3^{-/-} following RRV infection. Furthermore, RRV E2 DM-infected mice had reduced levels of MBL within the quadriceps muscle as well as reduced C3 deposition and cleavage products compared to RRV WT-infected mice. Together, these

data suggest that the E2 glycans regulate MBL-dependent complement activation leading to disease.

Glycans on infected cells versus on the virion.

The finding that MBL does not bind to the RRV virion particles, but does appear to bind to the E2 glycans on the infected cell, is intriguing in that the glycans should be the same on the infected cell and on the virion itself since the glycoproteins at the plasma membrane of the infected cell are incorporated into the virion particle. The three CRDs that make up each subunit of MBL are separated by a constant distance of 45Å, and thus require distinct spacing of carbohydrate ligands to efficiently bind and activate complement (211). Thus, one possible explanation for why MBL may recognize the infected cell rather than the virion is that the array of viral glycoproteins lying on the plasma membrane may provide the particular spacing and repeating array of carbohydrate ligands needed to efficiently bind MBL and activate complement whereas the glycans on the spherical virion particle may not. Structural analysis of the positions and spacing of the glycans on the surface of the infected cell compared to the virus would be needed to determine the spacing of the glycans are different between the two scenarios.

Recognition of the RRV N-linked glycans on the plasma membrane of the infected cell rather than the virion may also partially explain why MBL is pathologic in RRV-induced disease but protective in other virus systems. Since alphaviruses bud from the plasma membrane, the glycoproteins are prominently displayed on the cell surface, and allow for MBL deposition and complement activation directly on the infected host cell. Flaviviruses, such a WNV and DENV, bud from the ER and thus the glycoproteins

162

are only ever presented to MBL in virion form (136). Similarly, SARS-CoV forms virions within the cytoplasm of infected cells and mature virions are released by exocytosis (129). Thus, the interaction of flaviviruses and SARS-CoV with MBL may occur outside and away from host cells, and allow for complement activation and neutralization only on the virus. In contrast, recognition of the RRV E2 glycans on the infected cell by MBL may lead to complement activation on the infected cell, resulting in opsonization for killing and/or clearance by monocytes and macrophages.

Other possible ligands that could induce MBL-dependent complement activation following RRV infection.

Our work suggests that the RRV E2 N-linked glycans present on the surface of the infected cell act as a ligand for MBL binding and subsequent complement activation. However, MBL can bind to carbohydrate ligands that are not necessarily foreign in origin, such as N-linked glycans on receptors as well as other host proteins (223). Altered glycosylation of self-proteins has been demonstrated in tumor cells and in cells undergoing stress, leading to presentation of aberrantly glycosylated proteins on the surface of the cell (177, 229). Furthermore, alteration or loss of glycosyltransferase or glycosidase expression may lead to incomplete processing of the glycans resulting in hybrid or high mannose glycans on proteins being transported to the cell surface.

Alphaviruses induce host cell transcriptional shutoff, and thus it is possible that any proteins undergoing glycosylation at the time of shutoff may be aberrantly glycosylated. Some of these proteins may include surface proteins that are still transported to the surface of cell and could therefore be able to interact with MBL and

163

other carbohydrate binding proteins. Thus, in addition to recognition of the RRV glycoproteins on the surface of the infected cell, it is possible that MBL may also recognize aberrantly glycosylated host cell proteins. One possible experiment to address this possibility would be to generate the E2 glycan mutations in the context of a virus that is unable to induce host transcriptional shutoff, and determine the ability of these viruses to induce MBL deposition onto infected cells. Gorchakov *et al*. described an nsP2 mutant of SINV that is defective in its ability to induce shutoff, and a similar mutation could be made in RRV (60, 75). If the shutoff defective mutant virus with the WT glycans is still able to induce MBL deposition, while the mutant virus lacking the E2 glycans is not, this would provide strong evidence that the E2 glycans themselves are regulating MBL deposition onto infected cells.

4.2 Future Directions

Direct interaction between E2 glycans and MBL

We have developed two assays to determine if the E2 glycans contribute to MBL deposition on the surface of infected cells: western blot analysis of levels of MBL present with skeletal muscle cultures infected with either RRV WT or RRV E2 DM, as well as a visual analysis by immunofluorescence assay. In these assays, MBL is added exogenously to infected cells for 30 minutes to mimic *in vivo* conditions where MBL would interact with extracellular components of infected cells. Results from both assays indicate that the E2 glycans contribute to MBL deposition onto infected cells, despite similar levels of viral replication and/or viral antigen (Figures 3.1-3.3).

164

While these results indicate the E2 glycans regulate MBL deposition onto infected cells, we have not demonstrated a direct interaction between the RRV E2 glycans on the surface of the infected cell and MBL. Several additional experiments may be able to help determine if there is direct interaction between the glycans and MBL. Co-immunoprecipitation of the E2 glycoproteins and MBL from cells infected with either RRV WT or RRV E2 DM and incubated with exogenously added MBL would determine if a direct interaction between the RRV glycoproteins and MBL is dependent on the E2 glycans in the context of the infection.

Another approach would be to express either the WT or E2 DM glycoproteins from a plasmid and determine MBL deposition in the same assays described above. The advantage of this approach would be that the assay evaluates the contribution of the glycoproteins alone rather than in the context of viral infection. If MBL deposition occurs only onto the cells expressing the WT glycoproteins and not onto the cells expressing the E2 DM glycoproteins, it would suggest that the E2 glycans are indeed regulating MBL deposition onto the surface of cells. However, it is currently unclear if stable expression of the glycoproteins and maintenance of the mature glycoprotein spikes on the plasma membrane is feasible. An early study of SFV budding demonstrated that the glycoproteins at the plasma membrane do not accumulate in the absence of nucleocapsid interactions (256), and if this is the case, negative results would be difficult to interpret, since no binding of MBL to even WT glycoproteins could mean either that MBL binds to something else on the infected cell, or that the glycoproteins are not being maintained at the plasma membrane. IFA staining of unpermeabilized transfected cells for the RRV

165

structural proteins may be able to help determine if the glycoproteins are present on the surface of the cell.

MBL crosstalk with toll-like receptor pathways

The complement system has been recently shown to be involved in crosstalk with other innate immune pathways such as the toll-like receptor (TLR) family of receptors (82). MBL in particular appears to play a role in modulating signaling from various receptors. MBL bound to *S. aureus* bacteria enhanced signaling by TLR2 and TLR6 to generate a specific and robust response to *S. aureus* infection (108). MBL has also been reported to bind to TLR4 through the N-linked glycans on the receptor (212), and one study suggests that MBL binding to TLR4 can suppress LPS-induced pro-inflammatory responses (239). Intriguingly, TLR4 has a role in mediating RRV-induced disease (Neighbours L.M., Long K.M., and Heise M.T., unpublished data), thus it will be interesting to determine if MBL-TLR4 interactions contribute to RRV-induced disease.

Role of the complement system in pathogenesis of other arthritic alphaviruses.

The complement system appears to contribute to protection from encephalitic alphavirus infection yet enhances pathology following RRV infection (24, 79, 97, 98). However, the role of complement in the pathogenesis other arthritic alphaviruses, such as CHIKV, is currently unknown. Preliminary studies analyzing levels of circulating MBL in the serum of human CHIKV patients show elevated levels of MBL compared to uninfected healthy controls (Herrero, L. and Mahalingham, S., unpublished data). While additional studies in both mice and humans are needed to determine if there is a role for

MBL and complement in CHIKV pathogenesis, this preliminary data indicating that elevated levels of MBL are associated with CHIKV-associated polyarthritis suggest that MBL may play a role in other arthritic alphavirus infections.

Based on the results of the studies of this dissertation indicating a role for the RRV E2 glycans in mediating disease, similar mutations in the E2 glycans were generated in CHIKV in order to evaluate their potential role in CHIKV pathogenesis. Interestingly, the CHIKV mutant virus that lacks both of the E2 glycans (E2 N263; 345Q) induces a mild disease compared to CHIKV WT in mice, suggesting that the E2 glycans modulate CHIKV pathogenesis (McGee, C.E. and Heise, M.T., unpublished data). Whether the CHIKV E2 glycans regulate complement activation similar to the RRV E2 glycans remains to be seen; however this data highlights the importance of the viral N-linked glycans in arthritic alphavirus pathogenesis.

4.3 Conclusions and working model

The work described in this dissertation has identified critical pathologic roles for the host innate immune protein mannose binding lectin and the viral N-linked glycans in RRV pathogenesis. In this model, the E2 N-linked glycans on the surface of the infected cell induce MBL-dependent complement activation leading to development of RRV-induced disease. In addition to advancing our understanding of the molecular mechanisms that regulate RRV pathogenesis and identifying potential therapeutic targets, we have described novel pathologic roles for both MBL and viral N-linked glycans in viral pathogenesis.

Our current working model of how the interaction between the viral N-linked glycans and MBL contributes to RRV-induced disease is outlined in Figure 4.2 and is discussed below. As RRV replicates in host cells and tissues, the glycosylated envelope glycoproteins are expressed on the plasma membrane of the infected cell. Circulating MBL in the serum recognizes and binds to the E2 N-linked glycans that are present on the surface of infected cells to activate the complement cascade. Activation of complement produces the iC3b cleavage product that serves as a ligand to activate infiltrating inflammatory cells through CR3. Activation through CR3 initiates pro-inflammatory signaling that ultimately results in production of effector molecules and proteins that damage and kill iC3b-opsonized cells and tissues, resulting in the immunopathology that causes clinical disease.

Finally, arthritic alphaviruses are an important cause of infectious arthritis in many areas around the world, and have the potential to cause explosive epidemics of debilitating disease in millions of people. The work presented here advances our understanding of the mechanisms that contribute to development of RRV-induced disease, and suggest that targeting of MBL and the host complement system may be an effective therapeutic target for treatment of RRV and other arthritic alphaviruses.

Figure 4.1: MBL levels vary between Collaborative Cross founder strains.
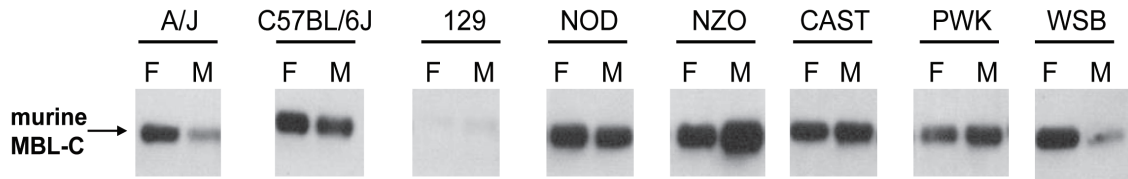
Figure 4.1:   MBL levels vary between Collaborative Cross founder strains.

To determine if baseline MBL levels varies between the founder mouse lines of the Collaborative Cross, western blot analysis using anti-mouse MBL-C antibodies was performed on equal volumes of serum from naïve male (M) and female (F) mice from each founder line.

Figure 4.2: Current model of how viral N-linked glycans and MBL contribute to RRV-induced disease.
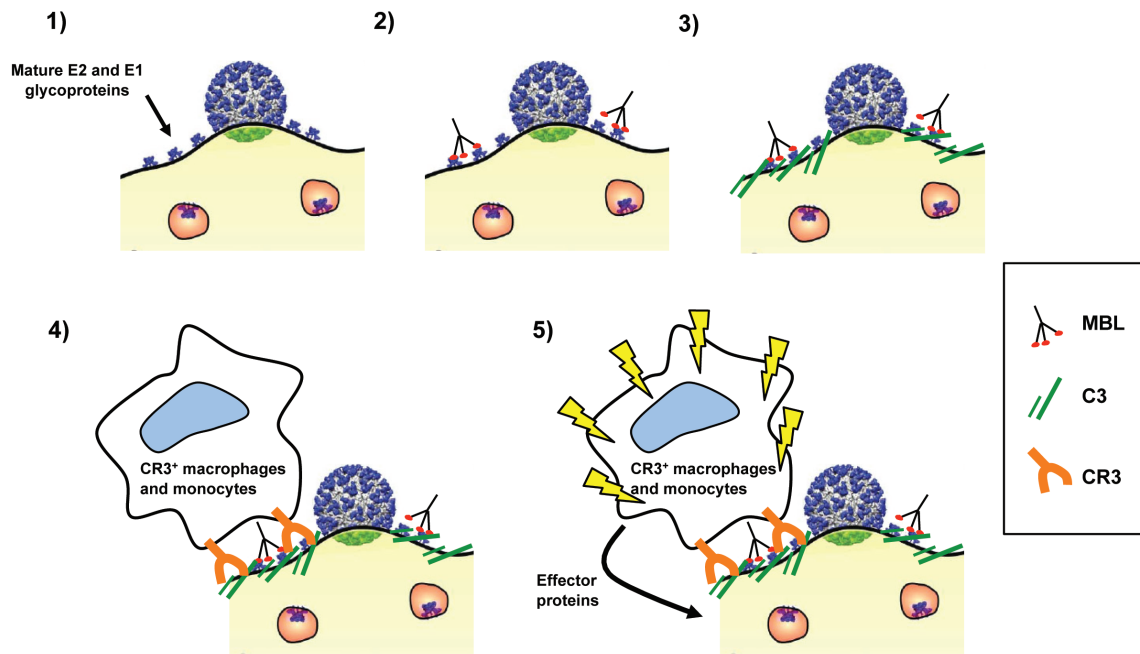
Figure 4.2: Current model of how viral N-linked glycans and MBL contribute to RRV-induced disease.

As RRV replicates in host cells and tissues, the glycosylated envelope glycoproteins are expressed on the plasma membrane of the infected cell (Step 1). Circulating MBL in the serum recognizes and binds to the E2 N-linked glycans present on the surface of infected cells to activate the complement system (Steps 2-3). Activation of complement produces the iC3b cleavage product that serves as a ligand to activate infiltrating inflammatory cells through CR3 (Step 3-4). Activation of the cells, indicated by lightening bolts, through CR3 initiates pro-inflammatory signaling that ultimately results in production of effector molecules and proteins that damage and kill iC3b-opsonized cells and tissues, resulting in the immunopathology that causes clinical disease (Step 5). Figure adapted from Li *et al.* with permission from Nature Publishing Group (133).

APPENDIX:

MECHANISMS OF TYPE I IFN INDUCTION IN MYELOID DENDRITIC CELLS BY MAMMALIAN CELL-DERIVED ROSS RIVER VIRUS.

A1.1 Introduction

Arthritic alphaviruses such as Ross River virus and chikungunya viruses are mosquito borne viruses that cause explosive epidemics of infectious arthritis in many areas around the world. These viruses are transmitted to humans by a mosquito vector and thus the virus is capable of infecting and replicating in both vertebrate and mosquito cells. The viruses that emerge from each of these different hosts have properties of the host cell, and one major difference between vertebrate and invertebrate cells is the glycosylation of proteins. As discussed in the introduction of this dissertation, asparagine (N)-linked glycosylation of viral proteins varies between mosquito and mammalian cells due to the lack of certain glycosidases in mosquito cells. Mosquito and other invertebrate cells produce high mannose glycans with mannose as the terminal residue, whereas vertebrate cells typically glycosylate proteins with complex or hybrid glycans, which have terminal sialic acid (215).

Early induction of type I interferon (IFN) is important for control of alphavirus replication (reviewed in (196)), and one of the major immune cell types capable of secreting large amounts of IFN is the dendritic cell (DC) population. DCs in the skin, such as Langerhan cells, are thought to be some of the first cells that come into contact with alphaviruses following infection by an infected mosquito (141). Prior studies demonstrated that mammalian cell-derived alphaviruses induce robust amounts of type I IFN from myeloid dendritic cells whereas mosquito cell-derived alphaviruses fail to

Authors: Bronwyn M. Gunn, Charles E. McGee, and Mark T. Heise

induce much IFN at all (209). The failure to induce IFN from dendritic cells by the mosquito-derived virus was independent of viral replication, and did not appear to occur through active suppression of type I IFN induction (209, 210). Rather, the mosquito-derived virus simply failed to activate IFN induction, whereas the mammalian-derived virus did. Additional studies indicated that the N-linked glycans on the mammalian-derived virus glycoproteins mediate IFN induction from mDCs (210). In particular, the two E2 N-linked glycans (E2 N200, N262) together were required for IFN production from mDCs. Analysis of the types of glycans that are typically glycosylated at the two sites revealed that the glycan at E2 N200 is typically a high mannose glycan, whereas the E2 N262 is predominantly a complex or hybrid glycan when produced in a mammalian cell (210). Together, this data suggests that the combination of the high mannose glycan and the complex glycan together induced IFN from mDCs. However, the mechanism by which the viral glycans induce type I IFN is unclear.

There are several classes of innate immune receptors that are present on DCs that mediate type I IFN production from DCs: the toll-like receptors (TLRs), C-type lectin receptors (CLRs), and the RIG-I like receptors (RLRs). These receptors are present either on the plasma membrane, within the endosome, or cytoplasmic and are involved in pathogen sensing. TLRs are present on the cell membrane as well as in the endosomes and engage a diverse set of bacterial, viral, and fungal ligands to induce the type I IFN system and NF-kB signaling pathways that initiate pro-inflammatory programs (reviewed in REF). While the list of ligands for the various TLRs is constantly growing, it is clear that some of the TLRs are activated by carbohydrate ligands. Viral glycoproteins from

173

several different viruses such as respiratory syncytial virus, measles, and human cytomegalovirus have been shown to activate TLR2 or TLR4 (15, 16, 36, 127).

CLRs are an emerging class of innate immune receptors that are typically found on the plasma membrane of immune cells and specifically recognize carbohydrate structures. DC-SIGN, CLEC5A, CLEC4A (DCIR) have been shown to interact with arboviruses, both flaviviruses and alphaviruses, to modulate pathogenesis (Long, K.M., and Heise M.T. manuscript under revision, (30, 31, 120)). Signaling from these receptors results in production of cytokines that regulate adaptive immunity (71). In addition, activation of certain CLRs leads to modulation of signaling pathways induced by other PRRs, such as TLRs (reviewed in (71)).

RLRs are cytoplasmic sensors that recognize nucleic acid within the cytoplasm and are required for type I IFN induction in response to many different viruses (reviewed in (139)). While RLRs do not directly recognize carbohydrate and protein structures, there is increasing evidence that the there is crosstalk between the RLRs and other PRR signaling pathways (179), and thus RLRs may play a secondary role in induction of type I IFN as a result of activation through other pathways.

In this study, we wanted to identify potential host sensors that recognized the viral N-linked glycans, leading to the production of type I IFN from mDCs. Given the localization and ligand specificity of the TLRs and CLRs, we hypothesized that these families of receptors may be recognizing the N-linked glycans on mammalian derived RRV. To determine if any of these sensors had a role in type I IFN induction, we took advantage of the availability of mice that are genetically deficient in the several different receptors: TLR2, TLR4, MyD88, DC-SIGN, and SIGN-R3. We derived mDCs from

these various mouse lines, and infected them with mammalian derived RRV and analyzed type I IFN production in the culture supernatant. However, we have not yet identified any particular receptor that mediates type I IFN production from mDCs in response to RRV infection.

A1.2 Materials and Methods

Viruses and cells. The viral stocks used in this study were generated from the infectious clone of the T48 strain of RRV (pRR64), kindly provided by Richard Kuhn (Purdue University) as described in (161). Briefly, viral RNA was generated through *in vitro* transcription of SacI-linearized pRR64 using the mMessage mMachine SP6 kit (Ambion) and electroportated into mammalian BHK-21 cells (ATCC). Viral titer was determined by plaque assay on BHK-21 cells. BHK-21 cells were grown in α-MEM (Gibco) supplemented with 10% donor calf serum (DCS), 10% tryptose phosphate, L-glutamine, penicillin, and streptomycin. C6/36 mosquito cells were grown in. L929 cells were grown in α-MEM (Gibco) supplemented with 10% donor calf serum (DCS), 10% tryptose phosphate, L-glutamine, penicillin, and streptomycin.

Generation of bone marrow derived dendritic cells (BMDCs). To generate BMDCs, bone marrow was extracted from the femurs and tibias of 8-10 week old mice, and cultured in low cluster 6-well plates in RPMI-10 (RPMI-1640 with 10% FBS, L-glutamine, b-mercaptoethanol, gentamicin, and penicillin, and streptomycin). To differentiate cells into BMDCs, cells were incubated in varying concentrations of GM-

CSF and IL-4 for 7 days as described in (209). Cells were either cryo-preserved or used immediately for experiments.

Infection of BMDC with RRV. BMDCs were plated at a density of 6 x 10^5 cells/well in RPMI-10 with GM-CSF and IL-4. Cells were infected either with diluent alone (mock) or with mammalian-derived RRV (mam-RRV) at an MOI of 10 or 20 for 2 hours in a 600µl volume. An addition 400µl of RPMI-10 with GM-CSF and IL-4 was added, and cells were incubated an additional 10 or 22 hours at 37C 5% CO2. At indicated time points (12 hpi or 24 hpi), culture supernatant was harvested by pelleting cells at 13000 RPM for 5 minutes, and transferring supernatant to a sterile eppendorf tube and stored at -80C until ready to assay.

Inhibition of endocytosis using dynasore. To inhibit endocytosis, differentiated BMDCs were incubated in RPMI-10 with GM-CSF and IL-4 containing either 80 µM of dynasore (Sigma Aldrich, St. Louis, MO) or DMSO vehicle for 30 minutes prior to infection with virus, and were maintained in the inhibitor following infection.

Type I IFN bioassay. Interferon bioassay was used to determine amounts of type I IFN as described in (209). Briefly, culture supernatants and interferon standards (NIH) were acidified to pH<2 with HCl overnight, and pH brought back to a neutral pH of 7-8 by NaOH. Samples were then UV-treated for 10 minutes to inactivate any residual virus. Samples were titrated by two-fold serial dilution onto L929 cells seeded in 96 well plates at a density of 8 x 10^3 cells/well, and incubated overnight. Following overnight

incubation, cells were challenged with EMCV at an MOI of 5 for 24 hours. Cell viability was determined by incubation in 6mg/ml of MTT (Sigma) for 3 hours. Residual MTT was removed, and the cells were dissolved in 0.4M HCl in isopropanol, and the absorbance 570nm of each well was measured on a microplate reader. To determine total amounts of IFN in each well, the well number at which had 50% cell viability was compared to the IFN standard and converted to international units (IU/ml).

Analysis of percent infection of BMDCs by RRV. Differentiated BMDCs were infected as above with either diluent, mam-RRVgfp or mos-RRVgfp at MOI 10. At 12 hpi, cells were harvested by pelleting and were fixed in 2% PFA overnight. Cells were analyzed for GFP expression on a CyAn flow cytometer (Becton Dickinson), and data was analyzed using Summit software.

Statistical analyses. Amounts of type I IFN production were analyzed for statistically significant differences by one-way ANOVA or students two tailed t-test between the various knockout lines and treatments ($p<0.05$ is considered significant). Statistical analyses were performed using GraphPad Prism 5.

A1.3 Results

Endocytosis of virus is required for type I IFN induction from BMDCs following mam-RRV infection.

Active viral replication by mammalian derived RRV was not required for induction of type I IFN from mDCs (209), suggesting that a cellular receptor is being activated during the entry stage of viral infection. This implies that the virus is interacting with the receptor during receptor binding and entry or during the internalization and fusion step. Both TLR2 and TLR4 are located at the plasma membrane as well as in the endosome and phagosome, where as CLRs are typically found at the plasma membrane. Furthermore, signaling through activation of RLRs required viral entry and release of viral RNA into the cytoplasm. To determine if type I IFN induction by mam-RRV required viral entry into the cell, we used a pharmacological inhibitor of dynamin, dynasore, to block clathrin-mediated endocytosis and entry of virus into the cell (142). Murine BMDCs were incubated in either 80μM of dynasore or DMSO vehicle prior to infection with mam-RRV, and type I IFN production was measured by type I IFN bioassay at 12 hpi. As shown in Figure A1.1, we observed a significant decrease in the amount of type I IFN production in cells treated with dynasore compared to vehicle treatment, indicating that endocytosis and/or viral entry is required for IFN induction following mamRRV infection.

TLR2 and TLR4 do not contribute to type I IFN induction from mDCs in response to mam-RRV.

Given that TLR2 and TLR4 can recognize to viral glycoproteins to initiate pro-inflammatory signaling as well as type I IFN production, we generated BMDCs from mice genetically deficient in either TLR2 or TLR4. To determine if either of the receptors mediated type I IFN induction from mDCs following mam-RRV infection, we infected either WT, TLR2$^{-/-}$ or TLR4$^{-/-}$ BMDCs with mam-RRV and measured type I IFN production at 12 hpi by type I IFN bioassay. Consistent with previous studies, mamRRV induced robust amounts of type I IFN from WT BMDCs (Figure A1.2). However, the induction of type I IFN was not dependent on either TLR2 or TLR4 as both TLR2$^{-/-}$ and TLR4$^{-/-}$ BMDCs produced comparable amounts of IFN to WT BMDCs (Figure A1.2).

While the results above indicated that neither TLR2 or TLR4 were required for IFN induction from mam-RRV infected BMDCs, it is possible that both receptors are capable of recognizing the N-linked glycans, and thus could compensate for each other. Multiple TLRs, including TLR2 and TLR4, signal through the adaptor protein MyD88, and thus we evaluated the production of type I IFN by mam-RRV in MyD88$^{-/-}$ BMDCs. As shown in Figure A1.2, MyD88$^{-/-}$ and WT BMDCs induced equivalent amounts of type I IFN following mam-RRV infection, suggesting that TLR signaling through MyD88 does not contribute to type I IFN induction in BMDCs. In addition to ruling out the role for TLR2 in IFN induction following mam-RRV infection, the use of MyD88$^{-/-}$ BMDCs also ruled out possible roles for TLR7, TLR9, TLR5, and TLR6 in mediating IFN induction by mam-RRV, since those receptors signal exclusively through MyD88 (117).

DC-SIGN and SIGN-R3 are not required for type I IFN induction from BMDCs following mam-RRV infection.

Type I IFN induction from mamRRV-infected BMDCs appears to require endocytosis and/or viral entry, yet neither TLR2 nor TLR4 mediated IFN induction following mamRRV infection, we next evaluated the role of CLRs in type I IFN induction. The CLRs DC-SIGN and SIGN-R3 can recognize and bind to high mannose glycans, and DC-SIGN has been reported to be an attachment factor for mosquito-derived alphaviruses that aids in viral entry into DCs (66, 71, 120). Thus, we hypothesized that DC-SIGN or SIGN-R3 mediated type IFN induction from BMDCs following mamRRV infection. To test this, we generated BMDCs from WT, DC-SIGN$^{-/-}$, or SIGN-R3$^{-/-}$ mice, and measured type I IFN induction following mam-RRV infection. As shown in Figure A1.3A, we did not observe any difference in type I IFN induction between WT, DC-SIGN$^{-/-}$ or SIGN-R3$^{-/-}$, suggesting that these receptors do not mediate IFN induction following mamRRV infection.

Mosquito cell-derived RRV infects BMDCs at a much higher efficiency than mammalian-cell derived RRV (209), and Klimstra *et al*. demonstrated that DC-SIGN and L-SIGN can act as dendritic cell attachment factors for mosquito cell-derived SINV (120). Therefore, we hypothesized that DC-SIGN might mediate efficient entry of mosRRV into BMDCs. To test this, we infected WT or DC-SIGN$^{-/-}$ BMDCs with a GFP-expressing mosRRV and determined percentage of viral infection by flow cytometry. Consistent with prior studies, we observed a significant increase in the number of cells infected with mosRRV compared to mamRRV in both the WT and DC-SIGN$^{-/-}$ BMDCs (Figure A1.2B). However, we did not observe any difference in the numbers of cells infected

180

with mos-RRV between WT and DC-SIGN$^{-/-}$ BMDCs, suggesting that DC-SIGN does not mediate efficient entry of mos-RRV into BMDCs (Figure A1.3B).

A1.4 Discussion and Future Directions

Early induction of type I IFN is critical in the control of alphavirus infection. Interestingly, mosquito and mammalian cell-derived RRV differentially induce type I IFN from myloid dendritic cells, and in particular, the RRV N-linked glycans on mammalian cell-derived RRV appear to be responsible for the differential type I IFN induction (209, 210). The mechanisms and/or host sensors that drive N-linked glycan mediated type I IFN induction are currently unknown. Innate immune pattern recognition receptors such as TLRs and CLRs can recognize carbohydrate structures on pathogens to activate host immune pathways. In this study we evaluated the role of these receptors in mediating type I IFN induction from BMDCs following infection with mam-RRV.

Prior studies indicated that viral replication was not necessarily required for IFN induction from mDCs (209), and suggests that the receptor involved in N-linked glycan recognition was either at the plasma membrane or located within endosomes. To distinguish between these two possibilities we used dynasore, which is an inhibitor of dynamin and clathrin mediated endocytosis. Our results indicated that endocytosis was required for IFN induction from mDCs following RRV infection. Both TLR2 and TLR4, which have been shown to recognize viral glycoproteins, can signal from the endosome and phagosomes (12). Therefore, we evaluated the role of TLR2 and TLR4 in type I IFN induction from mDCs. Surprisingly, neither receptor was required for type I IFN induction following mamRRV infection. Similar results were found with MyD88$^{-/-}$ mDCs,

suggesting that the MyD88-dependent TLRs do not mediate type I IFN from mDCs, definitively ruling out TLR2. While TLR4 signals through MyD88 at the plasma membrane, MyD88-independent TLR4 signaling can occur through the adaptor TRIF in the phagosome to mediate type I IFN induction (12, 252). We did not evaluate the role of TRIF-dependent TLRs in mediating type I IFN from mDCs in this study and needs to be tested, but our results with TLR4$^{-/-}$ BMDCs suggests that TLR4, regardless of whether it is at the plasma membrane or within phagosomes or endosomes, does not mediate N-linked glycan dependent type I IFN induction.

Since CLRs recognize glycan structures and the CLR DC-SIGN has been shown to interact with SINV, we next evaluated the role of DC-SIGN and one of its homologues SIGN-R3 in type I IFN from mDCs (120). However, neither DC-SIGN nor SIGN-R3 mediated type I IFN induction (Figure A1.3A). Furthermore, while DC-SIGN has been reported to be an attachment factor that enhances mosquito-derived SINV entry into DCs (120), DC-SIGN was not required for mos-RRV entry into DCs (Figure A1.3B). There are five mouse homologues to the human DC-SIGN (mouse DC-SIGN, SIGN-R1, SIGN-R2, SIGN-R3, and SIGN-R4) and while the SIGN-R3 is thought to be the one most closely related in carbohydrate binding specificity to the human DC-SIGN (169, 176), it is possible that one of the other DC-SIGN homologues can compensate in the absence of DC-SIGN in mouse cells and may partially explain our results.

RLRs such as RIG-I and MDA-5 contribute to type I IFN induction by alphaviruses (Cruz, CC and Heise MT unpublished data, (246, 248)) in fibroblasts. While RLRs are activated by RNA ligands and are unlikely to be directly activated by N-linked glycans on mamRRV, there is increasing evidence of cross-talk between RLRs and other

PRR families such as the NOD-like receptors, who can cross-talk with TLRs (179). Given that type I IFN from mDCs by mam-RRV required endocytosis, but not active viral replication, it is possible that RLRs may mediate some aspect of type I IFN induction by the N-linked glycans through cross talk with another PRR that does engage carbohydrates. In this scenario, a two-step induction process is required for type I IFN production: initial detection of viral N-linked glycans on incoming viruses by a CLR or TLR, subsequent recognition of viral RNA by the RLR, and synergy between the two pathways to produce robust amounts of type I IFN. We have not directly evaluated the role of IPS-1 or any of the RLRs in this study, and those experiments will need to be performed to determine the role of RLRs in mediating type I IFN production in mDCs following mam-RRV infection. Additional studies using BMDCs from mice deficient in both IPS-1 and various TLRs/CLRs may be useful in determining if there is synergy or interaction between the different pathways in type I IFN induction following RRV infection.

Future directions

In this study we have evaluated the role of several of the most likely innate immune receptors capable of recognizing viral glycoproteins in mediating type I IFN production from mDCs by the N-linked glycans on mamRRV. This has not been an exhaustive study by any means, and there are many more candidate receptors that may mediate IFN production from mDCs in response to mamRRV. In particular, other CLRs are attractive candidates to evaluate for their role in IFN production as well as a potential role in viral pathogenesis. For example, Langerin (CLEC4K), which is present on dermal

DCs called Langerhan cells that are in the skin, is an attractive candidate because of Langerhan cells are likely to be among the first cells to come into contact with mosRRV. Other receptors such as CLEC5A and CLEC4A (DCIR) have been shown to either interact with arboviruses or play a critical role in inflammatory diseases similar to alphavirus-induced arthritic diseases (30, 31, 114).

Rather than generating BMDCs from mice deficient in all of the different CLRs to evaluate their role in IFN induction, an alternative approach to determining if there is a role for any given CLR in IFN induction is to first determine if RRV interacts directly with candidate CLRs. Chen *et al*. have described a method to determine direct interaction between the carbohydrate recognition domains (CRDs) of various CLRs and viruses through expression of the CLR CRD fused to the Fc region of a human IgG and then performing an ELISA to determine if the virus bound to the CRD (30). We have taken a similar approach and generated constructs containing the CRDs of the CLRs outlined in Table A1.1. To produce the CLR.Fc fusion proteins, we transfected the constructs into HEK293T cells, and collected the supernatant 72 hours post transfection, and subsequently purified the CLR.Fc using a protein G column. The ELISA assay is currently undergoing optimization, and thus we do not have any interaction data so far; however, this panel of CLR.Fc fusion proteins provides us with a set of reagents to explore the roles of CLRs in alphavirus pathogenesis.

In summary, interactions between viral N-linked glycans and the innate immune system is an emerging field of study, and there is mounting evidence that these interactions play a critical role in modulating the host immune response and viral

pathogenesis. Dissecting these interactions by first identifying the host innate immune sensors involved in recognition and signaling will help further our understanding of how the viral N-linked glycans are sensed by the host, and ultimately their role in pathogenesis.

A1.5 Acknowledgements

Figure A1.1: Endocytosis of virus is required for type I IFN induction from BMDCs following mamRRV infection.

Figure A1.1 Endocytosis of virus is required for type I IFN induction from BMDCs following mamRRV infection.

To determine if endocytosis was required for induction of type I IFN from mam-RRV, murine C57BL/6 BMDCs were incubated in 80μM dynasore (solid bars) or DMSO vehicle (open bars) and then either mock infected or infected with mam-RRV for 12 hours. Amounts of type I IFN in the culture supernatant at 12 hpi were determined by type I IFN bioassay on L929 cells. The bar represents the arithmetic mean ± SD of triplicate wells and is representative of at least two independent experiments. ***p<0.0001 by students t-test.

Figure A1.2: TLR2 and TLR4 do not contribute to type I IFN induction from mDCs in response to mam-RRV.
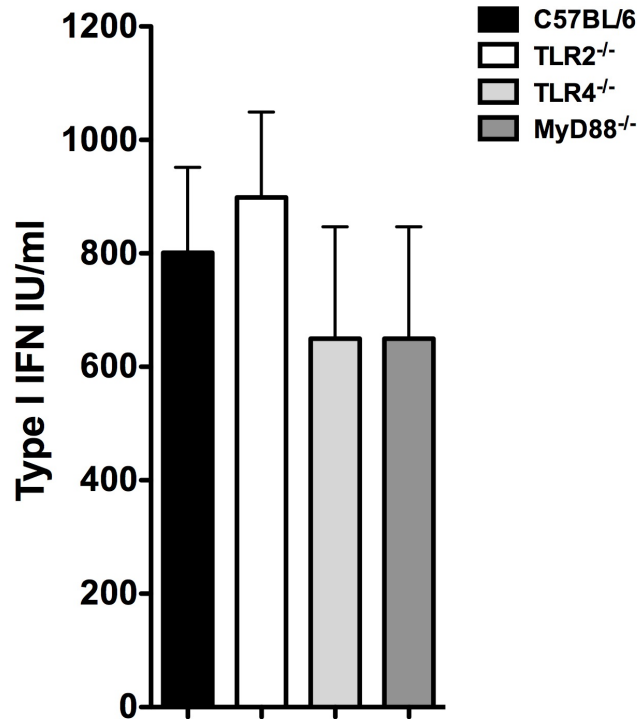
Figure A1.2 TLR2 and TLR4 do not contribute to type I IFN induction from mDCs in response to mam-RRV.

BMDCs derived from C57BL/6 WT (black bar), TLR2^{-/-} (open bar), TLR4^{-/-} (light grey bar), or MyD88^{-/-} (dark grey bar) were infected with mam-RRV at MOI 20. Amounts of type I IFN in the culture supernatant at 12 hpi were determined by type I IFN bioassay on L929 cells. n.s. by one-way ANOVA analysis with Bonferroni's muliple comparisons post-test. The bar represents the arithmetic mean ± SD of triplicate wells, and is representative of two independent experiments.

Figure A1.3: DC-SIGN and SIGN-R3 are not required for type I IFN induction from BMDCs following mamRRV infection.

A.
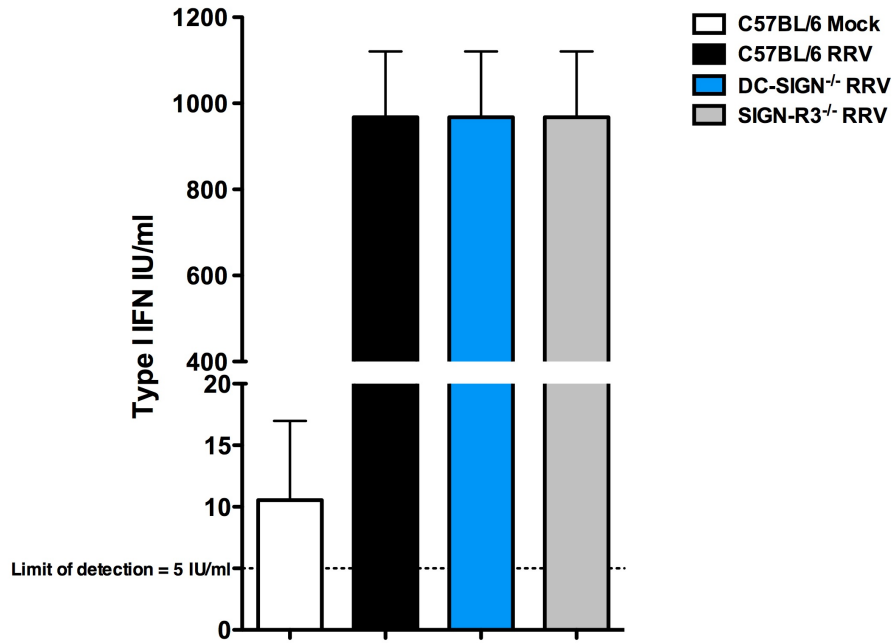
B.
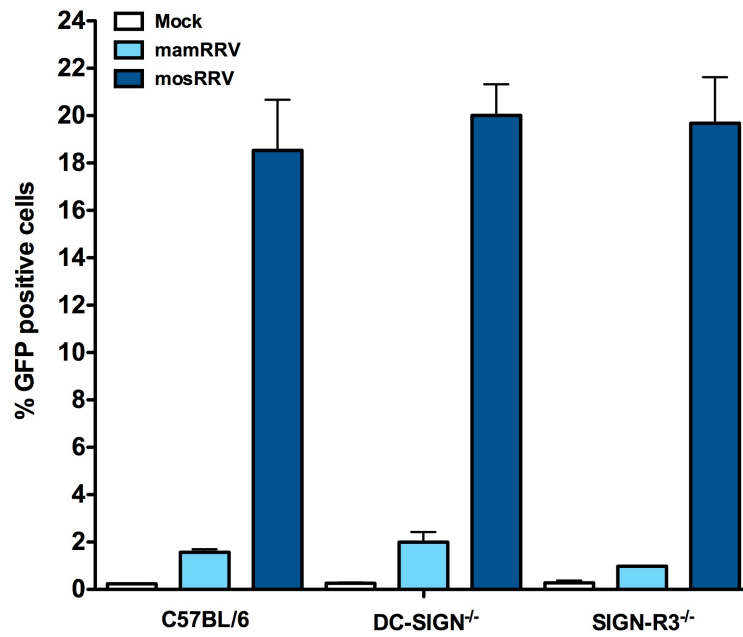
Figure A1.3: DC-SIGN and SIGN-R3 are not required for type I IFN induction from BMDCs following mamRRV infection.

(A) BMDCs from C57BL/6 WT (black bar), DC-SIGN$^{-/-}$ (blue bar), or SIGN-R3$^{-/-}$ (grey bar) were infected with mam-RRV at MOI 20. Amounts of type I IFN in the culture supernatant at 24 hpi were determined by interferon bioassay on L929 cells. The bar represents the arithmetic mean ± SD of triplicate wells.

(B) BMDCs from C57BL/6 WT, DC-SIGN$^{-/-}$, or SIGN-R3$^{-/-}$ were infected with diluent alone (mock; open bar), mam-RRVgfp (light blue bar) or mos-RRVgfp (dark blue bar) at MOI 10. Percent GFP^{+} cells were determined by flow cytometry. The bar represents the arithmetic mean ± SD of triplicate wells.

Table A1.1: CLR.Fc fusion constructs.

C-type Lectin receptor	Function	Ref.
CLEC5A/MDL-1	Pro-inflammatory cytokine induction; expressed on monocytes/macrophages; roles in DENV and JEV pathogenesis, inflammatory arthritis	(30, 31, 114)
CLEC4A/DCIR	ITIM containing CLR; expressed on DCs; role in CHIKV pathogenesis	Long, KM and Heise MT manuscript under review, (13)
CLEC4E/Mincle	Pro-inflammatory cytokine induction; expressed on neutrophils and macrophages	(253)
DC-SIGN	Expressed on DCs, macrophages; attachment factor for SINV, HIV, DENV	(72, 120, 224)
CLEC4M/L-SIGN	Expressed on endothelial cells; attachment factor for SINV	(120)
CLEC4K/Langerin	Expressed on Langerhan cells; roles in HIV pathogenesis	(41, 151)
CLEC4D/MCL	Expressed on monocytes/macrophages; pro-inflammatory cytokine production	(77)
CLEC12A/MICL	ITIM containing CLR; expressed on DCs, moncytes/macrophages	(146)
DCAR	ITAM containing CLR; pro-inflammatory cytokine induction; pairs with DCIR	(115, 116)

Table A1.1 CLR.Fc fusions constructs.

Initial panel of CLRs that we will evaluate for potential interaction with alphaviruses.

REFERENCES

1. **Aaskov, J. G., J. U. Mataika, G. W. Lawrence, V. Rabukawaqa, M. M. Tucker, J. A. Miles, and D. A. Dalglish.** 1981. An epidemic of Ross River virus infection in Fiji, 1979. Am J Trop Med Hyg **30:**1053-9.

2. **Acioli-Santos, B., L. Segat, R. Dhalia, C. A. Brito, U. M. Braga-Neto, E. T. Marques, and S. Crovella.** 2008. MBL2 gene polymorphisms protect against development of thrombocytopenia associated with severe dengue phenotype. Hum Immunol **69:**122-8.

3. **Ahn, A., M. R. Klimjack, P. K. Chatterjee, and M. Kielian.** 1999. An epitope of the Semliki Forest virus fusion protein exposed during virus-membrane fusion. J Virol **73:**10029-39.

4. **Ahn, A., R. J. Schoepp, D. Sternberg, and M. Kielian.** 1999. Growth and stability of a cholesterol-independent Semliki Forest virus mutant in mosquitoes. Virology **262:**452-6.

5. **Aliperti, G., and M. J. Schlesinger.** 1978. Evidence for an autoprotease activity of sindbis virus capsid protein. Virology **90:**366-9.

6. **Arpaia, N., and G. M. Barton.** 2012. Toll-like receptors: key players in antiviral immunity. Curr Opin Virol **1:**447-54.

7. **Avirutnan, P., R. E. Hauhart, M. A. Marovich, P. Garred, J. P. Atkinson, and M. S. Diamond.** 2011. Complement-mediated neutralization of dengue virus requires mannose-binding lectin. MBio **2**.

8. **Avirutnan, P., E. Mehlhop, and M. S. Diamond.** 2008. Complement and its role in protection and pathogenesis of flavivirus infections. Vaccine **26 Suppl 8:**I100-7.

9. **Banda, N. K., M. Takahashi, B. Levitt, M. Glogowska, J. Nicholas, K. Takahashi, G. L. Stahl, T. Fujita, W. P. Arend, and V. M. Holers.** 2010. Essential role of complement mannose-binding lectin-associated serine proteases-1/3 in the murine collagen antibody-induced model of inflammatory arthritis. J Immunol **185:**5598-606.

10. **Banda, N. K., M. Takahashi, K. Takahashi, G. L. Stahl, S. Hyatt, M. Glogowska, T. A. Wiles, Y. Endo, T. Fujita, V. M. Holers, and W. P. Arend.** 2011. Mechanisms of mannose-binding lectin-associated serine proteases-1/3 activation of the alternative pathway of complement. Mol Immunol **49:**281-9.

11. **Banda, N. K., J. M. Thurman, D. Kraus, A. Wood, M. C. Carroll, W. P. Arend, and V. M. Holers.** 2006. Alternative complement pathway activation is essential for inflammation and joint destruction in the passive transfer model of collagen-induced arthritis. J Immunol **177:**1904-12.

12. **Barton, G. M., and J. C. Kagan.** 2009. A cell biological view of Toll-like receptor function: regulation through compartmentalization. Nat Rev Immunol **9:**535-42.

13. **Bates, E. E., N. Fournier, E. Garcia, J. Valladeau, I. Durand, J. J. Pin, S. M. Zurawski, S. Patel, J. S. Abrams, S. Lebecque, P. Garrone, and S. Saeland.** 1999. APCs express DCIR, a novel C-type lectin surface receptor containing an immunoreceptor tyrosine-based inhibitory motif. J Immunol **163:**1973-83.

14. **Beinrohr, L., J. Dobo, P. Zavodszky, and P. Gal.** 2008. C1, MBL-MASPs and C1-inhibitor: novel approaches for targeting complement-mediated inflammation. Trends Mol Med **14:**511-21.

15. **Bieback, K., E. Lien, I. M. Klagge, E. Avota, J. Schneider-Schaulies, W. P. Duprex, H. Wagner, C. J. Kirschning, V. Ter Meulen, and S. Schneider-Schaulies.** 2002. Hemagglutinin protein of wild-type measles virus activates toll-like receptor 2 signaling. J Virol **76:**8729-36.

16. **Boehme, K. W., M. Guerrero, and T. Compton.** 2006. Human cytomegalovirus envelope glycoproteins B and H are necessary for TLR2 activation in permissive cells. J Immunol **177:**7094-102.

17. **Bonatti, S., G. Migliaccio, and K. Simons.** 1989. Palmitylation of viral membrane glycoproteins takes place after exit from the endoplasmic reticulum. J Biol Chem **264:**12590-5.

18. **Borgherini, G., P. Poubeau, A. Jossaume, A. Gouix, L. Cotte, A. Michault, C. Arvin-Berod, and F. Paganin.** 2008. Persistent arthralgia associated with chikungunya virus: a study of 88 adult patients on reunion island. Clin Infect Dis **47:**469-75.

19. **Borgherini, G., P. Poubeau, F. Staikowsky, M. Lory, N. Le Moullec, J. P. Becquart, C. Wengling, A. Michault, and F. Paganin.** 2007. Outbreak of chikungunya on Reunion Island: early clinical and laboratory features in 157 adult patients. Clin Infect Dis **44:**1401-7.

20. **Botto, M., D. Lissandrini, C. Sorio, and M. J. Walport.** 1992. Biosynthesis and secretion of complement component (C3) by activated human polymorphonuclear leukocytes. J Immunol **149:**1348-55.

21. **Bottomly, D., M. T. Ferris, L. D. Aicher, E. Rosenzweig, A. Whitmore, D. L. Aylor, B. L. Haagmans, L. E. Gralinski, B. G. Bradel-Tretheway, J. T. Bryan, D. W. Threadgill, F. P. de Villena, R. S. Baric, M. G. Katze, M. Heise, and S. K. McWeeney.** 2012. Expression quantitative trait Loci for extreme host response to influenza a in pre-collaborative cross mice. G3 (Bethesda) **2:**213-21.

22. **Brooke, C. B., D. J. Deming, A. C. Whitmore, L. J. White, and R. E. Johnston.** 2010. T cells facilitate recovery from Venezuelan equine encephalitis virus-induced encephalomyelitis in the absence of antibody. J Virol **84:**4556-68.

23. **Brooke, C. B., A. Schaefer, G. K. Matsushima, L. J. White, and R. E. Johnston.** 2011. Early activation of the host complement system is required to restrict CNS invasion and limit neuropathology during Venezuelan equine encephalitis virus infection. J Gen Virol.

24. **Brooke, C. B., A. Schafer, G. K. Matsushima, L. J. White, and R. E. Johnston.** 2011. Early activation of the host complement system is required to restrict central nervous system invasion and limit neuropathology during Venezuelan equine encephalitis virus infection. J Gen Virol **93:**797-806.

25. **Brown, K. S., S. D. Ryder, W. L. Irving, R. B. Sim, and T. P. Hickling.** 2007. Mannan binding lectin and viral hepatitis. Immunol Lett **108:**34-44.

26. **Burke, D., and K. Keegstra.** 1979. Carbohydrate structure of Sindbis virus glycoprotein E2 from virus grown in hamster and chicken cells. J Virol **29:**546-54.

27. **Burt, F. J., M. S. Rolph, N. E. Rulli, S. Mahalingam, and M. T. Heise.** 2012. Chikungunya: a re-emerging virus. Lancet **379:**662-71.

28. **Calandra, T., and T. Roger.** 2003. Macrophage migration inhibitory factor: a regulator of innate immunity. Nat Rev Immunol **3:**791-800.

29.   **Carey, D. E.** 1971. Chikungunya and dengue: a case of mistaken identity? J Hist Med Allied Sci **26:**243-62.

30.   **Chen, S. T., Y. L. Lin, M. T. Huang, M. F. Wu, S. C. Cheng, H. Y. Lei, C. K. Lee, T. W. Chiou, C. H. Wong, and S. L. Hsieh.** 2008. CLEC5A is critical for dengue-virus-induced lethal disease. Nature **453:**672-6.

31.   **Chen, S. T., R. S. Liu, M. F. Wu, Y. L. Lin, S. Y. Chen, D. T. Tan, T. Y. Chou, I. S. Tsai, L. Li, and S. L. Hsieh.** 2012. CLEC5A regulates Japanese encephalitis virus-induced neuroinflammation and lethality. PLoS Pathog **8:**e1002655.

32.   **Clarris, B. J., R. L. Doherty, J. R. Fraser, E. L. French, and K. D. Muirden.** 1975. Epidemic polyarthritis: a cytological, virological and immunochemical study. Aust N Z J Med **5:**450-7.

33.   **Coffey, L. L., E. Mertens, A. C. Brehin, M. D. Fernandez-Garcia, A. Amara, P. Despres, and A. Sakuntabhai.** 2009. Human genetic determinants of dengue virus susceptibility. Microbes Infect **11:**143-56.

34.   **Collard, C. D., R. Lekowski, J. E. Jordan, A. Agah, and G. L. Stahl.** 1999. Complement activation following oxidative stress. Mol Immunol **36:**941-8.

35.   **Collard, C. D., A. Vakeva, M. A. Morrissey, A. Agah, S. A. Rollins, W. R. Reenstra, J. A. Buras, S. Meri, and G. L. Stahl.** 2000. Complement activation after oxidative stress: role of the lectin complement pathway. Am J Pathol **156:**1549-56.

36.   **Compton, T., E. A. Kurt-Jones, K. W. Boehme, J. Belko, E. Latz, D. T. Golenbock, and R. W. Finberg.** 2003. Human cytomegalovirus activates inflammatory cytokine responses via CD14 and Toll-like receptor 2. J Virol **77:**4588-96.

37.   **Consortium, C. C.** 2012. The genome architecture of the Collaborative Cross mouse genetic reference population. Genetics **190:**389-401.

38.   **Cruz, C. C., M. S. Suthar, S. A. Montgomery, R. Shabman, J. Simmons, R. E. Johnston, T. E. Morrison, and M. T. Heise.** 2010. Modulation of type I IFN induction by a virulence determinant within the alphavirus nsP1 protein. Virology **399:**1-10.

39. **Davis, N. L., F. B. Grieder, J. F. Smith, G. F. Greenwald, M. L. Valenski, D. C. Sellon, P. C. Charles, and R. E. Johnston.** 1994. A molecular genetic approach to the study of Venezuelan equine encephalitis virus pathogenesis. Arch Virol Suppl **9:**99-109.

40. **de Curtis, I., and K. Simons.** 1988. Dissection of Semliki Forest virus glycoprotein delivery from the trans-Golgi network to the cell surface in permeabilized BHK cells. Proc Natl Acad Sci U S A **85:**8052-6.

41. **de Witte, L., A. Nabatov, M. Pion, D. Fluitsma, M. A. de Jong, T. de Gruijl, V. Piguet, Y. van Kooyk, and T. B. Geijtenbeek.** 2007. Langerin is a natural barrier to HIV-1 transmission by Langerhans cells. Nat Med **13:**367-71.

42. **Deresiewicz, R. L., S. J. Thaler, L. Hsu, and A. A. Zamani.** 1997. Clinical and neuroradiographic manifestations of eastern equine encephalitis. N Engl J Med **336:**1867-74.

43. **DeTulleo, L., and T. Kirchhausen.** 1998. The clathrin endocytic pathway in viral infection. EMBO J **17:**4585-93.

44. **Dinarello, C. A.** 2009. Immunological and inflammatory functions of the interleukin-1 family. Annu Rev Immunol **27:**519-50.

45. **Ding, M. X., and M. J. Schlesinger.** 1989. Evidence that Sindbis virus NSP2 is an autoprotease which processes the virus nonstructural polyprotein. Virology **171:**280-4.

46. **Doherty, R. L., J. G. Carley, M. J. Mackerras, and E. N. Marks.** 1963. Studies of arthropod-borne virus infections in Queensland. III. Isolation and characterization of virus strains from wild-caught mosquitoes in North Queensland. Aust J Exp Biol Med Sci **41:**17-39.

47. **Dommett, R. M., N. Klein, and M. W. Turner.** 2006. Mannose-binding lectin in innate immunity: past, present and future. Tissue Antigens **68:**193-209.

48. **Drickamer, K., M. S. Dordal, and L. Reynolds.** 1986. Mannose-binding proteins isolated from rat liver contain carbohydrate-recognition domains linked to collagenous tails. Complete primary structures and homology with pulmonary surfactant apoprotein. J Biol Chem **261:**6878-87.

49. **Edwards, J., and D. T. Brown.** 1991. Sindbis virus infection of a Chinese hamster ovary cell mutant defective in the acidification of endosomes. Virology **182:**28-33.

50. **Ehlers, M. R.** 2000. CR3: a general purpose adhesion-recognition receptor essential for innate immunity. Microbes Infect **2:**289-94.

51. **Eisen, D. P., and R. M. Minchinton.** 2003. Impact of mannose-binding lectin on susceptibility to infectious diseases. Clin Infect Dis **37:**1496-505.

52. **Eisen, S., A. Dzwonek, and N. J. Klein.** 2008. Mannose-binding lectin in HIV infection. Future Virol **3:**225-233.

53. **Ezekowitz, R. A., L. E. Day, and G. A. Herman.** 1988. A human mannose-binding protein is an acute-phase reactant that shares sequence homology with other vertebrate lectins. J Exp Med **167:**1034-46.

54. **Ezekowitz, R. A., M. Kuhlman, J. E. Groopman, and R. A. Byrn.** 1989. A human serum mannose-binding protein inhibits in vitro infection by the human immunodeficiency virus. J Exp Med **169:**185-96.

55. **Fraser, J. R., and G. J. Becker.** 1984. Mononuclear cell types in chronic synovial effusions of Ross River virus disease. Aust N Z J Med **14:**505-6.

56. **Fraser, J. R., and A. L. Cunningham.** 1980. Incubation time of epidemic polyarthritis. Med J Aust **1:**550-1.

57. **Fraser, J. R., A. L. Cunningham, B. J. Clarris, J. G. Aaskov, and R. Leach.** 1981. Cytology of synovial effusions in epidemic polyarthritis. Aust N Z J Med **11:**168-73.

58. **Fraser, J. R., A. L. Cunningham, J. D. Mathews, and A. Riglar.** 1988. Immune complexes and Ross River virus disease (epidemic polyarthritis). Rheumatol Int **8:**113-7.

59. **Frolov, I., R. Hardy, and C. M. Rice.** 2001. Cis-acting RNA elements at the 5' end of Sindbis virus genome RNA regulate minus- and plus-strand RNA synthesis. RNA **7:**1638-51.

60.   **Frolova, E. I., R. Z. Fayzulin, S. H. Cook, D. E. Griffin, C. M. Rice, and I. Frolov.** 2002. Roles of nonstructural protein nsP2 and Alpha/Beta interferons in determining the outcome of Sindbis virus infection. J Virol **76:**11254-64.

61.   **Fuchs, A., T. Y. Lin, D. W. Beasley, C. M. Stover, W. J. Schwaeble, T. C. Pierson, and M. S. Diamond.** 2010. Direct complement restriction of flavivirus infection requires glycan recognition by mannose-binding lectin. Cell Host Microbe **8:**186-95.

62.   **Fuchs, A., A. K. Pinto, W. J. Schwaeble, and M. S. Diamond.** 2011. The lectin pathway of complement activation contributes to protection from West Nile virus infection. Virology **412:**101-9.

63.   **Fujita, T.** 2002. Evolution of the lectin-complement pathway and its role in innate immunity. Nat Rev Immunol **2:**346-53.

64.   **Gaboriaud, C., N. M. Thielens, L. A. Gregory, V. Rossi, J. C. Fontecilla-Camps, and G. J. Arlaud.** 2004. Structure and activation of the C1 complex of complement: unraveling the puzzle. Trends Immunol **25:**368-73.

65.   **Gadjeva, M., S. R. Paludan, S. Thiel, V. Slavov, M. Ruseva, K. Eriksson, G. B. Lowhagen, L. Shi, K. Takahashi, A. Ezekowitz, and J. C. Jensenius.** 2004. Mannan-binding lectin modulates the response to HSV-2 infection. Clin Exp Immunol **138:**304-11.

66.   **Galustian, C., C. G. Park, W. Chai, M. Kiso, S. A. Bruening, Y. S. Kang, R. M. Steinman, and T. Feizi.** 2004. High and low affinity carbohydrate ligands revealed for murine SIGN-R1 by carbohydrate array and cell binding approaches, and differing specificities for SIGN-R3 and langerin. Int Immunol **16:**853-66.

67.   **Gardner, C. L., G. D. Ebel, K. D. Ryman, and W. B. Klimstra.** 2011. Heparan sulfate binding by natural eastern equine encephalitis viruses promotes neurovirulence. Proc Natl Acad Sci U S A **108:**16026-31.

68.   **Gardner, J., I. Anraku, T. T. Le, T. Larcher, L. Major, P. Roques, W. A. Schroder, S. Higgs, and A. Suhrbier.** 2010. Chikungunya virus arthritis in adult wild-type mice. J Virol **84:**8021-32.

69.   **Garmashova, N., R. Gorchakov, E. Frolova, and I. Frolov.** 2006. Sindbis virus nonstructural protein nsP2 is cytotoxic and inhibits cellular transcription. J Virol **80:**5686-96.

70.   **Garmashova, N., R. Gorchakov, E. Volkova, S. Paessler, E. Frolova, and I. Frolov.** 2007. The Old World and New World alphaviruses use different virus-specific proteins for induction of transcriptional shutoff. J Virol **81:**2472-84.

71.   **Geijtenbeek, T. B., and S. I. Gringhuis.** 2009. Signalling through C-type lectin receptors: shaping immune responses. Nat Rev Immunol **9:**465-79.

72.   **Geijtenbeek, T. B., D. S. Kwon, R. Torensma, S. J. van Vliet, G. C. van Duijnhoven, J. Middel, I. L. Cornelissen, H. S. Nottet, V. N. KewalRamani, D. R. Littman, C. G. Figdor, and Y. van Kooyk.** 2000. DC-SIGN, a dendritic cell-specific HIV-1-binding protein that enhances trans-infection of T cells. Cell **100:**587-97.

73.   **Gomez de Cedron, M., N. Ehsani, M. L. Mikkola, J. A. Garcia, and L. Kaariainen.** 1999. RNA helicase activity of Semliki Forest virus replicase protein NSP2. FEBS Lett **448:**19-22.

74.   **Gonzalez, S. F., V. Lukacs-Kornek, M. P. Kuligowski, L. A. Pitcher, S. E. Degn, Y. A. Kim, M. J. Cloninger, L. Martinez-Pomares, S. Gordon, S. J. Turley, and M. C. Carroll.** 2010. Capture of influenza by medullary dendritic cells via SIGN-R1 is essential for humoral immunity in draining lymph nodes. Nat Immunol **11:**427-34.

75.   **Gorchakov, R., E. Frolova, and I. Frolov.** 2005. Inhibition of transcription and translation in Sindbis virus-infected cells. J Virol **79:**9397-409.

76.   **Gorsuch, W. B., E. Chrysanthou, W. J. Schwaeble, and G. L. Stahl.** 2012. The complement system in ischemia-reperfusion injuries. Immunobiology **217:**1026-33.

77.   **Graham, L. M., V. Gupta, G. Schafer, D. M. Reid, M. Kimberg, K. M. Dennehy, W. G. Hornsell, R. Guler, M. A. Campanero-Rhodes, A. S. Palma, T. Feizi, S. K. Kim, P. Sobieszczuk, J. A. Willment, and G. D. Brown.** 2012. The C-type lectin receptor CLECSF8 (CLEC4D) is expressed by myeloid cells and triggers cellular activation through Syk kinase. J Biol Chem **287:**25964-74.

78. **Griffin, D. E.** 2007. Alphaviruses, p. 1023-1067. *In* D. M. Knipe, Howley, P. M. (ed.), Fields' Virology. Lippincott Williams & Wilkins, Philadelphia.

79. **Gunn, B. M., T. E. Morrison, A. C. Whitmore, L. K. Blevins, L. Hueston, R. J. Fraser, L. J. Herrero, R. Ramirez, P. N. Smith, S. Mahalingam, and M. T. Heise.** 2012. Mannose binding lectin is required for alphavirus-induced arthritis/myositis. PLoS Pathog **8:**e1002586.

80. **Gupta, B., C. Agrawal, S. K. Raghav, S. K. Das, R. H. Das, V. P. Chaturvedi, and H. R. Das.** 2005. Association of mannose-binding lectin gene (MBL2) polymorphisms with rheumatoid arthritis in an Indian cohort of case-control samples. J Hum Genet **50:**583-91.

81. **Hahn, C. S., and J. H. Strauss.** 1990. Site-directed mutagenesis of the proposed catalytic amino acids of the Sindbis virus capsid protein autoprotease. J Virol **64:**3069-73.

82. **Hajishengallis, G., and J. D. Lambris.** 2010. Crosstalk pathways between Toll-like receptors and the complement system. Trends Immunol **31:**154-63.

83. **Hansen, S., L. Selman, N. Palaniyar, K. Ziegler, J. Brandt, A. Kliem, M. Jonasson, M. O. Skjoedt, O. Nielsen, K. Hartshorn, T. J. Jorgensen, K. Skjodt, and U. Holmskov.** 2010. Collectin 11 (CL-11, CL-K1) is a MASP-1/3-associated plasma collectin with microbial-binding activity. J Immunol **185:**6096-104.

84. **Hardy, R. W., and C. M. Rice.** 2005. Requirements at the 3' end of the sindbis virus genome for efficient synthesis of minus-strand RNA. J Virol **79:**4630-9.

85. **Hardy, W. R., and J. H. Strauss.** 1989. Processing the nonstructural polyproteins of sindbis virus: nonstructural proteinase is in the C-terminal half of nsP2 and functions both in cis and in trans. J Virol **63:**4653-64.

86. **Harley, D., A. Sleigh, and S. Ritchie.** 2001. Ross River virus transmission, infection, and disease: a cross-disciplinary review. Clin Microbiol Rev **14:**909-32, table of contents.

87. **Harrison, S. C., A. David, J. Jumblatt, and J. E. Darnell.** 1971. Lipid and protein organization in sindbis virus. J Mol Biol **60:**533-8.

88. **Harrison, S. C., R. K. Strong, S. Schlesinger, and M. J. Schlesinger.** 1992. Crystallization of Sindbis virus and its nucleocapsid. J Mol Biol **226:**277-80.

89. **Hart, M. L., K. A. Ceonzo, L. A. Shaffer, K. Takahashi, R. P. Rother, W. R. Reenstra, J. A. Buras, and G. L. Stahl.** 2005. Gastrointestinal ischemia-reperfusion injury is lectin complement pathway dependent without involving C1q. J Immunol **174:**6373-80.

90. **Hart, M. L., M. Saifuddin, K. Uemura, E. G. Bremer, B. Hooker, T. Kawasaki, and G. T. Spear.** 2002. High mannose glycans and sialic acid on gp120 regulate binding of mannose-binding lectin (MBL) to HIV type 1. AIDS Res Hum Retroviruses **18:**1311-7.

91. **Hazelton, R. A., C. Hughes, and J. G. Aaskov.** 1985. The inflammatory response in the synovium of a patient with Ross River arbovirus infection. Aust N Z J Med **15:**336-9.

92. **Heil, M. L., A. Albee, J. H. Strauss, and R. J. Kuhn.** 2001. An amino acid substitution in the coding region of the E2 glycoprotein adapts Ross River virus to utilize heparan sulfate as an attachment moiety. J Virol **75:**6303-9.

93. **Heise, M. T., D. A. Simpson, and R. E. Johnston.** 2000. A single amino acid change in nsP1 attenuates neurovirulence of the Sindbis-group alphavirus S.A.AR86. J Virol **74:**4207-13.

94. **Herrero, L. J., M. Nelson, A. Srikiatkhachorn, R. Gu, S. Anantapreecha, G. Fingerle-Rowson, R. Bucala, E. Morand, L. L. Santos, and S. Mahalingam.** 2011. Critical role for macrophage migration inhibitory factor (MIF) in Ross River virus-induced arthritis and myositis. Proc Natl Acad Sci U S A **108:**12048-53.

95. **Hill, J. H., and P. A. Ward.** 1971. The phlogistic role of C3 leukotactic fragments in myocardial infarcts of rats. J Exp Med **133:**885-900.

96. **Hirsch, R. L., D. E. Griffin, and J. A. Winkelstein.** 1980. Role of complement in viral infections: participation of terminal complement components (C5 to C9) in recovery of mice from Sindbis virus infection. Infect Immun **30:**899-901.

97.   **Hirsch, R. L., D. E. Griffin, and J. A. Winkelstein.** 1978. The effect of complement depletion on the course of Sindbis virus infection in mice. J Immunol **121:**1276-8.

98.   **Hirsch, R. L., D. E. Griffin, and J. A. Winkelstein.** 1980. The role of complement in viral infections. II. the clearance of Sindbis virus from the bloodstream and central nervous system of mice depleted of complement. J Infect Dis **141:**212-7.

99.   **Hirsch, R. L., J. A. Winkelstein, and D. E. Griffin.** 1980. The role of complement in viral infections. III. Activation of the classical and alternative complement pathways by Sindbis virus. J Immunol **124:**2507-10.

100.   **Hoarau, J. J., M. C. Jaffar Bandjee, P. Krejbich Trotot, T. Das, G. Li-Pat-Yuen, B. Dassa, M. Denizot, E. Guichard, A. Ribera, T. Henni, F. Tallet, M. P. Moiton, B. A. Gauzere, S. Bruniquet, Z. Jaffar Bandjee, P. Morbidelli, G. Martigny, M. Jolivet, F. Gay, M. Grandadam, H. Tolou, V. Vieillard, P. Debre, B. Autran, and P. Gasque.** 2010. Persistent chronic inflammation and infection by Chikungunya arthritogenic alphavirus in spite of a robust host immune response. J Immunol **184:**5914-27.

101.   **Hobman, T., Chantler, J. .** 2007. Rubella Virus. *In* D. M. Knipe, Howley, P. M. (ed.), Fields Virology. Lippincott Williams & Wilkins, Phildelphia.

102.   **Hoffmann, J. A., F. C. Kafatos, C. A. Janeway, and R. A. Ezekowitz.** 1999. Phylogenetic perspectives in innate immunity. Science **284:**1313-8.

103.   **Holers, V. M.** 2003. The complement system as a therapeutic target in autoimmunity. Clin Immunol **107:**140-51.

104.   **Hubbard, S. C.** 1988. Regulation of glycosylation. The influence of protein structure on N-linked oligosaccharide processing. J Biol Chem **263:**19303-17.

105.   **Ikeda, K., T. Sannoh, N. Kawasaki, T. Kawasaki, and I. Yamashina.** 1987. Serum lectin with known structure activates complement through the classical pathway. J Biol Chem **262:**7451-4.

106.   **Iobst, S. T., M. R. Wormald, W. I. Weis, R. A. Dwek, and K. Drickamer.** 1994. Binding of sugar ligands to Ca(2+)-dependent animal lectins. I. Analysis of

mannose binding by site-directed mutagenesis and NMR. J Biol Chem **269:**15505-11.

107. **Ip, W. K., K. H. Chan, H. K. Law, G. H. Tso, E. K. Kong, W. H. Wong, Y. F. To, R. W. Yung, E. Y. Chow, K. L. Au, E. Y. Chan, W. Lim, J. C. Jensenius, M. W. Turner, J. S. Peiris, and Y. L. Lau.** 2005. Mannose-binding lectin in severe acute respiratory syndrome coronavirus infection. J Infect Dis **191:**1697-704.

108. **Ip, W. K., K. Takahashi, K. J. Moore, L. M. Stuart, and R. A. Ezekowitz.** 2008. Mannose-binding lectin enhances Toll-like receptors 2 and 6 signaling from the phagosome. J Exp Med **205:**169-81.

109. **Jacobsen, S., P. Garred, H. O. Madsen, N. H. Heegaard, M. L. Hetland, K. Stengaard-Pedersen, P. Junker, T. Lottenburger, T. Ellingsen, L. Smedegaard Andersen, I. Hansen, H. Skjodt, J. K. Pedersen, U. B. Lauridsen, A. J. Svendsen, U. Tarp, J. Podenphant, H. Lindegaard, A. Vestergaard, M. Ostergaard, and K. Horslev-Petersen.** 2009. Mannose-binding lectin gene polymorphisms are associated with disease activity and physical disability in untreated, anti-cyclic citrullinated peptide-positive patients with early rheumatoid arthritis. J Rheumatol **36:**731-5.

110. **Jacobsen, S., H. O. Madsen, M. Klarlund, T. Jensen, H. Skjodt, K. E. Jensen, A. Svejgaard, and P. Garred.** 2001. The influence of mannose binding lectin polymorphisms on disease outcome in early polyarthritis. TIRA Group. J Rheumatol **28:**935-42.

111. **Ji, X., G. G. Olinger, S. Aris, Y. Chen, H. Gewurz, and G. T. Spear.** 2005. Mannose-binding lectin binds to Ebola and Marburg envelope glycoproteins, resulting in blocking of virus interaction with DC-SIGN and complement-mediated virus neutralization. J Gen Virol **86:**2535-42.

112. **Jordan, J. E., M. C. Montalto, and G. L. Stahl.** 2001. Inhibition of mannose-binding lectin reduces postischemic myocardial reperfusion injury. Circulation **104:**1413-8.

113. **Jose, J., J. E. Snyder, and R. J. Kuhn.** 2009. A structural and functional perspective of alphavirus replication and assembly. Future Microbiol **4:**837-56.

114. **Joyce-Shaikh, B., M. E. Bigler, C. C. Chao, E. E. Murphy, W. M. Blumenschein, I. E. Adamopoulos, P. G. Heyworth, S. Antonenko, E. P.**

Bowman, T. K. McClanahan, J. H. Phillips, and D. J. Cua. 2010. Myeloid DAP12-associating lectin (MDL)-1 regulates synovial inflammation and bone erosion associated with autoimmune arthritis. J Exp Med **207:**579-89.

115. **Kaden, S. A., S. Kurig, K. Vasters, K. Hofmann, K. S. Zaenker, J. Schmitz, and G. Winkels.** 2009. Enhanced dendritic cell-induced immune responses mediated by the novel C-type lectin receptor mDCAR1. J Immunol **183:**5069-78.

116. **Kanazawa, N., K. Tashiro, K. Inaba, and Y. Miyachi.** 2003. Dendritic cell immunoactivating receptor, a novel C-type lectin immunoreceptor, acts as an activating receptor through association with Fc receptor gamma chain. J Biol Chem **278:**32645-52.

117. **Kawai, T., and S. Akira.** 2011. Toll-like receptors and their crosstalk with other innate receptors in infection and immunity. Immunity **34:**637-50.

118. **Keane, T. M., L. Goodstadt, P. Danecek, M. A. White, K. Wong, B. Yalcin, A. Heger, A. Agam, G. Slater, M. Goodson, N. A. Furlotte, E. Eskin, C. Nellaker, H. Whitley, J. Cleak, D. Janowitz, P. Hernandez-Pliego, A. Edwards, T. G. Belgard, P. L. Oliver, R. E. McIntyre, A. Bhomra, J. Nicod, X. Gan, W. Yuan, L. van der Weyden, C. A. Steward, S. Bala, J. Stalker, R. Mott, R. Durbin, I. J. Jackson, A. Czechanski, J. A. Guerra-Assuncao, L. R. Donahue, L. G. Reinholdt, B. A. Payseur, C. P. Ponting, E. Birney, J. Flint, and D. J. Adams.** 2011. Mouse genomic variation and its effect on phenotypes and gene regulation. Nature **477:**289-94.

119. **Kilpatrick, D. C.** 1998. Phospholipid-binding activity of human mannan-binding lectin. Immunol Lett **61:**191-5.

120. **Klimstra, W. B., E. M. Nangle, M. S. Smith, A. D. Yurochko, and K. D. Ryman.** 2003. DC-SIGN and L-SIGN can act as attachment receptors for alphaviruses and distinguish between mosquito cell- and mammalian cell-derived viruses. J Virol **77:**12022-32.

121. **Klimstra, W. B., K. D. Ryman, and R. E. Johnston.** 1998. Adaptation of Sindbis virus to BHK cells selects for use of heparan sulfate as an attachment receptor. J Virol **72:**7357-66.

122. **Knight, R. L., K. L. Schultz, R. J. Kent, M. Venkatesan, and D. E. Griffin.** 2009. Role of N-linked glycosylation for sindbis virus infection and replication in vertebrate and invertebrate systems. J Virol **83:**5640-7.

123. **Kojouharova, M., K. Reid, and M. Gadjeva.** 2010. New insights into the molecular mechanisms of classical complement activation. Mol Immunol **47:**2154-60.

124. **Krarup, A., S. Thiel, A. Hansen, T. Fujita, and J. C. Jensenius.** 2004. L-ficolin is a pattern recognition molecule specific for acetyl groups. J Biol Chem **279:**47513-9.

125. **Kuhn, R. J.** 2007. Togaviridae: The Viruses and Their Replication. *In* D. M. Knipe, Howley, P. M. (ed.), Fields' Virology. Lippincott Williams & Wilkins, Philadelphia.

126. **Kuroki, Y., T. Honma, H. Chiba, H. Sano, M. Saitoh, Y. Ogasawara, H. Sohma, and T. Akino.** 1997. A novel type of binding specificity to phospholipids for rat mannose-binding proteins isolated from serum and liver. FEBS Lett **414:**387-92.

127. **Kurt-Jones, E. A., L. Popova, L. Kwinn, L. M. Haynes, L. P. Jones, R. A. Tripp, E. E. Walsh, M. W. Freeman, D. T. Golenbock, L. J. Anderson, and R. W. Finberg.** 2000. Pattern recognition receptors TLR4 and CD14 mediate response to respiratory syncytial virus. Nat Immunol **1:**398-401.

128. **La Linn, M., J. A. Eble, C. Lubken, R. W. Slade, J. Heino, J. Davies, and A. Suhrbier.** 2005. An arthritogenic alphavirus uses the alpha1beta1 integrin collagen receptor. Virology **336:**229-39.

129. **Lai, M. M. C., Perlman, S., and Anderson, L.J.** 2007. Coronaviridae. *In* D. M. Knipe, Howley, P. M. (ed.), Fields Virology. Lippincott Williams & Wilkins, Philadelphia.

130. **Lescar, J., A. Roussel, M. W. Wien, J. Navaza, S. D. Fuller, G. Wengler, and F. A. Rey.** 2001. The Fusion glycoprotein shell of Semliki Forest virus: an icosahedral assembly primed for fusogenic activation at endosomal pH. Cell **105:**137-48.

131. **Levine, B., J. M. Hardwick, B. D. Trapp, T. O. Crawford, R. C. Bollinger, and D. E. Griffin.** 1991. Antibody-mediated clearance of alphavirus infection from neurons. Science **254:**856-60.

132. **Li, B., D. J. Allendorf, R. Hansen, J. Marroquin, C. Ding, D. E. Cramer, and J. Yan.** 2006. Yeast beta-glucan amplifies phagocyte killing of iC3b-opsonized tumor cells via complement receptor 3-Syk-phosphatidylinositol 3-kinase pathway. J Immunol **177:**1661-9.

133. **Li, L., J. Jose, Y. Xiang, R. J. Kuhn, and M. G. Rossmann.** 2010. Structural changes of envelope proteins during alphavirus fusion. Nature **468:**705-8.

134. **Lidbury, B. A., N. E. Rulli, A. Suhrbier, P. N. Smith, S. R. McColl, A. L. Cunningham, A. Tarkowski, N. van Rooijen, R. J. Fraser, and S. Mahalingam.** 2008. Macrophage-derived proinflammatory factors contribute to the development of arthritis and myositis after infection with an arthrogenic alphavirus. J Infect Dis **197:**1585-93.

135. **Lidbury, B. A., C. Simeonovic, G. E. Maxwell, I. D. Marshall, and A. J. Hapel.** 2000. Macrophage-induced muscle pathology results in morbidity and mortality for Ross River virus-infected mice. J Infect Dis **181:**27-34.

136. **Lindenbach, B. D., Thiel, H-J., and Rice, C.M.** 2007. Flaviviridae: The Viruses and Their Replication. *In* D. M. Knipe, Howley, P. M. (ed.), Fields Virology. Lippincott Williams & Wilkins, Philadelphia.

137. **Lipscombe, R. J., M. Sumiya, A. V. Hill, Y. L. Lau, R. J. Levinsky, J. A. Summerfield, and M. W. Turner.** 1992. High frequencies in African and non-African populations of independent mutations in the mannose binding protein gene. Hum Mol Genet **1:**709-15.

138. **Liu, H., L. Jensen, S. Hansen, S. V. Petersen, K. Takahashi, A. B. Ezekowitz, F. D. Hansen, J. C. Jensenius, and S. Thiel.** 2001. Characterization and quantification of mouse mannan-binding lectins (MBL-A and MBL-C) and study of acute phase responses. Scand J Immunol **53:**489-97.

139. **Loo, Y. M., and M. Gale, Jr.** 2011. Immune signaling by RIG-I-like receptors. Immunity **34:**680-92.

140. **Ludwig, G. V., J. P. Kondig, and J. F. Smith.** 1996. A putative receptor for Venezuelan equine encephalitis virus from mosquito cells. J Virol **70:**5592-9.

141. **MacDonald, G. H., and R. E. Johnston.** 2000. Role of dendritic cell targeting in Venezuelan equine encephalitis virus pathogenesis. J Virol **74:**914-22.

142.	**Macia, E., M. Ehrlich, R. Massol, E. Boucrot, C. Brunner, and T. Kirchhausen.** 2006. Dynasore, a cell-permeable inhibitor of dynamin. Dev Cell **10:**839-50.

143.	**Madsen, H. O., P. Garred, J. A. Kurtzhals, L. U. Lamm, L. P. Ryder, S. Thiel, and A. Svejgaard.** 1994. A new frequent allele is the missing link in the structural polymorphism of the human mannan-binding protein. Immunogenetics **40:**37-44.

144.	**Madsen, H. O., P. Garred, S. Thiel, J. A. Kurtzhals, L. U. Lamm, L. P. Ryder, and A. Svejgaard.** 1995. Interplay between promoter and structural gene variants control basal serum level of mannan-binding protein. J Immunol **155:**3013-20.

145.	**Madsen, H. O., M. L. Satz, B. Hogh, A. Svejgaard, and P. Garred.** 1998. Different molecular events result in low protein levels of mannan-binding lectin in populations from southeast Africa and South America. J Immunol **161:**3169-75.

146.	**Marshall, A. S., J. A. Willment, H. H. Lin, D. L. Williams, S. Gordon, and G. D. Brown.** 2004. Identification and characterization of a novel human myeloid inhibitory C-type lectin-like receptor (MICL) that is predominantly expressed on granulocytes and monocytes. J Biol Chem **279:**14792-802.

147.	**Matsushita, M., Y. Endo, S. Taira, Y. Sato, T. Fujita, N. Ichikawa, M. Nakata, and T. Mizuochi.** 1996. A novel human serum lectin with collagen- and fibrinogen-like domains that functions as an opsonin. J Biol Chem **271:**2448-54.

148.	**Mayne, J. T., J. R. Bell, E. G. Strauss, and J. H. Strauss.** 1985. Pattern of glycosylation of Sindbis virus envelope proteins synthesized in hamster and chicken cells. Virology **142:**121-33.

149.	**Mehlhop, E., and M. S. Diamond.** 2006. Protective immune responses against West Nile virus are primed by distinct complement activation pathways. J Exp Med **203:**1371-81.

150.	**Mehlhop, E., K. Whitby, T. Oliphant, A. Marri, M. Engle, and M. S. Diamond.** 2005. Complement activation is required for induction of a protective antibody response against West Nile virus infection. J Virol **79:**7466-77.

151. **Merad, M., F. Ginhoux, and M. Collin.** 2008. Origin, homeostasis and function of Langerhans cells and other langerin-expressing dendritic cells. Nat Rev Immunol **8:**935-47.

152. **Mi, S., R. Durbin, H. V. Huang, C. M. Rice, and V. Stollar.** 1989. Association of the Sindbis virus RNA methyltransferase activity with the nonstructural protein nsP1. Virology **170:**385-91.

153. **Mi, S., and V. Stollar.** 1991. Expression of Sindbis virus nsP1 and methyltransferase activity in Escherichia coli. Virology **184:**423-7.

154. **Michelow, I. C., C. Lear, C. Scully, L. I. Prugar, C. B. Longley, L. M. Yantosca, X. Ji, M. Karpel, M. Brudner, K. Takahashi, G. T. Spear, R. A. Ezekowitz, E. V. Schmidt, and G. G. Olinger.** 2011. High-dose mannose-binding lectin therapy for Ebola virus infection. J Infect Dis **203:**175-9.

155. **Mims, C. A., F. A. Murphy, W. P. Taylor, and I. D. Marshall.** 1973. Pathogenesis of Ross River virus infection in mice. I. Ependymal infection, cortical thinning, and hydrocephalus. J Infect Dis **127:**121-8.

156. **Mizuno, Y., Y. Kozutsumi, T. Kawasaki, and I. Yamashina.** 1981. Isolation and characterization of a mannan-binding protein from rat liver. J Biol Chem **256:**4247-52.

157. **Mocsai, A., M. Zhou, F. Meng, V. L. Tybulewicz, and C. A. Lowell.** 2002. Syk is required for integrin signaling in neutrophils. Immunity **16:**547-58.

158. **Morrison, T. E., R. J. Fraser, P. N. Smith, S. Mahalingam, and M. T. Heise.** 2007. Complement contributes to inflammatory tissue destruction in a mouse model of Ross River virus-induced disease. J Virol **81:**5132-43.

159. **Morrison, T. E., L. Oko, S. A. Montgomery, A. C. Whitmore, A. R. Lotstein, B. M. Gunn, S. A. Elmore, and M. T. Heise.** 2011. A mouse model of chikungunya virus-induced musculoskeletal inflammatory disease: evidence of arthritis, tenosynovitis, myositis, and persistence. Am J Pathol **178:**32-40.

160. **Morrison, T. E., J. D. Simmons, and M. T. Heise.** 2008. Complement receptor 3 promotes severe ross river virus-induced disease. J Virol **82:**11263-72.

161. **Morrison, T. E., A. C. Whitmore, R. S. Shabman, B. A. Lidbury, S. Mahalingam, and M. T. Heise.** 2006. Characterization of Ross River virus tropism and virus-induced inflammation in a mouse model of viral arthritis and myositis. J Virol **80:**737-49.

162. **Mukhopadhyay, S., W. Zhang, S. Gabler, P. R. Chipman, E. G. Strauss, J. H. Strauss, T. S. Baker, R. J. Kuhn, and M. G. Rossmann.** 2006. Mapping the structure and function of the E1 and E2 glycoproteins in alphaviruses. Structure **14:**63-73.

163. **Mylonas, A. D., A. M. Brown, T. L. Carthew, B. McGrath, D. M. Purdie, N. Pandeya, P. C. Vecchio, L. G. Collins, I. D. Gardner, F. J. de Looze, E. J. Reymond, and A. Suhrbier.** 2002. Natural history of Ross River virus-induced epidemic polyarthritis. Med J Aust **177:**356-60.

164. **Nascimento, E. J., A. M. Silva, M. T. Cordeiro, C. A. Brito, L. H. Gil, U. Braga-Neto, and E. T. Marques.** 2009. Alternative complement pathway deregulation is correlated with dengue severity. PLoS One **4:**e6782.

165. **Neuvonen, M., A. Kazlauskas, M. Martikainen, A. Hinkkanen, T. Ahola, and K. Saksela.** 2011. SH3 domain-mediated recruitment of host cell amphiphysins by alphavirus nsP3 promotes viral RNA replication. PLoS Pathog **7:**e1002383.

166. **Ng, L. F., A. Chow, Y. J. Sun, D. J. Kwek, P. L. Lim, F. Dimatatac, L. C. Ng, E. E. Ooi, K. H. Choo, Z. Her, P. Kourilsky, and Y. S. Leo.** 2009. IL-1beta, IL-6, and RANTES as biomarkers of Chikungunya severity. PLoS One **4:**e4261.

167. **Ogden, C. A., A. deCathelineau, P. R. Hoffmann, D. Bratton, B. Ghebrehiwet, V. A. Fadok, and P. M. Henson.** 2001. C1q and mannose binding lectin engagement of cell surface calreticulin and CD91 initiates macropinocytosis and uptake of apoptotic cells. J Exp Med **194:**781-95.

168. **Palaniyar, N., J. Nadesalingam, H. Clark, M. J. Shih, A. W. Dodds, and K. B. Reid.** 2004. Nucleic acid is a novel ligand for innate, immune pattern recognition collectins surfactant proteins A and D and mannose-binding lectin. J Biol Chem **279:**32728-36.

169. **Park, C. G., K. Takahara, E. Umemoto, Y. Yashima, K. Matsubara, Y. Matsuda, B. E. Clausen, K. Inaba, and R. M. Steinman.** 2001. Five mouse homologues of the human dendritic cell C-type lectin, DC-SIGN. Int Immunol **13:**1283-90.

170. **Peng, X., L. Gralinski, M. T. Ferris, M. B. Frieman, M. J. Thomas, S. Proll, M. J. Korth, J. R. Tisoncik, M. Heise, S. Luo, G. P. Schroth, T. M. Tumpey, C. Li, Y. Kawaoka, R. S. Baric, and M. G. Katze.** 2012. Integrative deep sequencing of the mouse lung transcriptome reveals differential expression of diverse classes of small RNAs in response to respiratory virus infection. MBio **2**.

171. **Peranen, J., P. Laakkonen, M. Hyvonen, and L. Kaariainen.** 1995. The alphavirus replicase protein nsP1 is membrane-associated and has affinity to endocytic organelles. Virology **208:**610-20.

172. **Perera, C., H. P. McNeil, and C. L. Geczy.** 2010. S100 Calgranulins in inflammatory arthritis. Immunol Cell Biol **88:**41-9.

173. **Perera, P. Y., T. N. Mayadas, O. Takeuchi, S. Akira, M. Zaks-Zilberman, S. M. Goyert, and S. N. Vogel.** 2001. CD11b/CD18 acts in concert with CD14 and Toll-like receptor (TLR) 4 to elicit full lipopolysaccharide and taxol-inducible gene expression. J Immunol **166:**574-81.

174. **Pletnev, S. V., W. Zhang, S. Mukhopadhyay, B. R. Fisher, R. Hernandez, D. T. Brown, T. S. Baker, M. G. Rossmann, and R. J. Kuhn.** 2001. Locations of carbohydrate sites on alphavirus glycoproteins show that E1 forms an icosahedral scaffold. Cell **105:**127-36.

175. **Powers, A. M., A. C. Brault, Y. Shirako, E. G. Strauss, W. Kang, J. H. Strauss, and S. C. Weaver.** 2001. Evolutionary relationships and systematics of the alphaviruses. J Virol **75:**10118-31.

176. **Powlesland, A. S., E. M. Ward, S. K. Sadhu, Y. Guo, M. E. Taylor, and K. Drickamer.** 2006. Widely divergent biochemical properties of the complete set of mouse DC-SIGN-related proteins. J Biol Chem **281:**20440-9.

177. **Rabinovich, G. A., Y. van Kooyk, and B. A. Cobb.** 2012. Glycobiology of immune responses. Ann N Y Acad Sci **1253:**1-15.

178. **Raju, R., and H. V. Huang.** 1991. Analysis of Sindbis virus promoter recognition in vivo, using novel vectors with two subgenomic mRNA promoters. J Virol **65:**2501-10.

179. **Ramos, H. J., and M. Gale, Jr.** 2011. RIG-I like receptors and their signaling crosstalk in the regulation of antiviral immunity. Curr Opin Virol **1:**167-76.

180. **Reed, D. S., T. Larsen, L. J. Sullivan, C. M. Lind, M. G. Lackemeyer, W. D. Pratt, and M. D. Parker.** 2005. Aerosol exposure to western equine encephalitis virus causes fever and encephalitis in cynomolgus macaques. J Infect Dis **192:**1173-82.

181. **Rezza, G., L. Nicoletti, R. Angelini, R. Romi, A. C. Finarelli, M. Panning, P. Cordioli, C. Fortuna, S. Boros, F. Magurano, G. Silvi, P. Angelini, M. Dottori, M. G. Ciufolini, G. C. Majori, and A. Cassone.** 2007. Infection with chikungunya virus in Italy: an outbreak in a temperate region. Lancet **370:**1840-6.

182. **Rice, C. M., and J. H. Strauss.** 1982. Association of sindbis virion glycoproteins and their precursors. J Mol Biol **154:**325-48.

183. **Ricklin, D., G. Hajishengallis, K. Yang, and J. D. Lambris.** 2010. Complement: a key system for immune surveillance and homeostasis. Nat Immunol **11:**785-97.

184. **Rikkonen, M., J. Peranen, and L. Kaariainen.** 1994. ATPase and GTPase activities associated with Semliki Forest virus nonstructural protein nsP2. J Virol **68:**5804-10.

185. **Rivas, F., L. A. Diaz, V. M. Cardenas, E. Daza, L. Bruzon, A. Alcala, O. De la Hoz, F. M. Caceres, G. Aristizabal, J. W. Martinez, D. Revelo, F. De la Hoz, J. Boshell, T. Camacho, L. Calderon, V. A. Olano, L. I. Villarreal, D. Roselli, G. Alvarez, G. Ludwig, and T. Tsai.** 1997. Epidemic Venezuelan equine encephalitis in La Guajira, Colombia, 1995. J Infect Dis **175:**828-32.

186. **Roberts, A., F. Pardo-Manuel de Villena, W. Wang, L. McMillan, and D. W. Threadgill.** 2007. The polymorphism architecture of mouse genetic resources elucidated using genome-wide resequencing data: implications for QTL discovery and systems genetics. Mamm Genome **18:**473-81.

187. **Robinson, D., N. C. Phillips, and B. Winchester.** 1975. Affinity chromatography of human liver alpha-D-mannosidase. FEBS Lett **53:**110-2.

188. **Robinson, M. C.** 1955. An epidemic of virus disease in Southern Province, Tanganyika Territory, in 1952-53. I. Clinical features. Trans R Soc Trop Med Hyg **49:**28-32.

189. **Robinson, M. J., D. Sancho, E. C. Slack, S. LeibundGut-Landmann, and C. Reis e Sousa.** 2006. Myeloid C-type lectins in innate immunity. Nat Immunol **7:**1258-65.

190. **Rose, P. P., S. L. Hanna, A. Spiridigliozzi, N. Wannissorn, D. P. Beiting, S. R. Ross, R. W. Hardy, S. A. Bambina, M. T. Heise, and S. Cherry.** 2011. Natural resistance-associated macrophage protein is a cellular receptor for sindbis virus in both insect and mammalian hosts. Cell Host Microbe **10:**97-104.

191. **Rosen, L., D. J. Gubler, and P. H. Bennett.** 1981. Epidemic polyarthritis (Ross River) virus infection in the Cook Islands. Am J Trop Med Hyg **30:**1294-302.

192. **Rossi, V., S. Cseh, I. Bally, N. M. Thielens, J. C. Jensenius, and G. J. Arlaud.** 2001. Substrate specificities of recombinant mannan-binding lectin-associated serine proteases-1 and -2. J Biol Chem **276:**40880-7.

193. **Rulli, N. E., A. Guglielmotti, G. Mangano, M. S. Rolph, C. Apicella, A. Zaid, A. Suhrbier, and S. Mahalingam.** 2009. Amelioration of alphavirus-induced arthritis and myositis in a mouse model by treatment with bindarit, an inhibitor of monocyte chemotactic proteins. Arthritis Rheum **60:**2513-23.

194. **Russell, R. C.** 2002. Ross River virus: ecology and distribution. Annu Rev Entomol **47:**1-31.

195. **Ryman, K. D., C. L. Gardner, C. W. Burke, K. C. Meier, J. M. Thompson, and W. B. Klimstra.** 2007. Heparan sulfate binding can contribute to the neurovirulence of neuroadapted and nonneuroadapted Sindbis viruses. J Virol **81:**3563-73.

196. **Ryman, K. D., and W. B. Klimstra.** 2008. Host responses to alphavirus infection. Immunol Rev **225:**27-45.

197. **Ryman, K. D., W. B. Klimstra, K. B. Nguyen, C. A. Biron, and R. E. Johnston.** 2000. Alpha/beta interferon protects adult mice from fatal Sindbis virus infection and is an important determinant of cell and tissue tropism. J Virol **74:**3366-78.

198. **Saevarsdottir, S., K. Steinsson, G. Grondal, and H. Valdimarsson.** 2007. Patients with rheumatoid arthritis have higher levels of mannan-binding lectin than their first-degree relatives and unrelated controls. J Rheumatol **34:**1692-5.

199. **Sahu, A., T. R. Kozel, and M. K. Pangburn.** 1994. Specificity of the thioester-containing reactive site of human C3 and its significance to complement activation. Biochem J **302 (Pt 2):**429-36.

200. **Saifuddin, M., M. L. Hart, H. Gewurz, Y. Zhang, and G. T. Spear.** 2000. Interaction of mannose-binding lectin with primary isolates of human immunodeficiency virus type 1. J Gen Virol **81:**949-55.

201. **Schafer, A., C. B. Brooke, A. C. Whitmore, and R. E. Johnston.** 2011. The role of the blood-brain barrier during Venezuelan equine encephalitis virus infection. J Virol **85:**10682-90.

202. **Schilte, C., T. Couderc, F. Chretien, M. Sourisseau, N. Gangneux, F. Guivel-Benhassine, A. Kraxner, J. Tschopp, S. Higgs, A. Michault, F. Arenzana-Seisdedos, M. Colonna, L. Peduto, O. Schwartz, M. Lecuit, and M. L. Albert.** 2010. Type I IFN controls chikungunya virus via its action on nonhematopoietic cells. J Exp Med **207:**429-42.

203. **Schoneboom, B. A., K. M. Catlin, A. M. Marty, and F. B. Grieder.** 2000. Inflammation is a component of neurodegeneration in response to Venezuelan equine encephalitis virus infection in mice. J Neuroimmunol **109:**132-46.

204. **Schoneboom, B. A., M. J. Fultz, T. H. Miller, L. C. McKinney, and F. B. Grieder.** 1999. Astrocytes as targets for Venezuelan equine encephalitis virus infection. J Neurovirol **5:**342-54.

205. **Schwaeble, W. J., N. J. Lynch, J. E. Clark, M. Marber, N. J. Samani, Y. M. Ali, T. Dudler, B. Parent, K. Lhotta, R. Wallis, C. A. Farrar, S. Sacks, H. Lee, M. Zhang, D. Iwaki, M. Takahashi, T. Fujita, C. E. Tedford, and C. M. Stover.** 2011. Targeting of mannan-binding lectin-associated serine protease-2 confers protection from myocardial and gastrointestinal ischemia/reperfusion injury. Proc Natl Acad Sci U S A **108:**7523-8.

206. **Scott, T. W., and S. C. Weaver.** 1989. Eastern equine encephalomyelitis virus: epidemiology and evolution of mosquito transmission. Adv Virus Res **37:**277-328.

207. **Sefton, B. M.** 1977. Immediate glycosylation of Sindbis virus membrane proteins. Cell **10:**659-68.

208. **Seppanen, M., M. L. Lokki, M. Lappalainen, E. Hiltunen-Back, A. T. Rovio, S. Kares, M. Hurme, and J. Aittoniemi.** 2009. Mannose-binding lectin 2 gene polymorphism in recurrent herpes simplex virus 2 infection. Hum Immunol **70:**218-21.

209. **Shabman, R. S., T. E. Morrison, C. Moore, L. White, M. S. Suthar, L. Hueston, N. Rulli, B. Lidbury, J. P. Ting, S. Mahalingam, and M. T. Heise.** 2007. Differential induction of type I interferon responses in myeloid dendritic cells by mosquito and mammalian-cell-derived alphaviruses. J Virol **81:**237-47.

210. **Shabman, R. S., K. M. Rogers, and M. T. Heise.** 2008. Ross River virus envelope glycans contribute to type I interferon production in myeloid dendritic cells. J Virol **82:**12374-83.

211. **Sheriff, S., C. Y. Chang, and R. A. Ezekowitz.** 1994. Human mannose-binding protein carbohydrate recognition domain trimerizes through a triple alpha-helical coiled-coil. Nat Struct Biol **1:**789-94.

212. **Shimizu, T., C. Nishitani, H. Mitsuzawa, S. Ariki, M. Takahashi, K. Ohtani, N. Wakamiya, and Y. Kuroki.** 2009. Mannose binding lectin and lung collectins interact with Toll-like receptor 4 and MD-2 by different mechanisms. Biochim Biophys Acta **1790:**1705-10.

213. **Shirako, Y., E. G. Strauss, and J. H. Strauss.** 2000. Suppressor mutations that allow sindbis virus RNA polymerase to function with nonaromatic amino acids at the N-terminus: evidence for interaction between nsP1 and nsP4 in minus-strand RNA synthesis. Virology **276:**148-60.

214. **Shope, R. E., and S. G. Anderson.** 1960. The virus aetiology of epidemic exanthem and polyarthritis. Med J Aust **47(1):**156-8.

215. **Stanley, P., Schachter, H., and Taniguchi, N. .** 2009. N-Glycans. *In* A. Varki, Cummings, R.D., Esko, J.D., et al. (ed.), Essentials of Glycobiology, 2nd edition. Cold Spring Laboratory Press, Cold Spring Harbor, NY.

216. **Stoermer, K. A., A. Burrack, L. Oko, S. A. Montgomery, L. B. Borst, R. G. Gill, and T. E. Morrison.** 2012. Genetic ablation of arginase 1 in macrophages and neutrophils enhances clearance of an arthritogenic alphavirus. J Immunol **189:**4047-59.

217. **Stoermer, K. A., and T. E. Morrison.** 2011. Complement and viral pathogenesis. Virology **411:**362-73.

218. **Strauss, E. G., R. J. De Groot, R. Levinson, and J. H. Strauss.** 1992. Identification of the active site residues in the nsP2 proteinase of Sindbis virus. Virology **191:**932-40.

219. **Strauss, J. H., and E. G. Strauss.** 1994. The alphaviruses: gene expression, replication, and evolution. Microbiol Rev **58:**491-562.

220. **Stuart, L. M., K. Takahashi, L. Shi, J. Savill, and R. A. Ezekowitz.** 2005. Mannose-binding lectin-deficient mice display defective apoptotic cell clearance but no autoimmune phenotype. J Immunol **174:**3220-6.

221. **Suhrbier, A., M. C. Jaffar-Bandjee, and P. Gasque.** 2012. Arthritogenic alphaviruses--an overview. Nat Rev Rheumatol **8:**420-9.

222. **Sumiya, M., M. Super, P. Tabona, R. J. Levinsky, T. Arai, M. W. Turner, and J. A. Summerfield.** 1991. Molecular basis of opsonic defect in immunodeficient children. Lancet **337:**1569-70.

223. **Takahashi, K., W. E. Ip, I. C. Michelow, and R. A. Ezekowitz.** 2006. The mannose-binding lectin: a prototypic pattern recognition molecule. Curr Opin Immunol **18:**16-23.

224. **Tassaneetrithep, B., T. H. Burgess, A. Granelli-Piperno, C. Trumpfheller, J. Finke, W. Sun, M. A. Eller, K. Pattanapanyasat, S. Sarasombath, D. L. Birx, R. M. Steinman, S. Schlesinger, and M. A. Marovich.** 2003. DC-SIGN (CD209) mediates dengue virus infection of human dendritic cells. J Exp Med **197:**823-9.

225. **Tesh, R. B., R. G. McLean, D. A. Shroyer, C. H. Calisher, and L. Rosen.** 1981. Ross River virus (Togaviridae: Alphavirus) infection (epidemic polyarthritis) in American Samoa. Trans R Soc Trop Med Hyg **75:**426-31.

226. **Thiel, S., T. Vorup-Jensen, C. M. Stover, W. Schwaeble, S. B. Laursen, K. Poulsen, A. C. Willis, P. Eggleton, S. Hansen, U. Holmskov, K. B. Reid, and J. C. Jensenius.** 1997. A second serine protease associated with mannan-binding lectin that activates complement. Nature **386:**506-10.

227. **Tsetsarkin, K. A., D. L. Vanlandingham, C. E. McGee, and S. Higgs.** 2007. A single mutation in chikungunya virus affects vector specificity and epidemic potential. PLoS Pathog **3:**e201.

228. **van de Geijn, F. E., J. M. Hazes, K. Geleijns, M. Emonts, B. C. Jacobs, B. C. Dufour-van den Goorbergh, and R. J. Dolhain.** 2008. Mannose-binding lectin polymorphisms are not associated with rheumatoid arthritis--confirmation in two large cohorts. Rheumatology (Oxford) **47:**1168-71.

229. **Varki, A.** 2009. Essentials of glycobiology, 2nd ed. Cold Spring Harbor Laboratory Press, Cold Spring Harbor, N.Y.

230. **Vashishtha, M., T. Phalen, M. T. Marquardt, J. S. Ryu, A. C. Ng, and M. Kielian.** 1998. A single point mutation controls the cholesterol dependence of Semliki Forest virus entry and exit. J Cell Biol **140:**91-9.

231. **Vasiljeva, L., A. Merits, P. Auvinen, and L. Kaariainen.** 2000. Identification of a novel function of the alphavirus capping apparatus. RNA 5'-triphosphatase activity of Nsp2. J Biol Chem **275:**17281-7.

232. **Vasudevan, S. S., N. H. Lopes, P. N. Seshiah, T. Wang, C. B. Marsh, D. J. Kereiakes, C. Dong, and P. J. Goldschmidt-Clermont.** 2003. Mac-1 and Fas activities are concurrently required for execution of smooth muscle cell death by M-CSF-stimulated macrophages. Cardiovasc Res **59:**723-33.

233. **Vetvicka, V., B. P. Thornton, and G. D. Ross.** 1996. Soluble beta-glucan polysaccharide binding to the lectin site of neutrophil or natural killer cell complement receptor type 3 (CD11b/CD18) generates a primed state of the receptor capable of mediating cytotoxicity of iC3b-opsonized target cells. J Clin Invest **98:**50-61.

234. **von Bonsdorff, C. H., and S. C. Harrison.** 1978. Hexagonal glycoprotein arrays from Sindbis virus membranes. J Virol **28:**578-83.

235. **von Bonsdorff, C. H., and S. C. Harrison.** 1975. Sindbis virus glycoproteins form a regular icosahedral surface lattice. J Virol **16:**141-5.

236. **Voss, J. E., M. C. Vaney, S. Duquerroy, C. Vonrhein, C. Girard-Blanc, E. Crublet, A. Thompson, G. Bricogne, and F. A. Rey.** 2010. Glycoprotein

organization of Chikungunya virus particles revealed by X-ray crystallography. Nature **468:**709-12.

237. **Walsh, M. C., T. Bourcier, K. Takahashi, L. Shi, M. N. Busche, R. P. Rother, S. D. Solomon, R. A. Ezekowitz, and G. L. Stahl.** 2005. Mannose-binding lectin is a regulator of inflammation that accompanies myocardial ischemia and reperfusion injury. J Immunol **175:**541-6.

238. **Wang, K. S., R. J. Kuhn, E. G. Strauss, S. Ou, and J. H. Strauss.** 1992. High-affinity laminin receptor is a receptor for Sindbis virus in mammalian cells. J Virol **66:**4992-5001.

239. **Wang, M., Y. Chen, Y. Zhang, L. Zhang, X. Lu, and Z. Chen.** 2011. Mannan-binding lectin directly interacts with Toll-like receptor 4 and suppresses lipopolysaccharide-induced inflammatory cytokine secretion from THP-1 cells. Cell Mol Immunol **8:**265-75.

240. **Weaver, S. C., and A. D. Barrett.** 2004. Transmission cycles, host range, evolution and emergence of arboviral disease. Nat Rev Microbiol **2:**789-801.

241. **Weaver, S. C., R. Rico-Hesse, and T. W. Scott.** 1992. Genetic diversity and slow rates of evolution in New World alphaviruses. Curr Top Microbiol Immunol **176:**99-117.

242. **Weaver, S. C., R. Winegar, I. D. Manger, and N. L. Forrester.** 2012. Alphaviruses: population genetics and determinants of emergence. Antiviral Res **94:**242-57.

243. **Weis, W. I., K. Drickamer, and W. A. Hendrickson.** 1992. Structure of a C-type mannose-binding protein complexed with an oligosaccharide. Nature **360:**127-34.

244. **Weiss, B., H. Nitschko, I. Ghattas, R. Wright, and S. Schlesinger.** 1989. Evidence for specificity in the encapsidation of Sindbis virus RNAs. J Virol **63:**5310-8.

245. **White, L. J., J. G. Wang, N. L. Davis, and R. E. Johnston.** 2001. Role of alpha/beta interferon in Venezuelan equine encephalitis virus pathogenesis: effect of an attenuating mutation in the 5' untranslated region. J Virol **75:**3706-18.

246. **White, L. K., T. Sali, D. Alvarado, E. Gatti, P. Pierre, D. Streblow, and V. R. Defilippis.** 2011. Chikungunya virus induces IPS-1-dependent innate immune activation and protein kinase R-independent translational shutoff. J Virol **85:**606-20.

247. **Williams, M. C., J. P. Woodall, and J. D. Gillett.** 1965. O'nyong-Nyong Fever: An Epidemic Virus Diesease in East Africa. Vii. Virus Isolations from Man and Serological Studies up to July 1961. Trans R Soc Trop Med Hyg **59:**186-97.

248. **Wollish, A. C., M. T. Ferris, L. K. Blevins, Y. M. Loo, M. Gale, Jr., and M. T. Heise.** 2012. An attenuating mutation in a neurovirulent Sindbis virus strain interacts with the IPS-1 signaling pathway in vivo. Virology.

249. **Wouters, D., A. E. Voskuyl, E. T. Molenaar, B. A. Dijkmans, and C. E. Hack.** 2006. Evaluation of classical complement pathway activation in rheumatoid arthritis: measurement of C1q-C4 complexes as novel activation products. Arthritis Rheum **54:**1143-50.

250. **Wu, M. F., S. T. Chen, A. H. Yang, W. W. Lin, Y. L. Lin, N. J. Chen, I. S. Tsai, L. Li, and S. L. Hsieh.** 2012. CLEC5A is critical for dengue virus-induced inflammasome activation in human macrophages. Blood.

251. **Xia, Y., V. Vetvicka, J. Yan, M. Hanikyrova, T. Mayadas, and G. D. Ross.** 1999. The beta-glucan-binding lectin site of mouse CR3 (CD11b/CD18) and its function in generating a primed state of the receptor that mediates cytotoxic activation in response to iC3b-opsonized target cells. J Immunol **162:**2281-90.

252. **Yamamoto, M., S. Sato, H. Hemmi, K. Hoshino, T. Kaisho, H. Sanjo, O. Takeuchi, M. Sugiyama, M. Okabe, K. Takeda, and S. Akira.** 2003. Role of adaptor TRIF in the MyD88-independent toll-like receptor signaling pathway. Science **301:**640-3.

253. **Yamasaki, S., E. Ishikawa, M. Sakuma, H. Hara, K. Ogata, and T. Saito.** 2008. Mincle is an ITAM-coupled activating receptor that senses damaged cells. Nat Immunol **9:**1179-88.

254. **Ying, H., X. Ji, M. L. Hart, K. Gupta, M. Saifuddin, M. R. Zariffard, and G. T. Spear.** 2004. Interaction of mannose-binding lectin with HIV type 1 is sufficient for virus opsonization but not neutralization. AIDS Res Hum Retroviruses **20:**327-35.

255.   **Zacho, R. M., L. Jensen, R. Terp, J. C. Jensenius, and S. Thiel.** 2012. Studies of the pattern recognition molecule H-ficolin: specificity and purification. J Biol Chem **287:**8071-81.

256.   **Zhao, H., and H. Garoff.** 1992. Role of cell surface spikes in alphavirus budding. J Virol **66:**7089-95.

257.   **Zhou, Y., K. Lu, S. Pfefferle, S. Bertram, I. Glowacka, C. Drosten, S. Pohlmann, and G. Simmons.** 2010. A single asparagine-linked glycosylation site of the severe acute respiratory syndrome coronavirus spike glycoprotein facilitates inhibition by mannose-binding lectin through multiple mechanisms. J Virol **84:**8753-64.

258.   **Ziemiecki, A., and H. Garofff.** 1978. Subunit composition of the membrane glycoprotein complex of Semliki Forest virus. J Mol Biol **122:**259-69.

259.   **Zipfel, P. F., and C. Skerka.** 2009. Complement regulators and inhibitory proteins. Nat Rev Immunol **9:**729-40.